Efficient solvers for power flow equations: parametric solutions with accuracy control assessment

Raquel García-Blanco

EFFICIENT SOLVERS FOR POWER FLOW EQUATIONS: PARAMETRIC SOLUTIONS WITH ACCURACY CONTROL ASSESSMENT

Raquel García-Blanco

Doctoral Thesis
Barcelona, 2016

EFFICIENT SOLVERS FOR POWER FLOW EQUATIONS: PARAMETRIC SOLUTIONS WITH ACCURACY CONTROL ASSESSMENT

Raquel García-Blanco

UPC

Doctoral Thesis
Advisors: Pedro Díez and Francisco Chinesta
Barcelona, 2016

Departament d'Enginyeria Civil i Ambiental
Programa de Doctorat de Matemàtica Aplicada

ABSTRACT

Efficient solvers for power flow equations: parametric solutions with accuracy control assessment

Raquel García-Blanco

The Power Flow model is extensively used to predict the behavior of electric grids and results in solving a nonlinear algebraic system of equations. Modeling the grid is essential for design optimization and control. Both applications require a fast response for multiple queries to a parametric family of power flow problems. Different solvers have been introduced especially designed for the algebraic nonlinear power flow equations, providing efficient solutions for single problems, even when the number of degrees of freedom is considerably large. However, there is no existing methodology providing an explicit solution of the Parametric Power Flow problem (viz. a computational vademecum, explicit in terms of the parameters).

This work aims precisely at designing algorithms producing computational vademecums for the Parametric Power Flow problem. Once these solutions are available, solving for different values of the parameters is an extremely fast (real-time) post-process and therefore both the optimal design and the control problem can readily be addressed.

In a first phase, a new family of iterative solvers for the non-parametric version of the problem is devised. The method is based on a hybrid formulation of the problem combined with an alternated search directions scheme. These methods are designed such that it can be generalized to deal with the parametric version of the problem following a Proper Generalized Decomposition (PGD) strategy.

The solver for the parametric problem is conceived by performing the operations involving the unknowns in a PGD fashion. The algorithm follows the basic steps of the algebraic solver, but some operations are carried out in a PGD framework, that is requiring a nested iterative algorithm. The PGD solver is accompanied with an error assessment technique that allows monitoring the convergence of the iterative procedures and deciding the number of terms required to meet the accuracy prescriptions. Different examples of realistic grids and standard benchmark tests are used to demonstrate the performance of the proposed methodologies.

a mis niñas, Caro, Cris y Noe porque a pesar de estar separadas, siempre estáis a mi lado.

Por último, agradecer a toda mi familia por escucharme, ayudarme y apoyarme siempre en todo lo que me he propuesto durante estos años, en particular a mi tía Eva, cuyo apoyo he sentido siempre aún estando lejos. Gracias a mi hermana Tatiana por ser mi compañera de viaje y la que me hace reír cuando lo necesito, y por supuesto a los motores de mi vida, Papá y Mamá, sabéis que sin vosotros no hubiera sido posible.

Raquel García-Blanco
Ceuta, 2016

Contents

CONTENTS

x

Chapter 1

Introduction

1.1 Motivation

Electricity is a common form of energy used in all countries since it is the backbone of industrial expansion. It is essential for technological development and plays a decisive role in social progress. Consequently, electric power systems constitute a fundamental framework of contemporary society. Accordingly, during the last decades, networks around the world have been continuously expanding and growing in terms of complexity and demand of the power.

In response to this evolution, the necessity of modeling, simulating and monitoring power systems in order to make predictions and design them emerged. Power flow analysis, which is a branch of the power system engineering, is one of the tools used to perform these actions. Specifically, power flow analysis is applied to phenomena related to:

- Transmission and distribution of electrical power

- Energy generation and management

- Power system planning: operation and expansion

- Optimal control and contingency analysis

- Real-time monitoring, decision making and security risk assessment for reaching stability and reliability

Apart from these applications, one of the most significant is the *design planning and verification*. Due to the increased power demands, some countries share their concern about the state and management of physical networks. For instance, they have the urge to expand grids in order to meet the power demands. Nevertheless, this action requires the early simulation of the whole procedure for avoiding unnecessary failures and assuring the viability of the process. The effect of expanding a grid may be catastrophic unless the management of resources follow a reliable plan which is based on analyzing all the possible outputs in the network simulation under some constraints.

The design and verification of networks is connected to another remarkable application of the power systems analysis, the *optimization* of power systems. This is due to the fact that construction of large power plants or grids could suppose high costs in addition to legal problems such as obtaining environmental permits for construction of new lines ensuring the reduction of the greenhouse emissions. Hence, optimizing grids instead of updating them might be beneficial in some circumstances. As a result, both applications are related to electricity production and environment.

In order to generate electricity safely, industry incorporates sources of generation, called distributed generators (DG) in the case of distribution systems or just generators for transmission systems. In Shrivastava et al. (2012) is reported that distributed power generation is a technology that could help to enable efficient and renewable energy production. Distributed generation is related to the use of small generating unit installed at strategic point of electric power system, sometimes connected directly to the customer site. DG technologies includes engines, small wind turbines or fuel cells and photo-voltaic system. The introduction of DG technologies can bring benefits to a power grid. These advantages, see Abookazemi et al. (2010) and Mithulananthan et al. (2004), can be divided into:

1. Technical: including wide ranges of benefits such as efficiency, grid reinforcement (providing backup power during utility system outages), power loss

reduction, reliability and security increase, load factors and voltage profile improvement and incremental power quality supply.

2. Economical: reducing transmission and distribution operating cost and decreasing the electricity price generating power to save peak periods.

3. Environmental: covering the reductions in emission of greenhouse gases and also sound pollutions.

These benefits depend on the characteristics of DG units such as photovoltaic or wind system, characteristics of the loads and network configuration. Originally, networks were designed for unidirectional power flows, from higher voltages to lower voltages, rather than to accommodate generators. Accordingly, the erroneous location may have different consequences like increase system losses, reverse power flows or increments in line losses and voltage rise. For these reasons, it is necessary to avoid these failures optimizing the DG units size, locate and configuration.

Design network and optimization aim at providing efficiency and security guaranteeing all the desirable benefits of the introduction of generators. Therefore, these procedures must be analyzed and tested previously. For instance, Gupta (2016) states that the intermittent and fluctuating nature of wind power injected into the grid causes variations in bus voltages and line power flows of transmission systems. Hence, for the prosperous integration of wind generation in the grid, these variations need to be analyzed, estimated and quantified. In general, successful operations of power system with generators are subject to power system planning and contingency analysis with uncertainty. In such way, the *Uncertainty Quantification* (UQ) measures the error and uncertainties, being another relevant application. Related to this application, network analysis from the probabilistic point of view is another tool for handling uncertainty in performance assessment and risk calculations.

1.1.1 Classical problem statement

The power flow problem computes the flow of the electrical power in a power system determining its state. The power flow equations are a system of nonlinear equations modeling the relation between powers and voltages. The basic formulation of these

very well-known equations was originally illustrated in G.W.Stagg and A.H.El-Abiad (1968); Elgerd (1972); Wasley and Shlash (1974). The main object of the power flow solution was described by Wasley and Shlash (1974) as: to obtain the individual phase voltages at all nodes or buses in the network corresponding to specified system conditions.

An electric network can be characterized by:

- The topology of the grid, described by the number of lines, the number of buses and their connectivity.

- The admittance matrix $\mathbf{Y} \in \mathbb{C}^{n \times n}$ including the material characteristics of the devices conforming the grid (wires and other system devices like transformers). Note that n is the number of degrees of freedom and in the case of a three-phase systems, n is tripled. The material characteristics of wires for each line allows to build primitive admittance matrices. Assembling these matrices, the global admittance matrix $\mathbf{Y}$ is obtained. Generally, the sparsity of $\mathbf{Y}$ is associated with the lines-buses connectivity. The unit of each component of this matrix is the siemens (S).

- The complex power source vector $S \in \mathbb{C}^n$, describing the power supplied and/or extracted at each phase of each node. Its unit is the volt-ampere (VA) and it is defined at each node from the demand value and the power factor.

- The voltage vector $V \in \mathbb{C}^n$ measured in volt (V) and the injected current vector $I \in \mathbb{C}^n$ whose unit is the ampere (A).

- The vector $I_0 \in \mathbb{C}^n$ accounting for the current originated by the slack node. Introducing a slack node is necessary to guarantee the solvability of the problem. The complex voltage in this node is known, and therefore it is not reevaluated. This is equivalent to reduce the dimension of the original admittance matrix by deleting the slack bus row and column, see Dimitrovski and Tomsovic (2004); Grainer and Stevenson (2008); S. M. L. Kabir and Alam (2014).

The input data characterizing the power flow problem is the complex vector S and the admittance matrix $\mathbf{Y}$. Consequently, the unknowns of the problem are the voltages and nodal intensities collecting in vectors of n components V and I. At each bus, the nonlinear relation between the voltage, the current and the complex power is provided by the following equation:

$$S = V \odot I^{*}, \tag{1.1}$$

where I^{*} denotes the complex conjugate of the current vector I, and the symbol $\odot$ denotes the Hadamard product of vectors (component-wise product). Furthermore, Kirchhoff's law leads to the following algebraic system of equations:

$$\mathbf{Y}V = I + I_0, \tag{1.2}$$

which, using (1.1) results in a nonlinear algebraic system of equations for the unknown V:

$$\mathbf{Y}V = S^{*} \oslash V^{*} + I_0 = I_{\text{bus}}(V), \tag{1.3}$$

where the symbol $\oslash$ denotes the component-wise quotient between vectors. These governing equations are a nonlinear, specifically quadratic, complex system of n equations and n unknowns. Note that these equations are also seen as $V^{*} \odot (\mathbf{Y}V - I_0) = S^{*}$.

The admittance matrix and power source in Cartesian form are $\mathbf{Y} = \Re(\mathbf{Y}) + i\Im(\mathbf{Y})$ and $S = \Re(S) + i\Im(S) = P + iQ$ respectively where $\Re(\cdot)$ and $\Im(\cdot)$ stand for the real and the imaginary part of the matrix or vector and i is the imaginary unit. Hence, the vector of voltages reads $V = \Re(V) + i\Im(V)$. The notation $V = V^{\text{Re}} + iV^{\text{Im}}$ is also adopted, to shorten some expressions in the following. Moreover, the vector V is also expressed in polar form (module-argument form, α_l being the argument of V_l), such that each component reads $V_l = |V_l| \left[\cos(\alpha_l) + i\sin(\alpha_l) \right]$, for $l = 1, \ldots, n$, now the power flow equations (1.3) read as,

$$\begin{cases} P_l = \displaystyle\sum_{k=1}^{n} |V_l||V_k| [\mathbf{Y}_{lk}^{\text{Re}} \cos(\alpha_l - \alpha_k) + \mathbf{Y}_{lk}^{\text{Im}} \sin(\alpha_l - \alpha_k)] - P_0 \\ Q_l = \displaystyle\sum_{k=1}^{n} |V_l||V_k| [-\mathbf{Y}_{lk}^{\text{Im}} \cos(\alpha_l - \alpha_k) + \mathbf{Y}_{lk}^{\text{Re}} \sin(\alpha_l - \alpha_k)] - Q_0 \end{cases}, \tag{1.4}$$

Type of bus	$|V|$	α	P	Q
Slack	datum	datum	unknown	unknown
PQ	unknown	unknown	datum	datum
PV	datum	unknown	datum	unknown

Table 1.1: Classification of the buses in an electrical network

where the module and argument of the slack node are known, thus the term V^*I_0 is also known and from now on it is called $S_0 = P_0 + iQ_0$. Furthermore, $\theta_{lk} = \alpha_l - \alpha_k$ is defined as the difference in voltage angle between the l-th and k-th buses, hence the system of equations now is,

$$
\begin{cases}
P_l = \sum\limits_{k=1}^{n} |V_l||V_k|[\mathbf{Y}_{lk}^{\mathrm{Re}} \cos(\theta_{lk}) + \mathbf{Y}_{lk}^{\mathrm{Im}} \sin(\theta_{lk})] - P_0 \\
Q_l = \sum\limits_{k=1}^{n} |V_l||V_k|[-\mathbf{Y}_{lk}^{\mathrm{Im}} \cos(\theta_{lk}) + \mathbf{Y}_{lk}^{\mathrm{Re}} \sin(\theta_{lk})] - Q_0
\end{cases}
. \quad (1.5)
$$

This is a nonlinear real system of $2n$ equations and $2n$ unknowns. For each node in the network, that is $l = 1, \ldots, n$, the active power P_l and the reactive power Q_l are known, while the $|V_l|$ and α_l are unknown variables.

Equations (1.3) and (1.5) are equivalent, the choice of one rather than the other depends on the type of nodes in the network and the available data. In a network, different types of nodes are considered, see table 1.1. If there are PQ nodes, where the values of P and Q are known, both equations are used. However, in the case of the PV nodes where just P and $|V|$ are given, equation (1.5) is more suitable.

1.1.2 Parametric problem statement

Solving the power flow problem provides the state of the network for a given configuration of the materials and loads. In practice, analyzing an electric grid requires solving the same problem with a large number of configurations. Describing these scenarios is easily done introducing parameters defining the concept of Parametric Power Flow problem. The novelty of this methodology is the fact that diverse parameters of the power flow problem are now considered as variables rather than input quantities. Typical examples of parameters are the location and nominal

power, denoted by q and r, of some distributed generator or just generator, and the time t that modulates the power S.

The general form of the Parametric Power Flow problem is described by taking the voltage V, the power source S and the current I no longer vectors of nodal values but functions of the problems parameters, for instance $S(q, r, t)$. Consequently, the solution of equation (1.3) also depends on these parameters, namely $V(q, r, t)$. Thus, the equation reads as:

$$\mathbf{Y}V(q, r, t) = S(q, r, t)^* \oslash V(q, r, t)^* + I_0 \,. \tag{1.6}$$

In practice, this brings the problem from a simple nonlinear algebraic equation in $\mathbb{C}^n$ into a multidimensional setup: formally, V is now in $[L_2(I_q) \times L_2(I_r) \times L_2(I_t)]^n$, that is, each component of V is a function taking values for $(q, r, t) \in I_q \times I_r \times I_t$ where I_q, I_r and I_t are intervals in $\mathbb{R}$. Further details are shown in chapter 3.

1.2 State of the art in power flow solvers

In this section a brief state of the art of the most significant and classical methods for solving the power flow equations is presented.

1.2.1 Y-matrix and Z-matrix methods

Over the last eighty years, numerous methods have been proposed in order to solve the power flow equation. The first practical technique was described by Ward and Hale (1956) in the fifties. During the same decade, methods called Y-matrix also appeared, see Glimn and Stagg (1957); Brown and Tinney (1957). These methods are a straightforward fixed-point iteration from (1.3). Thus, an approximated value $V^{[\gamma]}$ is used to compute the next iteration $V^{[\gamma+1]}$ such that

$$\mathbf{Y}V^{[\gamma+1]} = S^* \oslash V^{[\gamma]^*} + I_0 \,, \tag{1.7}$$

by solving, in each iterative step, a linear system of equations with matrix $\mathbf{Y}$. These methods are consistent and were successfully employed in many examples but they do not guarantee converge. Actually, they fail in converging for many examples.

This difficulty was overcame through the introduction of the Z-matrix methods, for instance, Hale and Goodrich (1959); Gupta and Humphrey Davies (1961); Brameller and Denmead (1962); Brown et al. (1960, 1963, 1968). The main idea of these methods is to invert the system admittance matrix $\mathbf{Y}$ obtaining the impedance matrix $\mathbf{Z}$ using a technique based on Kron's concept of network tearing using the system data. This procedure is faster than the standard matrix inversion and avoids the necessity of complete re-inversion when such minor changes in the network are required. These changes are made directly to the inverted matrix, thus the computation time involved for such modifications is a small fraction of that needed for a complete matrix inversion, more details are given in Brameller and Denmead (1962). Besides, when it comes to networks under fault conditions, the Y-matrix approach requires an iterative solution of the entire network for each fault condition. However, one of the distinct advantages of this method is that, once the matrix is formed, all fault calculations may be obtained with a minimum of arithmetic operations involving only related portions of the matrix, as is shown in Brown et al. (1960).

Many techniques have been proposed to modify the traditional Z-matrix building algorithms. Among those methods, the Gauss implicit Z-matrix method is the most generally used method, see Ou and Lin (2009). Furthermore, some novel studies about the convergence analysis of this method including PV nodes and DG have emerged in the current decade, for example, He et al. (2012); Chiang et al. (2014); Zhao et al. (2016); Yang (2016).

1.2.2 Gauss-Seidel and Newton-Raphson methods

Around the sixties, the notable Gauss-Seidel (GS) and Newton-Raphson (NR) methods for power flow calculations were also presented by Glimn and Stagg (1957); Taylor and Treece (1967) and Ness (1959); Tinney and Hart (1967) respectively. Both are iterative methods and their equations are:

- Gauss-Seidel

  At iteration γ, the solution $V^{[\gamma+1]}$ is obtained solving the below system of

equations:

$$\mathbf{Y}_L V^{[\gamma+1]} = S^* \oslash V^{[\gamma]*} - \mathbf{Y}_U V^{[\gamma]} + I_0 \,, \tag{1.8}$$

being $\mathbf{Y}_U$ the upper triangular part and $\mathbf{Y}_L$ the lower triangular part of $\mathbf{Y}$ plus its diagonal. In the literature, Gauss-Seidel method is also classified as an Y-matrix method since the calculation of the solution depends on the admittance matrix.

- Newton-Raphson

Before defining NR equations, it is necessary to consider the Cartesian representation of the vectors and matrices involved in the power flow equations because the conjugate function is not a holomorphic function and complex derivation is not formally defined. By introducing the real and imaginary parts of voltages, currents, powers and admittances as separate variables, the following quantities are defined:

$$\hat{\mathbf{Y}} = \begin{bmatrix} \mathbf{Y}^{\mathrm{Re}} & -\mathbf{Y}^{\mathrm{Im}} \\ \mathbf{Y}^{\mathrm{Im}} & \mathbf{Y}^{\mathrm{Re}} \end{bmatrix} \quad , \quad \hat{V} = \begin{bmatrix} V^{\mathrm{Re}} \\ V^{\mathrm{Im}} \end{bmatrix},$$

$$\hat{I}_{\mathrm{bus}} = \begin{bmatrix} I_{\mathrm{bus}}^{\mathrm{Re}} \\ I_{\mathrm{bus}}^{\mathrm{Im}} \end{bmatrix} = \begin{bmatrix} I_0^{\mathrm{Re}} \\ I_0^{\mathrm{Im}} \end{bmatrix} + \begin{bmatrix} \left(P \odot V^{\mathrm{Re}} + Q \odot V^{\mathrm{Im}}\right) \oslash \left(V^{\mathrm{Re}} \odot V^{\mathrm{Re}} + V^{\mathrm{Im}} \odot V^{\mathrm{Im}}\right) \\ \left(P \odot V^{\mathrm{Im}} - Q \odot V^{\mathrm{Re}}\right) \oslash \left(V^{\mathrm{Re}} \odot V^{\mathrm{Re}} + V^{\mathrm{Im}} \odot V^{\mathrm{Im}}\right) \end{bmatrix}, \tag{1.9}$$

where $\hat{\mathbf{Y}} \in \mathbb{R}^{2n \times 2n}$ and $\hat{V}, \hat{I}_{\mathrm{bus}} \in \mathbb{R}^{2n}$ are duplicating dimensions of the complex matrices and vectors. The power flow equations can be written now as:

$$\hat{\mathbf{Y}}\hat{V} = \hat{I}_{\mathrm{bus}}(\hat{V})\,. \tag{1.10}$$

Newton-Raphson method consists in iteratively updating $\hat{V}$ with an increment $\Delta\hat{V}$, that is $\hat{V}^{[\gamma+1]} = \hat{V}^{[\gamma]} + \Delta\hat{V}$. In the following the dependence on γ is eliminated in the superscript to simplify notation. Thus, the resulting algorithm reads

$$\hat{\mathbf{J}}\Delta\hat{V} = -\hat{\mathbf{Y}}\hat{V} + \hat{I}_{\mathrm{bus}}(\hat{V})\,, \tag{1.11}$$

where the Jacobian $\hat{\mathbf{J}}$ is the partial derivative of the right-hand-side of (1.11) (the residual) with respect to $\hat{V}$, that is

$$\hat{\mathbf{J}} = \hat{\mathbf{Y}} - \begin{bmatrix} \hat{\mathbf{J}}_{11} & \hat{\mathbf{J}}_{12} \\ \hat{\mathbf{J}}_{21} & \hat{\mathbf{J}}_{22} \end{bmatrix} \tag{1.12}$$

where $\hat{\mathbf{J}}_{kl}$ for $k, l = 1, 2$ are diagonal matrices in $\mathbb{R}^{n \times n}$ (component l of $\hat{I}_{\text{bus}}(\hat{V})$ depends only on component l of $\hat{V}$, see (1.9)) such that

$$\hat{\mathbf{J}}_{11} = \frac{\partial I_{\text{bus}}^{\text{Re}}}{\partial V^{\text{Re}}}, \quad \hat{\mathbf{J}}_{12} = \frac{\partial I_{\text{bus}}^{\text{Re}}}{\partial V^{\text{Im}}}, \quad \hat{\mathbf{J}}_{21} = \frac{\partial I_{\text{bus}}^{\text{Im}}}{\partial V^{\text{Re}}} \quad \text{and} \quad \hat{\mathbf{J}}_{22} = \frac{\partial I_{\text{bus}}^{\text{Im}}}{\partial V^{\text{Im}}}.$$

Particularly,

$$\left[\hat{\mathbf{J}}_{11} \right]_{ll} = \frac{P_l(|V_l|^2 - V_l^{\text{Re}}) + 2Q_l V_l^{\text{Re}} V_l^{\text{Im}}}{|V_l|^4},$$

$$\left[\hat{\mathbf{J}}_{12} \right]_{ll} = \frac{Q_l |V_l|^2 - P_l V_l^{\text{Re}} + 2Q_l (V_l^{\text{Im}})^2}{|V_l|^4},$$

$$\left[\hat{\mathbf{J}}_{21} \right]_{ll} = \frac{-Q_l |V_l|^2 - P_l V_l^{\text{Im}} - 2Q_l (V_l^{\text{Re}})^2}{|V_l|^4},$$

$$\left[\hat{\mathbf{J}}_{22} \right]_{ll} = \frac{P_l(|V_l|^2 - V_l^{\text{Im}} - 2Q_l V_l^{\text{Re}} V_l^{\text{Im}}}{|V_l|^4},$$

for $l = 1, \ldots n$.

Both GS and NR methods enjoy of low memory usage and competent ratios of convergence, better in the case of NR which has an optimal quadratic rate, although the computational time increases because of the assembling of the Jacobian matrix at every single iteration. For that reason, diverse approaches have appeared over the years.

In the case of NR methods, it is worthy mentioning different modifications of the original problem introducing decomposition of the Jacobian matrix as is illustrated in references Cheng (1997); Garcia et al. (2000), reformulating the original equations to accommodate the introduction of generation devices like in Li et al. (2011); Sameni et al. (2012) or decreasing the computational time thorough the application of third-, fourth- and fifth-order Newton-like methods as is discussed in Derakhshandeh and Pourbagher (2016).

Similarly, the GS approach has been improved by Teng (2002); Maffei et al. (2015) using block version of its initial equations or by Yang (2016) combining with the implicit Z-matrix bus method for unbalanced distribution networks. The initial references of the three type of methods (Z-matrix bus, GS and NR) are shown in the reviews Laughton and Davies (1964); Stott (1974) while an extensively recent study of them can also be found Gómez-Expósito et al. (2008).

Additionally to the improved methods mentioned above, since NR methods emerged, a great effort has been made to overcome the problem of updating the Jacobian when the size of the test systems was considerable large. Consequently, a variety of formulations have been developed. These include:

- Newton-Krylov methods consisting in solving the Jacobian equation partially or combined with a Krylov subspace method as is shown in Yi-Shan and Hsiao-Dong (2010); Idema et al. (2010, 2012, 2013).

- Jacobian-free Newton-Krylov methods (JFNK) where a Krylov subspace is built up for correcting the Jacobian in NR strategy, see reference Knoll and Keyes (2004).

- Jacobian-free methods that analyze approaches as partial Jacobian update variants and inexact solutions, for instance De Leon and Semlyen (2002); Chen and Shen (2006).

Generally, despite the fact that these strategies does not include the whole Jacobian, the quadratic convergence is still granted. Apart from these approaches, the most popular is Fast Decoupled Load Flow method (FDLF) presented by Stott and Alsac (1974). It consists, mainly, in approximating the Jacobian using factorization, preconditioners or information obtained from the network in order to solve the Jacobian system quickly. In such a way, the matrices are kept constant hence NR method is reduced to a sequence of decoupled linear problems for the voltage magnitude and phase angle.

The application of the NR method for the equation (1.5) results in a nonlinear real system of $2n$ equations with $2n$ unknowns, the vectors $|V_l|$ and α_l for $l = 1, \ldots, n$. The equations read as:

$$\mathbf{J} \begin{bmatrix} \Delta\alpha \\ \Delta|V| \end{bmatrix} = - \begin{bmatrix} P_{res} \\ Q_{res} \end{bmatrix}, \tag{1.13}$$

where P_{res} and Q_{res} are the residuals of the equation and the Jacobian is

$$\mathbf{J} = \begin{bmatrix} \mathbf{J}_{11} & \mathbf{J}_{12} \\ \mathbf{J}_{21} & \mathbf{J}_{22} \end{bmatrix} = \begin{bmatrix} \frac{\partial P_{res}}{\partial\alpha} & \frac{\partial P_{res}}{\partial|V|} \\ \frac{\partial Q_{res}}{\partial\alpha} & \frac{\partial Q_{res}}{\partial|V|} \end{bmatrix}. \tag{1.14}$$

11

Specifically,

$$
[\mathbf{J}_{11}]_{lk} = \begin{cases} |V_l||V_k|[\mathbf{Y}^{\mathrm{Re}}_{lk}\sin(\theta_{lk}) - \mathbf{Y}^{\mathrm{Im}}_{lk}\cos(\theta_{lk})], & k \neq l \\ -\sum\limits_{m \neq l}^{n} |V_l||V_m|[\mathbf{Y}^{\mathrm{Re}}_{lm}\sin(\theta_{lm}) - \mathbf{Y}^{\mathrm{Im}}_{lm}\cos(\theta_{lm})], & k = l \end{cases}
$$

$$
[\mathbf{J}_{12}]_{lk} = \begin{cases} |V_l|[\mathbf{Y}^{\mathrm{Re}}_{lk}\cos(\theta_{lk}) + \mathbf{Y}^{\mathrm{Im}}_{lk}\sin(\theta_{lk})], & k \neq l \\ \sum\limits_{m \neq l}^{n} |V_m|[\mathbf{Y}^{\mathrm{Re}}_{lm}\cos(\theta_{lm}) + \mathbf{Y}^{\mathrm{Im}}_{lm}\sin(\theta_{lm})] + 2\mathbf{Y}^{\mathrm{Re}}_{ll}|V_l|, & k = l \end{cases}
$$

$$
[\mathbf{J}_{21}]_{lk} = \begin{cases} -|V_l||V_k|[\mathbf{Y}^{\mathrm{Re}}_{lk}\cos(\theta_{lk}) + \mathbf{Y}^{\mathrm{Im}}_{lk}\sin(\theta_{lk})], & k \neq l \\ -\sum\limits_{m \neq l}^{n} |V_l||V_m|[\mathbf{Y}^{\mathrm{Re}}_{lm}\cos(\theta_{lm}) + \mathbf{Y}^{\mathrm{Im}}_{lm}\sin(\theta_{lm})], & k = l \end{cases}
$$

$$
[\mathbf{J}_{22}]_{lk} = \begin{cases} |V_l|[\mathbf{Y}^{\mathrm{Re}}_{lk}\sin(\theta_{lk}) - \mathbf{Y}^{\mathrm{Im}}_{lk}\cos(\theta_{lk})], & k \neq l \\ \sum\limits_{m \neq l}^{n} |V_m|[\mathbf{Y}^{\mathrm{Re}}_{lm}\sin(\theta_{lm}) - \mathbf{Y}^{\mathrm{Im}}_{lm}\cos(\theta_{lm})] - 2\mathbf{Y}^{\mathrm{Im}}_{ll}|V_l|, & k = l \end{cases}
$$

for $l, k, m = 1, \ldots n$.

Taking into account that for $k \neq l$,

$$
[\mathbf{J}_{11}]_{lk} = |V_k|\,[\mathbf{J}_{22}]_{lk} \quad \text{and} \quad [\mathbf{J}_{21}]_{lk} = -|V_k|\,[\mathbf{J}_{12}]_{lk}\,,
$$

the algorithm is rewritten as

$$
\tilde{\mathbf{J}} \begin{bmatrix} \Delta\alpha \\ \frac{\Delta|V|}{|V|} \end{bmatrix} = - \begin{bmatrix} P_{res} \\ Q_{res} \end{bmatrix}, \tag{1.15}
$$

where

$$
\tilde{\mathbf{J}} = \begin{bmatrix} \tilde{\mathbf{J}}_{11} & \tilde{\mathbf{J}}_{12} \\ \tilde{\mathbf{J}}_{21} & \tilde{\mathbf{J}}_{22} \end{bmatrix}, \quad \text{explicitly,} \tag{1.16}
$$

$$
\left[\tilde{\mathbf{J}}_{11}\right]_{lk} = \begin{cases} [\mathbf{J}_{11}]_{lk}, & k \neq l \\ -Q_l + \mathbf{Y}_{ll}^{\mathrm{Im}}|V_l|^2, & k = l \end{cases}
$$

$$
\left[\tilde{\mathbf{J}}_{12}\right]_{lk} = \begin{cases} -[\mathbf{J}_{21}]_{lk}, & k \neq l \\ P_l + \mathbf{Y}_{ll}^{\mathrm{Re}}|V_l|^2, & k = l \end{cases}
$$

$$
\left[\tilde{\mathbf{J}}_{21}\right]_{lk} = \begin{cases} [\mathbf{J}_{21}]_{lk}, & k \neq l \\ P_l - \mathbf{Y}_{ll}^{\mathrm{Re}}|V_l|^2, & k = l \end{cases}
$$

$$
\left[\tilde{\mathbf{J}}_{22}\right]_{lk} = \begin{cases} [\mathbf{J}_{11}]_{lk}, & k \neq l \\ Q_l - \mathbf{Y}_{ll}^{\mathrm{Im}}|V_l|^2, & k = l \end{cases}
$$

for $l, k = 1, \ldots n$.

As mentioned before, FDLF method is a variation of Newton-Raphson method. It is achieved by only inverting the Jacobian matrix once it is simplified assuming the below statements:

- It is observed that real power P was barely influenced by changes in voltage magnitude V, thus, all the derivative are considered to be zero. Similarly, Q was relatively insensitive to changes in α. This means that $\left[\tilde{\mathbf{J}}_{12}\right]_{lk} = \left[\tilde{\mathbf{J}}_{21}\right]_{lk} = 0$.

- The difference between angles $\theta_{lk} = \alpha_l - \alpha_k$ is usually small, $\cos(\theta_{lk})$ is taken by 1 and $\sin(\theta_{lk})$ as 0, for $l, k = 1, \ldots, n$.

- The magnitude of some voltages is also assumed to be 1.

Applying these assumptions to equation (1.15) and dividing equations by $|V_k|$ in both sides, the system to be solved is:

$$
\begin{bmatrix} \mathbf{U}' & 0 \\ 0 & \mathbf{U}'' \end{bmatrix} \begin{bmatrix} \Delta\alpha \\ \Delta|V| \end{bmatrix} = - \begin{bmatrix} \frac{P_{res}}{|V|} \\ \frac{Q_{res}}{|V|} \end{bmatrix}, \tag{1.17}
$$

where $\mathbf{U}' = -\mathbf{Y}^{\mathrm{Im}}$ and $\mathbf{U}''$ is built taking the elements of $-\mathbf{Y}^{\mathrm{Im}}$ that correspond to the PV nodes.

Later, FDLF has been developed for unbalanced radial distribution system in reference Zimmerman and Chiang (1995), for three phase distribution networks

in Lin and Teng (2000) and for transmission system using an optimal multiplier in Bijwe et al. (2009). From the mathematical point of view, some authors as in references Wu (1977); Monticelli et al. (1990) have addressed its theoretical background.

1.2.3 Holomorphic Embedding Load Flow methods

Besides this deficiency in terms of the Jacobian assembly, the traditional power flow methods suffer from the fact that there is no guarantee of convergence to the physical or high voltage solution. There exists the possibility that some iterative solvers converge to spurious non-operative solutions or simply fail to converge in a number of cases. The reason behind that behavior could be either the dependency between the initial estimate and the final approximation, see Stott (1971); Iwamoto and Tamura (1981); Schaffer and Tylavsky (1988) or the system operability making the algorithm not being able to find the operative solution. This might happen when the value of network parameters move outside of the standard operating range due to contingencies as is discussed in Tripathy et al. (1982). In the case of NR methods, it has been demonstrated by Thorp and Naqavi (1997); Thorp et al. (1990) that the nature of the power flow solution are fractal.

Overcoming both adversities was a challenge which motivated numerous authors. On one hand, methods based on truncated Taylor expansions in a polar or Cartesian coordinate form were proposed by Sauer (1981); Xu et al. (1998); De Souza et al. (2007). A suitable one is the second order load flow technique presented by Sachdev and Medicherla (1977) which requires less iterations and have better convergence characteristics than conventional NR technique. On the other hand, the recent Holomorphic Embedding Load Flow Method (HELM) based on analytical continuation illustrated in Trias (2012, 2015) was introduced. It is based on a technique that extends the domain of analytic functions relying on Padé approximants. The method extends the voltage variables into analytic functions in the complex plane providing a non-iterative procedure for constructing the complex power series of voltages.

If a simple two buses system is considered, the Z-matrix method applied to the

scalar version of equation (1.3) reads as:

$$V = \mathbf{Z}[S^* \oslash V^*] + V_0, \tag{1.18}$$

where $V_0 = \mathbf{Z}I_0$. Rewriting equation (1.18) using the notation $U = V/V_0$, the following equation is obtained,

$$U = 1 + \frac{\sigma}{U^*}, \tag{1.19}$$

where $\sigma = \frac{\mathbf{Z}S^*}{|V_0|^2}$. This above equation (1.19) can be seen as a continued fraction approximation of the solution,

$$U = 1 + \cfrac{\sigma}{1 + \cfrac{\sigma^*}{1 + \cfrac{\sigma}{1 + \dots}}}. \tag{1.20}$$

As mentioned above, the Holomorphic Embedding method is based on analytical continuation and a continued fraction is defined. In this particular case, (1.20) is also seen as the same continued fraction resulting from the application of the Holomorphic Embedding method to the same simple system, see Trias (2012). This continued fraction suggests the use of Padé approximants and its convergents corresponds to the application of the fixed point equation (1.18). Therefore, the iterative solutions found with the Z-matrix method, coincide with the ones found with the HELM as the number of coefficients of the Padé approximant is increased.

In a general case, Holomorphic Embedding changes σ by $s\sigma$ in equation (1.19) and defines a system of two equations:

$$\begin{cases} F(s) = 1 + \frac{s\sigma}{\bar{F}(s)} \\ \bar{F}(s) = 1 + \frac{s\sigma^*}{F(s)} \end{cases} \tag{1.21}$$

with $\bar{F}(s) = F^*(s^*)$. In this way, the functions $F(s)$ and $\bar{F}(s)$ are holomorphic. Note that $F(s = 1)$ recovers the solution U of equation (1.19). The procedure is to consider the power series expansion of $F(s)$ about $s = 0$ since $F(s)$ and $\bar{F}(s)$ are holomorphic. The embedded equations (1.21) allow to seek the coefficients of the power series as the solution of a succession of linear systems. Particularly, the

15

derivates of the function $F(s)$ evaluated in $s = 0$ are:

$$F(0) = 1$$
$$F^{(1)}(0) = \sigma$$
$$F^{(2)}(0) = -2\sigma\sigma^*$$
$$F^{(3)}(0) = 6(\sigma^2\sigma^* + \sigma(\sigma^*)^2)$$
$$F^{(4)}(0) = -72(\sigma^2(\sigma^*)^2) - 24(\sigma(\sigma^*)^3 + \sigma^3\sigma^*) \qquad (1.22)$$
$$F^{(5)}(0) = -60(\sigma^2\sigma^*) + 600(\sigma^3(\sigma^*)^2) + 720(\sigma^2(\sigma^*)^3)+$$
$$+ 120(\sigma^4\sigma^*)$$
$$\ldots$$
$$F^{(l)}(0) = \ldots$$

Using these derivates, the Padé approximation $P_{ap}(s)$ is computed and the solution $U = F(s = 1)$ is approximated by $P_{ap}(s = 1)$, that is to say, using Padé approximants, the solution at $s = 1$ can be constructed.

The Padé approximants are a particular type of rational approximation for power series. They have been used extensively because their convergence has been known to be much better than the convergence of power series. For instance, these approximants are usually superior to Taylor series when the functions to be approximated are complex with singularities (poles), because the use of rational functions allows them to be well-represented. In the case of the power flow equation, Stahl's results reveal that Padé approximants are suitable for analytic continuation. In fact, these results confer the method very strong additional guarantees: if the approximants converge at $s = 1$, the result is guaranteed to be the analytic continuation of the high voltage branch at $s = 1$; conversely, if the Padé approximants do not converge at $s = 1$ then it is guaranteed that there is no solution (that is, the system is beyond voltage collapse). More details are given in Trias (2012).

After this initial proposal, an extension from alternating current to direct current-based systems has been presented by Trias and Marn (2016). Other authors have also explored this approach, for instance Subramanian et al. (2013); Rao et al. (2015). The main advantage of this sort of strategies is its reliability finding a stable solution for any set of power flow equations. If the starting solu-

tion is an operative one, there is guarantee that the algorithm converges fast to a solution which is in the branch of the operative solutions.

1.2.4   Parametric solvers for probabilistic and optimization problems

All the solvers described in the above sections are related to the resolution of the algebraic version of the power flow problem. However, there exists a category where a parametric representation of the problem described in section 1.1.2 is involved. Two particular cases are the Probabilistic Load Flow (PLF) and the Optimal Power Flow (OPF) where a power flow solver is called as many times as particular system configurations need to be evaluated.

The concept of Probabilistic Load Flow was first proposed in the seventies by Borkowska (1974) taking into consideration uncertainty of the nodes data. Another historical reference where the definition of the Stochastic Load Flow appeared for the first time is Dopazo et al. (1975). Since then, many papers have been published. In review Li and Zhang (2009), it is claimed that Probabilistic Load Flow methods can be divided into three categories:

- Simulation methods: an example is discussed in Fang et al. (2014), Monte Carlo method which simulates power flow calculations based on deterministic samples. It is well-known as a flexible and robust method but also as time-consuming because of the need of repeating calculations.

- Analytical methods: based on convolution techniques or cumulant method are claimed to be more effective computationally, as references Allan and Al-Shakarchi (1977) and Zhang and Lee (2004) state.

- Approximate methods: the most common are the method of moments and the point estimate method, see for example Su (2005).

Apart from this classification, another remarkable methods for solving the probabilistic load problems using techniques as combinatorics, Hybrid Latin Hypercube Sampling and Cholesky Decomposition, polynomial normal transformation and Quasi Monte Carlo Simulation have been analyzed by Rau and Necsulescu (1990),

Yu et al. (2009) and Fang et al. (2014). Over these decades, PLF has been applied to different phenomena as:

- Branch outages, photo-voltaic and wind power through distributed generators

- Wind farm power generation and energy storage

- Planning and design analysis of distribution system

- Optimization for reaching systems reliability

The Optimal Power Flow solution was presented in the sixties by Dommel and Tinney (1968). The idea of the classical OPF is a power flow problem in which certain controllable variables are to be adjusted to minimize an objective function such as the cost of active power generation or losses, see Sun et al. (1984).

Particularly, Georgilakis and Hatziargyriou (2013) defines the optimal distributed generation placement problem (ODGP) claiming that it provides the best locations and sizes of DGs to optimize electrical distribution networks. When ODGP is solved, the objective function can be single or multi-objective. On one hand, the main single-objective functions are: minimization of energy losses, minimization of system average interruption duration index (SAIDI), minimization of cost, etc. On the other hand, in Shareef and Kumar (2014), ODGP multi-objective formulations are classified as multi-objective function with weights, goal multi-objective index and multi-objective formulation considering more than one often contrasting objectives. The aim in this thesis is to minimize the annual losses based on the optimal allocation of DG units. New methodologies have been proposed with the same objective, for instance Martinez and Guerra (2012); Atwa and El-Saadany (2011); Griffin, Tomsovic, and Law (Griffin et al.).

Improved versions of the OPF as is described in Yong and Lasseter (2000) emerged later on and also the number of applications increase notably. Some of them are based on the same ideas as the Probabilistic Load Flow applications, other are economic and pollution dispatch or maximum interchange, however one stands out the optimization problem in presence of distributed generation, mainly wind farms or turbines. Diverse strategies has been addressed in order to solve

this particular application as can be seen in Shrivastava et al. (2012) using the following techniques:

- Analytical: zero point analysis focusing on the point of the feeder where the power flow is zero or the $\frac{2}{3}$ ruled used for capacitor placement in radial distribution system are examples of this category, see Willis (2000).

- Exact formulas: references Acharya et al. (2006); Rau and Wan (1994) present exact methods such as the exact loss formula or the gradient method.

- Evolutionary: diverse strategies belong to this category, such as Monte Carlo method, Hereford Ranch Algorithm (HRA) and Genetic Algorithm (GA) based on genetic concepts, Fuzzy System algorithm built using the fuzzy set theory, Ant Colony optimization specially designed to deal with large search spaces since it dynamically creates the search routes such as real ants do, Tabu Search that explores the whole solution space randomly based on the local search and Particle Swarm optimization inspired by social behavior of bird flocking among others. Details about these methods can be found in references El-Khattam et al. (2003), Kim, Park, Park, and Singh (Kim et al.); Mithulananthan et al. (2004), Gandomkar et al. (2005),Kim et al. (2002), Favuzza et al. (2007),Nara et al. (2001),Abido (2002).

The optimal placement of distributed generators problem is solved using the probabilistic approaches mentioned above or the deterministic ones. Further information about methods and techniques proposed for solving OPF and PLF are shown in Huneault and Galiana (1991); Frank et al. (2012); Chen et al. (2008).

1.3 Objectives

The general objective of this thesis is to propose improved methods for solving both versions (algebraic and parametric) of the power flow problem. These methods are aimed to guarantee a priori the accuracy of the obtained solutions and provide computationally efficient simulations. The present thesis aims at contributing in the research field of reduced order techniques applied to electric power systems by proposing alternative methods able to control the accuracy of the solution.

19

1. INTRODUCTION

These are focused on the resolution of the power flow problem overcoming classical adversities in this area, and also including error indicators that measure the quality of the approximation while it is computed. In order to meet this main objective, the work was focused on achieving the following specific goals:

1. *Application of Reduced Order Model techniques*

   The idea of applying these approaches is the possibility of making real-time decisions in terms of controlling the state of the networks. This requires network simulations under different configurations in order to consider all the potential outputs. Initially, the Reduced Basis (RB) method and the Proper Orthogonal Decomposition (POD) were suitable. However, the resolution of optimization problems involves parametrized solutions, hence the application of the Proper Generalized Decomposition (PGD) method emerged naturally.

2. *Application of the error assessment procedure to the proposed power flow solvers*

   Once the computational cost of each simulation of the power flow problem is assured to be low, the focal point is to guarantee the quality of the computed solution. The standard procedure of the error assessment applied to many other fields was believed to be convenient. Thus, the challenge is to control the process of building the solution in terms of accuracy taking into account a specific quantity of interest. As a result, the precision of approximated solutions would be controlled by truncating the number of terms in the sum of the PGD approximation.

3. *Introduction of an effective solver for the power flow problem able to circumvent classical difficulties*

   In order to carry out the objectives above, the fundamental step is to introduce a new method able to overcome adversities associated with standard power flow solvers such as guarantee of convergence or affordable computational time at each simulation without the calculation of the Jacobian matrices.

The remainder of this document includes four additional chapters 2, 3, 4 and 5 and the papers associated with the contributions of this thesis.

In chapter 2, the proposed solver for the algebraic power flow equation is presented while chapter 3 details the extension of this method combined with the Proper Generalized technique to the parametric version of the problem. Chapter 4 introduces the error assessment in the context of the power flow problem and finally in chapter 5 an overview of the main contributions, the conclusions and future research are described.

The appendix contains the papers where the contributions are discussed in detail. Paper A describes the family of iterative solvers for power systems obtained applying the ASDM to the power flow equation. Papers B and C present an approach for reduced order solutions of the parametrized power flow solutions. Paper D provides tools to monitor the error associated with the parametric solver guaranteeing the quality of the PGD solution.

Chapter 2

A family of iterative solvers for power systems

There still exist difficulties in solving the power flow equations. One of them is to guarantee the convergence to the physical solution. The other one is that some methods, such as Newton-Raphson (NR) or Fast Decoupled Load Flow (FDLF), are subject to the assemble of the Jacobian matrix. This procedure may be computationally unfordable if the number of nodes in the network is considerably large.

Thus, the goal is to proposed a method which is able to circumvent both adversities and also to accommodate the parametric version of the problem so that the Proper Generalized Decomposition technique is applied easily. The Alternating Search Direction method (ASDM) is suitable for overcoming both difficulties taking advantage of the algebraic structure of the governing equation. This method requires the choice of the search directions enforcing the convergence to the operative solution and providing fast convergence to the solution, at least, the convergence rate is close as possible to the Newton-Raphson methods. Furthermore, in terms of implementation, the choice of the search directions is advisable to be a constant matrix in the linear problem.

2.1 The method of Alternating Search Directions

The method of Alternating Search Directions was initially described in Ladevèze and Simmonds (1999). The studied models belong to domains of mechanics such as plasticity. In that cases, it is possible to distinguish between different relations in the same equations. For instance, linear and nonlinear relations, or it may happen that a relation in a point of the domain just involves quantities defined in the same point, that is to say, there is a local relation. On the contrary, if there are more points involved, the relation is global. The main idea of the method is to separated these relations, equations global and linear and equations local but nonlinear. Thus, the resolution of the model is performed in two different stages adding two search directions resulting in a iterative scheme.

In the derivation of the power flow equations is observed that, (1.3) is formed combining nonlinear but local relations in equation (1.1) with global and linear relations in equation (1.2). Hence, following the ASDM strategy, the problem is duplicated keeping the two unknowns I and V as in the original formulation. Consequently, a single iteration in the original fixed-point equation (1.3) becomes a combination of two steps, one per equation. Additional relations between voltages and currents need to be described in order the problem to be well-posed. These linear relations, called search directions, are representing by the matrices $\boldsymbol{\alpha}$ and $\boldsymbol{\beta}$, both considered at the beginning in $\mathbb{C}^{n \times n}$.

Thus, each iteration γ consists in computing $(V, I)^{[\gamma+1]}$ from the previous approximation $(V, I)^{[\gamma]}$. The first step consists in finding an intermediate approximation $(V, I)^{[\gamma+\frac{1}{2}]}$ from the linear system given the matrix $\boldsymbol{\alpha}$,

$$\begin{cases} I^{[\gamma+\frac{1}{2}]} - I^{[\gamma]} = \boldsymbol{\alpha}(V^{[\gamma+\frac{1}{2}]} - V^{[\gamma]}), \\ \mathbf{Y}V^{[\gamma+\frac{1}{2}]} = I^{[\gamma+\frac{1}{2}]} + I_0. \end{cases} \tag{2.1}$$

Similarly, the second step computes $(V, I)^{[\gamma+1]}$ for a given diagonal matrix $\boldsymbol{\beta}$ updating the following system, such that

$$\begin{cases} I^{[\gamma+1]} - I^{[\gamma+\frac{1}{2}]} = \boldsymbol{\beta}(V^{[\gamma+1]} - V^{[\gamma+\frac{1}{2}]}), \\ V^{*[\gamma+1]} \odot I^{[\gamma+1]} = S^*. \end{cases} \tag{2.2}$$

Initially, $\boldsymbol{\alpha}$ and $\boldsymbol{\beta}$ are matrices of dimension $n \times n$. However, if the matrix $\boldsymbol{\beta}$ is non-diagonal, equation (2.2) would keep the global relation between the voltages. Accordingly, from now on β is a diagonal matrix or vector. For an approximated solution at iteration γ, $V^{[\gamma]}$, the algorithm is implemented following two steps:

1. Step one consists in solving the linear system

$$V^{[\gamma+\frac{1}{2}]} = (\mathbf{Y} - \boldsymbol{\alpha})^{-1} \left(S^* \oslash V^{[\gamma]*} - \boldsymbol{\alpha} V^{[\gamma]} + I_0 \right). \qquad (2.3)$$

   Once the search direction $\boldsymbol{\alpha}$ is known, the LU decomposition of the matrix $\mathbf{Y} - \boldsymbol{\alpha}$ is performed.

2. Step two involves the solution of n decoupled second order equations

$$\beta \odot V^{[\gamma+1]*} \odot V^{[\gamma+1]} + V^{[\gamma+1]*} \odot \left[(\mathbf{Y} - \beta) V^{[\gamma+\frac{1}{2}]} - I_0 \right] - S^* = 0. \qquad (2.4)$$

   Dividing by β (assuming that none of the elements of β is zero) the following vectors are defined

$$\begin{aligned} A &= \left[(\mathbf{Y} - \beta) V^{[\gamma+\frac{1}{2}]} - I_0 \right] \oslash \beta, \\ B &= -S^* \oslash \beta \quad \text{and} \quad Z = V^{[\gamma+1]} \oslash A. \end{aligned} \qquad (2.5)$$

   Now, the above equation can be written as

$$Z^* \odot Z + Z^* + C = 0. \qquad (2.6)$$

   where $C = B \oslash (\bar{A} \odot A)$. Duplicating the equation using Cartesian representation, the below equation is obtained,

$$\begin{cases} (Z^{\text{Re}})^2 + (Z^{\text{Im}})^2 + Z^{\text{Re}} + C^{\text{Re}} = 0 \\ -Z^{\text{Im}} + C^{\text{Im}} = 0 \end{cases}, \qquad (2.7)$$

   which yields:

$$Z = \frac{-1 \pm \sqrt{1 - 4((C^{\text{Im}})^2 + C^{\text{Re}})}}{2} - iC^{\text{Im}}. \qquad (2.8)$$

   In the above expression all the operations are intended as component-wise on the vectors Z and C. In order to reach the high voltage solution, the root corresponding to the sign plus is selected.

The algorithm can be resumed as follows:

1. Assemble the system by forming the matrix $\mathbf{Y}$ and the vectors S and I_0.

2. Select the search directions $\boldsymbol{\alpha}$ and β.

3. Factorize the matrix $(\mathbf{Y} - \boldsymbol{\alpha})$.

4. Evaluate the initial guess $V^{[0]}$.

5. Alternate steps (2.3) and (2.4) until the stagnation criterion for the approximated solution V and the relative error in the residual is less than an fixed tolerance.

Thus, every iteration consists of a backward and a forward substitution for the linear global stage, and the computation of the high voltage root of n decoupled quadratic equations, which can be done without the need of an iterative solver. The initial guess $V^{[0]}$ corresponds to the solution of the systems with no loads and only due to the slack node voltage. Note that this choice is not mandatory and the method can be started in other ways. Convergence is obtained even with arbitrary random starts for which NR diverges. There are several advantages associated with this approach:

- If $\boldsymbol{\alpha}$ is constant, the matrix factorization needed to solve system (2.3) is only performed once.

- Equations (2.4) can be solved analytically. The final equation is a group of n decoupled second degree equations with two possible roots, demonstrating the existence of low and high voltage solutions in the power grid. During the iterative process, selecting the appropriate root, the convergence to the desired operative solution is guaranteed. Hence, the converged solution is by construction an operative solution, regardless of the choice of the initial guess.

- Since the pairs $(V, I)^{[\gamma+\frac{1}{2}]}$ and $(V, I)^{[\gamma+1]}$ fulfill equations (2.3) and (2.4) respectively and the algorithm is numerically consistent.

This family of algorithms is parameterized by the search directions $\boldsymbol{\alpha}$ and β, that is to say, the performance of this method is strongly dependent on the choice of these matrices.

2.1.1 Geometrical interpretation

The original formulation of the ASDM states that all the solutions of equation (2.1) are in a lineal manifold while the solutions of equation (2.2) are in a general curve manifold, hence the method is represented in a geometric scenario where the final solution is the intersection of the two manifolds.

The solutions of the simple two buses equation (1.18) are considered in this section in order to observe the geometrical representation in the 2-dimension space of the ASDM applied to the power flow problem. This second order equation has two solutions, although the operative solution is the high voltage one (the one resulting from the sign plus in the root). In this particular case, the manifolds are an hyperbola of equation $I = S^*/V^*$ and a line of equation $I = Y(V - V_0)$. The intersection of them as can be seen in figure 2.1 results in the two solutions, the high voltage and the low voltage one.

The proposed method can be identified with the following geometrical construction, illustrated in figure 2.1(a): starting from any point on the hyperbola (local problem), it is moved from there to the line (global problem) following a straight paths (continuous line) with constant slope α and then from the line back to the hyperbola with a straight path of slope β, until the intersection point is found. The same result is obtained for any other initial point either on the hyperbola or on the line. With this perspective, it is possible to see NR algorithms as a particularization of the discussed method for α equals to the local tangent to the hyperbola and $\beta \to \infty$, see table 2.1. Although Newton-Raphson method enjoys a faster convergence rate due to the variable α, it can be noticed from figure 2.1(b) that it is impossible to enforce the correct branch of the hyperbola, therefore the final solution depends on the initial guess.

Note that if the number of degrees of freedom n is higher than one, the line and hyperbola are replaced by their corresponding multidimensional manifolds, but the geometric scenario of the algorithm is the same, that is the solutions of

27
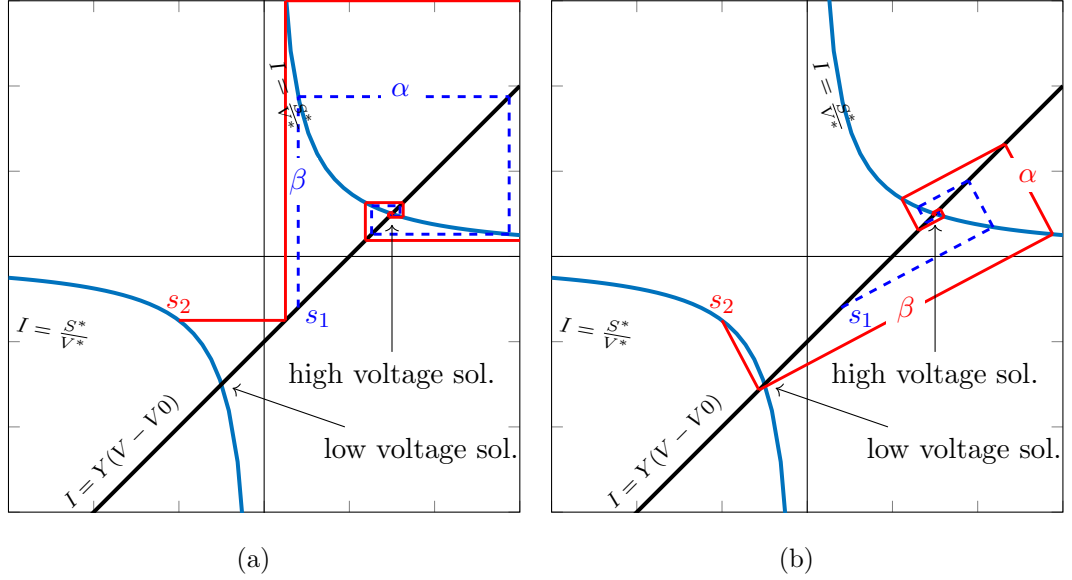
Figure 2.1: Graphic comparison between different search directions (α, β). The two trajectories (continuous red and dashed blue lines) are generated by choosing the first solution in the lower branch of the hyperbola (s_2) or on the line close to the upper branch of the hyperbola (s_1). (a)Generic alternating orthogonal directions. (b)NR method.

the global and local steps are alternated through linear search directions, until an intersection point is found.

2.1.2 Choices of the search directions

The matrix $\boldsymbol{\alpha}$ and the vector β are a fundamental feature in the described approach. Depending on the the choice of these matrices, the characteristics of the method in terms of convergence, computational time or accuracy might change during the iterative process.

Typically the unknown of the power flow problem is the voltage V, although most of the times the pair (V,I) is considered as an unknown. Note that once either V or I is computed, the other one is obtained fulfilling equation (1.2). In this case, current can be neglected from the two equations (2.1) and (2.2), and

Method	Choice for $\boldsymbol{\alpha}$	Choice for β
Gauss-Seidel	$\mathbf{Y}_U$	∞
Newton-Raphson	$\frac{\partial I_{bus}}{\partial V}$	∞
Z-matrix bus	0	∞

Table 2.1: Search directions for the classical methods

the iterative algorithm is formulated just for the unknown V, see equations (2.3) (2.4). Once equations depend just on V is easy to prove that for some choices of the matrices $\boldsymbol{\alpha}$ and $\boldsymbol{\beta}$ it is possible to recover some classical methods as is shown in table 2.1, more details are given in Borzacchiello et al. (2016).

Apart from these choices, based on the numerical examples, it has been demonstrated that the following alternative approach is a suitable choice:

$$\begin{cases} \boldsymbol{\alpha} = \mathrm{diag}\left(S^* \oslash |V_b|^2\right) \\ \beta \to \infty \end{cases}, \tag{2.9}$$

where V_b is the voltage base. The matrix $(\mathbf{Y} - \boldsymbol{\alpha})$ becomes a modified admittance matrix whose diagonal includes the linear part of the loads. This choice is optimal in many cases, since well designed grids are normally operating not far from the voltage V_b. A similar strategy was adopted by some authors and for the open source code OpenDSS, see Dugan and McDermott (2013). Indeed, the basic solution algorithm of OpenDSS can be seen as a particularization of the method of Alternating Search Directions when the values for $\boldsymbol{\alpha}$ and β are the same as in equation (2.9).

A common condition in all the methods discussed so far is the choice of β, which in practice means that the voltage of the local step is simply inherited from the global step, while the current is calculated using (2.2). Another choice which provides viable results although not optimal for β is the elements of the diagonal of $\mathbf{Y}$. Besides that, the matrix $\mathbf{Y} - \boldsymbol{\alpha}$ is preferable to be nonsingular and the matrices $\boldsymbol{\alpha}$ and diagonal matrix built using the vector β not to be equal, otherwise the method stagnates at the first iteration. Geometrically, these search directions would be parallel and the algorithm alternates between two same solutions indefinitely. In order to avoid this phenomenon, there exist another possibility considering $\boldsymbol{\alpha} = -\beta^{-1}$ which results in orthogonal search directions.

2.2   Numerical Example

This sections shows the performance of the proposed method in a distribution network. The test system is the IEEE 8500-node benchmark given in Arritt and Dugan (2010). It consists of approximately 4800 buses that are single-, two or three-phase. The total number of nodes, and therefore voltage unknowns, is around 8500. The test feeder is provided with balanced 120V secondary loads on the service transformers.

In order to compare the computed solutions using the ASDM, which is implemented using Matlab, a convergence error is defined. The error is the difference between the reference solution V and the approximated solution V_a measured in the norm of the maximum where the reference solutions are computed using OpenDSS and MATPOWER with tolerance close to the machine precision. To provide comparable results, the Z-matrix bus and OpenDSS solvers were implemented as particularizations of the ASDM by selecting the appropriate search directions. In this way, timing differences due to the particular implementation and different programming language are eliminated. For the same reason the NR algorithm is taken from a MATPOWER routine which also uses Matlab. Since the code execution depends on the particular system on which the test is run, a dimensionless time is obtained by dividing the run time by the time needed for a single NR iteration. The latter is obtained as an average over 1000 runs.

Figure 2.2 presents the convergence results. Due to the fact that at every iteration NR methods need to assemble and solve the Jacobian, the execution time is significant higher although NR has a faster (quadratic) convergence with respect to methods with fixed search directions. This is more evident in large systems, as the example IEEE-8500 feeder, for which the run time of the method of Alternating Search Directions becomes a fraction of a single NR iteration as can be seen in figures 2.2(a) and 2.2(b). Besides, there is no significant change in the diagrams of convergence when the calculations are performed for the cases of balanced and unbalanced loads and either between the different choices of the search directions.

In the light of the results in Borzacchiello et al. (2016), it is concluded that as the systems approaches the voltage instability point, the number of iteration
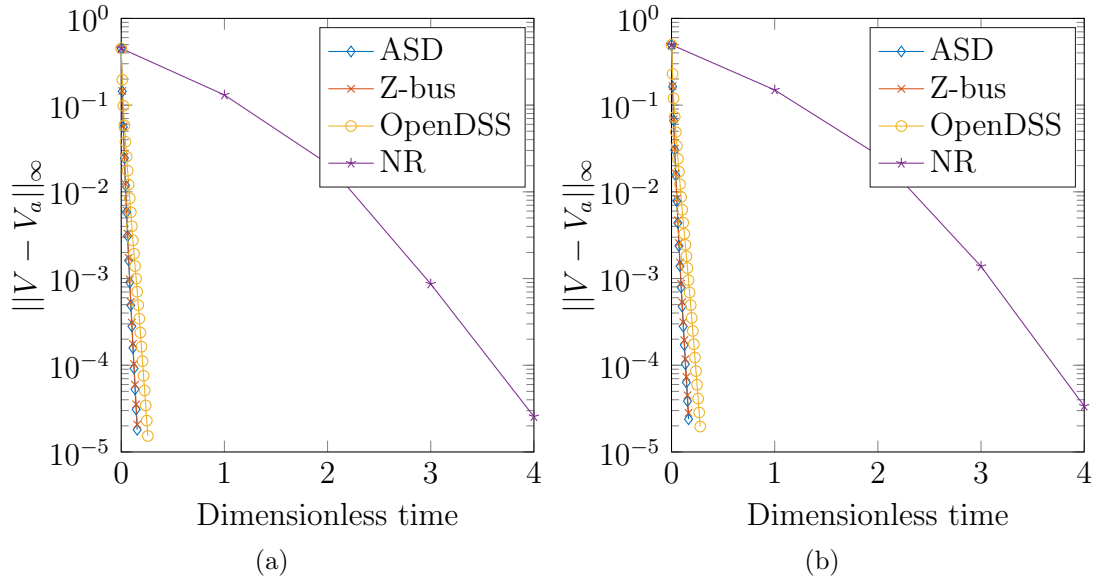
Figure 2.2: Convergence in the norm of the error for different iterative methods. (a)Case of the IEEE-8500 feeder with balanced loads. (b)Case of the IEEE-8500 feeder with unbalanced loads.

increases. Moreover, this paper studies in detail the implementation of controls included in the power flow formulation and analyzes the treatment of networks with PV nodes.

Chapter 3

Parametric power flow solution based on Proper Generalized Decomposition

The design verification and optimization of networks as applications of the power flow analysis requires to solve the power flow equations as many times as particular system configurations are considered. In order to represent these different schemes, the Parametric Power Flow problem was introduced in section 1.1.2. Consequently, the solutions now are sought in high dimensional spaces. This fact implies that the number of degrees of freedom increases exponentially. Thus, this method is potentially subject to the curse of dimensionality, that is, to a dramatic increment of the computational cost with the number of dimensions. Indeed, in D dimensions if each parameter assumes d possible states, the extensive exploration of the parametric space is associated to a volume of information that scales with d^D. In this context, Reduced Order Models (ROM) are especially indicated to remedy this deficiency.

In general, ROM aims to reduce the computational complexity of such problems. The concept of ROM techniques based on projection approaches implies to simplify the original problem extracting the relevant information out of a set of

representative problems and form a suitable basis to solve new problems once the parameters are changed. Some common strategies are:

- Reduced Basis (RB): approximates the solution of a system of nonlinear equations by the solution of a related system of much lower dimension, more details are given in Rozza (2008).

- Proper Orthogonal Decomposition method (POD): supplies an orthonormal basis taking into account empirical data of the initial model, hence the choice of the data set plays a crucial role, see Sirovich (1987); Pinnau (2008); Rios et al. (2010).

- Discrete Empirical Interpolation Method (DEIM): it is presented by Chaturantabut and Sorensen (2009a) as an improvement of the POD approximation because reduces the nonlinear terms in the full problem with a complexity proportional to the number of reduced variables.

ROM techniques have been applied in the field of power system engineering. For instance, grid equivalencing techniques like Ward reduction in Ward (1949) or POD in Parrilo et al. (1999) are commonly used to reduce the computational cost of power flow analysis of large systems. The combination of both POD and DEIM methods has been applied for model order reduction for semiconductors in electrical networks using DEIM to treat the reduction of nonlinear components as is shown in Hinze and Kunkel (2012). Electrical, thermal, and micro-electromechanical systems have been also studied in Hochman et al. (2011). More recently, works dealing with either OPF or PLF using order reduction techniques rely on Sparse Grid approaches like references Lin et al. (2014); Zhang and Li (2013); Tang et al. (2015) or Sparse Tensor Recovery in reference Zhang et al. (2015) emerged. Both techniques can be classified as collocation approaches, since the solution is reconstructed in the high dimensional space from the values it assumes in a set of particular and well-chosen points called the collocation points.

In this thesis, ROM techniques are not intended to reduce the degrees of freedom of the physical system but the computational complexity associated to the resolution of high-dimensional parametric equations. For that reason, Proper Gen-

eralized Decomposition (PGD) technique is suitable for the parametric power flow problem.

3.1   The Proper Generalized Decomposition

Proper Generalized Decomposition stands out in the ROM field since computes the solution without using precomputed results reducing also the dimensional complexity. PGD has proven to be an efficient method for the numerical solution of high dimensional and parametric equations, see Chinesta et al. (2010, 2011, 2013a,b). This strategy has been successfully applied to parametric problems in computational mechanics as is illustrated in Aghighi et al. (2013); Niroomandi et al. (2013).

The particular way in which the PGD method reduces the dimensional complexity is by approximating a multidimensional function by the sum of products of one-dimensional functions. This form, called separated variables representation, is computed using a greedy enrichment procedure, in which a single term per iteration is introduced in the summation. Each new term is determined using a fixed-point algorithm in which each function is updated individually, using an alternating minimization approach.

Generally, the application of PGD to linear problems is straightforward, nevertheless the extension to nonlinear problems could be really arduous depending on the particular problem to be solved. Diversified strategies exist, in this thesis, the combination of the nonlinear algebraic solver illustrated in chapter 2 with the PGD approach is detailed.

3.2   Parametrized power flow equations and separable approximation

The parameters considered in this section as the same as described in section 1.1.2. These are the location q, the power r of a generator and the time t representing the demand power during a year. Thus, the parametrized version of the Parametric Power Flow problem is described by taking S depending of these three parameters

in (1.6), that is,

$$S(q,r,t) = \sum_{h=1}^{H} \alpha_S^h \, S^h \, \breve{\mathcal{Q}}^h(q) \breve{\mathcal{R}}^h(r) \breve{\mathcal{T}}^h(t) \,, \qquad (3.1)$$

where H is the number of terms in the S expansion, and for $h = 1, \ldots, H$, α_S^h are positive scalars, $S^h \in \mathbb{C}^n$ are the unit vector modes of powers, and $\breve{\mathcal{Q}}^h(q)$, $\breve{\mathcal{R}}^h(r)$ and $\breve{\mathcal{T}}^h(t)$ are the unit parametric modes.

The output of PGD technique is a full parametric solution in a compact separated variables format, thus the PGD approximation of V, V_a, has a separated form. That means that it is a sum of M terms, each of them being the product of functions only depending on one of the parameters, namely

$$V(q,r,t) \approx V_a(q,r,t) = \sum_{m=1}^{M} \alpha_V^m \, V^m \mathcal{Q}^m(q) \mathcal{R}^m(r) \mathcal{T}^m(t) \,, \qquad (3.2)$$

where, for $m = 1, \ldots, M$, α_V^m are positive scalars, $V^m \in \mathbb{C}^n$ are the unit vector modes of voltages, and $\mathcal{Q}^m(q)$, $\mathcal{R}^m(r)$ and $\mathcal{T}^m(t)$ are the unit parametric modes. The modes are normalized (to have unit norm) and the positive scalar α_V^m collects the amplitude of each term.

In practice, the parametric dimensions are discretized in a Finite Element fashion. Let n_q, n_r and n_t denote the number of degrees of freedom discretizing the three parametric dimensions. Thus, function $\mathcal{Q}^m(q)$ is identified with vector $\mathcal{Q}^m \in \mathbb{C}^{n_q}$, similarly vectors $\mathcal{R}^m \in \mathbb{C}^{n_r}$ and $\mathcal{T}^m \in \mathbb{C}^{n_t}$ represent functions $\mathcal{R}^m(r)$ and $\mathcal{T}^m(t)$. Hence, the multivariate function $V_a(q,r,t)$ is also described by a $n \times n_q \times n_r \times n_t$ complex tensor $\mathbf{V}_a$, such that

$$\mathbf{V}_a = \sum_{m=1}^{M} \alpha_V^m \, V^m \otimes \mathcal{Q}^m \otimes \mathcal{R}^m \otimes \mathcal{T}^m \,. \qquad (3.3)$$

Similarly, $S(q,r,t)$ is identified with its tensorial version $\mathbf{S} \in \mathbb{C}^{n \times n_q \times n_r \times n_t}$ that reads

$$\mathbf{S} = \sum_{h=1}^{H} \alpha_S^h \, S^h \otimes \breve{\mathcal{Q}}^h \otimes \breve{\mathcal{R}}^h \otimes \breve{\mathcal{T}}^h \,. \qquad (3.4)$$

3.3 A PGD solver based on Z-matrix bus method

Equation (1.3) in the parametric context with the explicit parametric dependence reads as:

$$V_a^{[\gamma+1]}(q,r,t) = \mathbf{Y}^{-1}\left(S^*(q,r,t) \oslash V_a^{*[\gamma]}(q,r,t) + I_0\right).$$ (3.5)

Note that the equation above is an adaptation of the iterative strategy presented in chapter 2 when the choice for the matrices $\boldsymbol{\alpha}$ and β are 0 and ∞ respectively. It is worthy mentioning that any other combination of values for the matrix $\boldsymbol{\alpha}$ and the vector β is applicable, nevertheless in terms of computation and accuracy this choice is suitable. Following the ideas already presented, this equation is split into two steps:

1. First, given $V_a^{[\gamma]}(q,r,t)$ an intermediate quantity I is computed in a separated variables form such that

$$I(q,r,t) = S^*(q,r,t) \oslash V_a^{*[\gamma]}(q,r,t),$$ (3.6)

   Since the numerator S and the denominator $V_a^{[\gamma]}$ are separated variables functions, the evaluation of the quotient is not as trivial as in their algebraic version. For instance, for S and V_a in $\mathbb{C}^n$, computing $I = S^* \oslash V_a$ is a simple division for each component: $[I]_l = [S]_l^*/[V]_l^*$ for $l = 1,\ldots,n$. Therefore, PGD is applied in order to find a separated representation of $I(q,r,t)$.

2. Then, the second step consists in solving the global (but linear) system, that is in computing

$$V_a^{[\gamma+1]}(q,r,t) = \mathbf{Y}^{-1}\left(I(q,r,t) + I_0\right).$$ (3.7)

   This step does not present any additional difficulty since the matrix $\mathbf{Y}$ does not depend on the parameters q, r and t. For this reason, the factorization of the matrix can be stored and reused. Concluding that the voltage inherits the same parametric modes of the current, the modes for the voltage $V_a^{[\gamma+1]}$ can be straightforwardly computed multiplying by $\mathbf{Y}^{-1}$, for all $m = 1,\ldots,M$.

3.3.1 Overview of the algorithm

For each iteration γ, the problem to be solved is a problem of the type: find $I(q,r,t)$ such that $I(q,r,t) \odot V_a^{*[\gamma]}(q,r,t) = S^*(q,r,t)$. The standard PGD procedure consists in computing sequentially the terms of the PGD expansion of $I(q,r,t)$ (loop on M) and for each term iterate in the alternated directions scheme (this is going to be denoted as a loop on k). The PGD solver uses a greedy algorithm to compute these terms in the expansion (3.2) (or its tensorial form (3.3)). Thus, in this context, the PGD algorithm involves three nested loops:

1. The external one correspond to the nonlinear solver and iterates in γ.

2. The second is the greedy part of the PGD algorithm to solve (3.6) (loop on the number of terms of the PGD expansion M).

3. The inner loop iterates (for $k = 1, 2, \ldots$) in the alternated direction scheme for each of the parametric dimensions.

As an iterative solver, an initial solution is required. The initial solution is typically provided after the slack node intensity, that is to say, I_0 is the voltage circulating in the grid under no loads or generation, namely

$$V_a^{[0]} = \mathbf{Y}^{-1} I_0. \tag{3.8}$$

The computation of the parametric modes is done using the standard Finite Element approximations, although it may be done using other procedures. Following this approach, the modes are numerically describe as 1D functions. For instance, $\mathcal{Q}^m$ can be seen just as a set of values of $\mathcal{Q}^m(q)$ in some sampling points. The fact of identifying this set of points with a finite element 1D grid is not strictly necessary in this context but it can be helpful in the case some integral of the nodal modes needs to be computed. Thus, the underlying finite element space, typically $\mathcal{C}^0$ linear elements which is the simplest option. Note also that the continuity of the parametric modes is implicitly assumed and therefore the functional spaces where the modes are sought are, in practice, smaller than L_2.

The global idea of the PGD procedure is illustrated in algorithm 1.

Algorithm 1: PGD solver for the Power Flow problem

Data: I_0, S

`% Initialize`

$V_a^{[0]} = \mathbf{Y}^{-1} I_0$

`% Iterations of the nonlinear solver`

Loop on γ: **while** *[stopping criteria for γ do not hold (i.e.error > tolerance)]* **do**

    `% Computation of` $\quad I = S^* \oslash V_a^{*[\gamma]} \quad$ `à la PGD`

    Loop on M: **while** *[stopping criteria for M do not hold]* **do**

$$I = \underbrace{\sum_{m=1}^{M-1} V^m \mathcal{Q}^m(q) \mathcal{R}^m(r) \mathcal{T}^m(t)}_{\text{known}} + \underbrace{V^M \mathcal{Q}^M(q) \mathcal{R}^M(r) \mathcal{T}^M(t)}_{\text{unknown}};$$

        `% Iterations for alternated directions`

        Loop on k: **while** *[stopping criteria for k do not hold]* **do**

            Compute $(V^M)^{k+1}$ from $(\mathcal{Q}^M(q))^k$, $(\mathcal{R}^M(r))^k$ and $(\mathcal{T}^M(t))^k$;

            Compute $(\mathcal{Q}^M(q))^{k+1}$ from $(V^M)^{k+1}$, $(\mathcal{R}^M(r))^k$ and $(\mathcal{T}^M(t))^k$;

            Compute $(\mathcal{R}^M(r))^{k+1}$ from $(V^M)^{k+1}$, $(\mathcal{Q}^M(q))^{k+1}$ and $(\mathcal{T}^M(t))^k$;

            Compute $(\mathcal{T}^M(t))^{k+1}$ from $(V^M)^{k+1}$, $(\mathcal{Q}^M(q))^{k+1}$ and $(\mathcal{R}^M(r))^{k+1}$;

    `% Compute` $V_a^{[\gamma+1]} = \mathbf{Y}^{-1}(I + I_0)$

    $V^m \leftarrow \mathbf{Y}^{-1} V^m$ for $m = 1, \dots, M$;

    $V_a^{[\gamma+1]} = \mathbf{Y}^{-1} I + V_a^{[0]}$;

3.3.2 Stopping criteria

The three loops described in the algorithm 1 above stop using criteria based on the user prescribed tolerances. The criteria defined in this section are based on the residual of the equation and the stagnation between two consecutive approximations. Hence, the error indicators $\xi_\star^\square$, where $\square$ accounts for the type of error measured (taking two possible values: $\square = R$ for a purely residual estimate and $\square = S$ for a measure of the stationarity in the loop) and $\star$ denotes the loop where it is used (taking three possible values: $\star = \gamma$; $\star = M$; or $\star = k$) are introduced. Thus, the different stopping criteria are expressed as: *continue with the loop while*

$\xi_\star^\square > \text{tol}_\star^\square$, $\text{tol}_\star^\square$ being the different tolerances prescribed for the different criteria. The definitions of the different error indicators are listed below:

1. Loop in γ

$$\xi_\gamma^R = \frac{\|R(V_a^{[\gamma+1]})\|_2}{\|S\|_2}, \ \xi_\gamma^S = \frac{\|V_a^{[\gamma+1]} - V_a^{[\gamma]}\|_2}{\|V_a^{[\gamma+1]}\|_2} \tag{3.9}$$

where $R(V_a^{[\gamma+1]}) = S^* - V_a^* \odot (\mathbf{Y}V_a - I_0)$ is the residual of equation (1.3). Recall that $\|\cdot\|_2$ stands for either the L^2-norm or the Frobenius norm (depending on whether the argument is a vector or a matrix).

2. Loop in M

$$\xi_M^R = \frac{\|R(I)\|_2}{\|S\|_2}, \ \xi_M^S = \frac{|\alpha_I^M|}{|\alpha_I^1|} \tag{3.10}$$

where $R(I) = (S^* - V_a^* \odot I)$.

3. Loop in k

$$\begin{aligned} \xi_k^{S_1} = \frac{\|(V^M)^{k+1} - (V^M)^k\|_2}{\|(V^M)^{k+1}\|_2} \ , \ \xi_k^{S_2} = \frac{\|(\mathcal{R}^M)^{k+1} - (\mathcal{R}^M)^k\|_2}{\|(\mathcal{R}^M)^{k+1}\|_2} \\ \xi_k^{S_3} = \frac{\|(\mathcal{Q}^M)^{k+1} - (\mathcal{Q}^M)^k\|_2}{\|(\mathcal{Q}^M)^{k+1}\|_2} \ \text{ and } \ \xi_k^{S_4} = \frac{\|(\mathcal{T}^M)^{k+1} - (\mathcal{T}^M)^k\|_2}{\|(\mathcal{T}^M)^{k+1}\|_2} \end{aligned} \tag{3.11}$$

These stopping criteria are complemented by two more that measure the error which are discussed in detail in section 4.3.

3.4 Numerical results

This sections aims at analyzing how the PGD method works in the context of the Parametric Power Flow problem for an optimization problem in a distribution system. The system analyzed is the three-phase radial distribution grid extracted from Martinez and Guerra (2012, 2014) and it is represented in figure 3.1. This consists of 100 buses and a transformer, therefore the number of nodes, considering the slack bus, is $n = 306$.

The problem considered requires to determine the optimal location and size of a distributed generator in the distribution network in order to minimize the power losses over a year. The variables that need to be optimized are p, q, that is, the
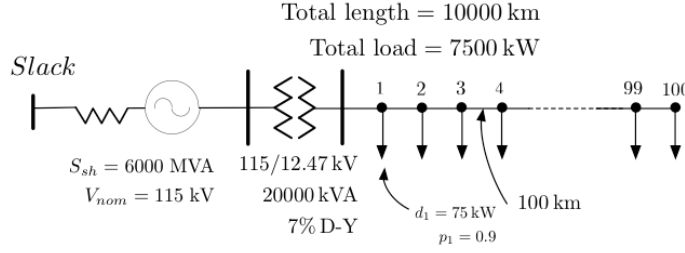
Figure 3.1: Diagram of the distribution grid.

location of the capacitor bank and the nominal power (in this case the distributed generator is a the capacitor bank since is a purely reactive power source) and the time t representing the hours of a year.

Traditional optimization algorithms require multiple solutions of the power flow problem to evaluate the cost function (in this case the power losses). Instead of following this approach, the described PGD solver computes the parametric solution of the problem as an explicit function of the parameters p, q and t, thus the evaluation of the objective function in the optimization algorithm does not require any further simulation. Consequently, simulation and optimization are now separate steps and any optimization algorithm can be elected since this is completely unrelated to the solution of the power flow.

The sought voltage solution is written as:

$$V_a(q, r, t) = \sum_{m=1}^{M} \alpha_V^m \, V^m \mathcal{Q}^m(q) \mathcal{R}^m(r) \mathcal{T}^m(t) \,. \tag{3.12}$$

Note that the number of terms M in the summation is also referred to as the rank of the approximation and is not known a priori but can be progressively increased in order to improve the accuracy of the solution. In practice, the numerical approximation of the parametric modes $\mathcal{Q}^m(q)$, $\mathcal{R}^m(r)$ and $\mathcal{T}^m(t)$ requires the discretization of the parametric space based on n_q, n_r and n_t discrete points. Particularly, the search space for optimization is defined by:

$$(q, r, t) \in I_q \times I_r \times I_t$$

where $I_q = [1, q_{max}]$, $I_r = [0, r_{max}]$ and $I_t = [0, t_{max}]$ with $q_{max} = 100$ the number of possible location for the DG (in this case, all the buses are potential candidates) and $r_{max} = 4 \cdot 10^3$ kVAR is the maximum reactive power that the DG can provide. Accordingly, the number of discretization points are $n_q = 100$ and $n_r = 100$. Moreover, $t_{max} = 8760$ h and the load variations are recorded hourly, therefore time is discretized in $n_t = 8760$ points.

When the time is included in the description of the solution, load profiles can be either obtained by direct measurements over time or, as in this case, generated with an appropriate model. Load and generation shapes data were obtained from reference Martinez and Guerra (2012) based on the models implemented in the software HOWER, see Lambert et al. (2006). For this case, the power can be written as a sum of five terms, one for the generator and four describing the loads variations in time:

$$S(q, r, t) = \sum_{h=1}^{4} \alpha_S^h \, S^h \breve{\mathcal{Q}}^h(q) \breve{\mathcal{R}}^h(r) \breve{\mathcal{T}}^h(t) + \breve{\alpha}\breve{S}\breve{\mathcal{Q}}(q)\breve{\mathcal{R}}(r)\breve{\mathcal{T}}(t) \,. \qquad (3.13)$$

Thus, the resulting Parametric Power Flow problem is four-dimensional (one physical coordinate and three parameters). The same problem is solved by Martinez and Guerra (2012) using Monte Carlo Simulation.

The prescribed tolerances in this example are $\mathrm{tol}_\gamma^\square = 10^{-5}$, $\mathrm{tol}_M^\square = 10^{-6}$ and $\mathrm{tol}_k^\square = 10^{-7}$ for $\square = S, R$. The convergence of the outer loop γ is shown in figure 3.2(a), where the number of the computed modes at each iteration is also reported. The nonlinear iterative method converges in 7 iterations and the separated representation of the converged solution is composed of 28 terms. The Euclidean norm of each term is also represented by the coefficients α_V in figure 3.2(b), these values are a measure of the relative weight of individual terms in the low rank approximation.

Once the solution is obtained, a separated variables representation for the losses can be computed as a part of the post-processing of the solution:

$$L(q, r, t) = \sum_{h=1}^{\tilde{H}} \tilde{\mathcal{Q}}^h(q) \tilde{\mathcal{R}}^h(r) \tilde{\mathcal{T}}^h(t) \qquad (3.14)$$

In the above expression the losses are also approximated using separated variables representation. The first 20 functions $\tilde{\mathcal{Q}}^h(q)$, $\tilde{\mathcal{R}}^h(r)$ and $\tilde{\mathcal{T}}^h(t)$, from the separated
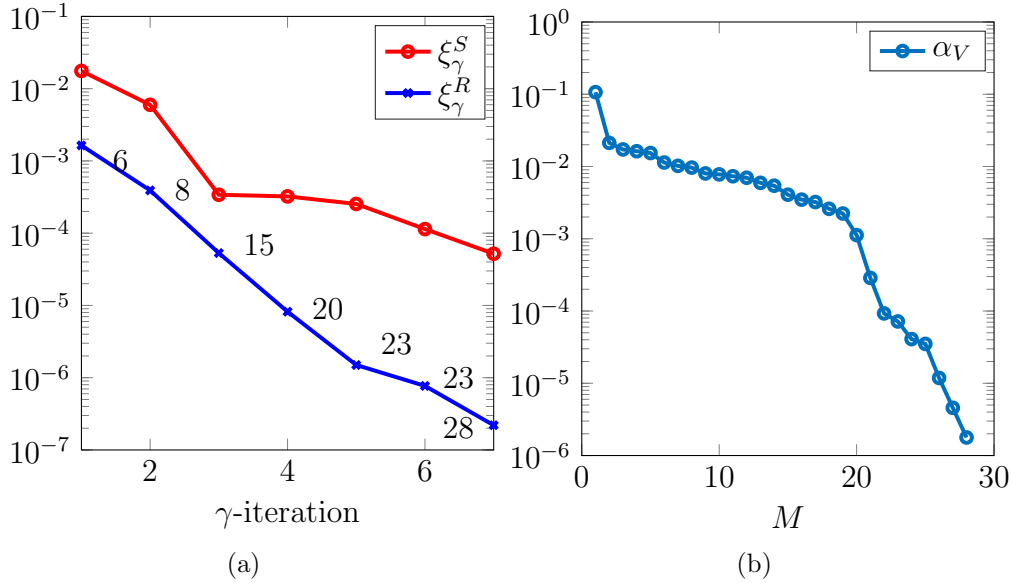
Figure 3.2: Parametric Power Flow solution with PGD. (a)Convergence diagram of nonlinear PGD solver with the iteration index γ. The numbers reported on the curve represent number of terms M that the solution contains at each nonlinear iteration γ. (b)Norm of each individual term in the separated representation of the converged solution for $m = 1, 2, \ldots, 28$.

variable representation of the losses are shown respectively in figures 3.3(a), 3.3(b) and 3.3(c) together with the reconstruction of the two dimensional loss function in figure 3.3(d). Note that this is possible since the losses for a combination of parameters (p, q) is taken as the sum of the losses associated with every hour t.

To understand the advantage of slow rank approximation, note that the computational work needed to obtain an equivalent solution with a traditional parametric sweep in the optimization space corresponds to $100 \times 100 \times 8760$ different calls of the power flow solver. This amounts to compute $306 \times 100 \times 100 \times 8760$ unknowns, whereas using PGD a separated variable approximation of the parametric solution only requires computing $28 \times (306 \times 100 + 100 + 8760)$ unknowns to have the desired accuracy. Therefore the reduced order solution is about 25×10^3 times smaller than the full order solution. This evidences how the separated variables approximation becomes more and more efficient as the dimensionality of the problem increases.
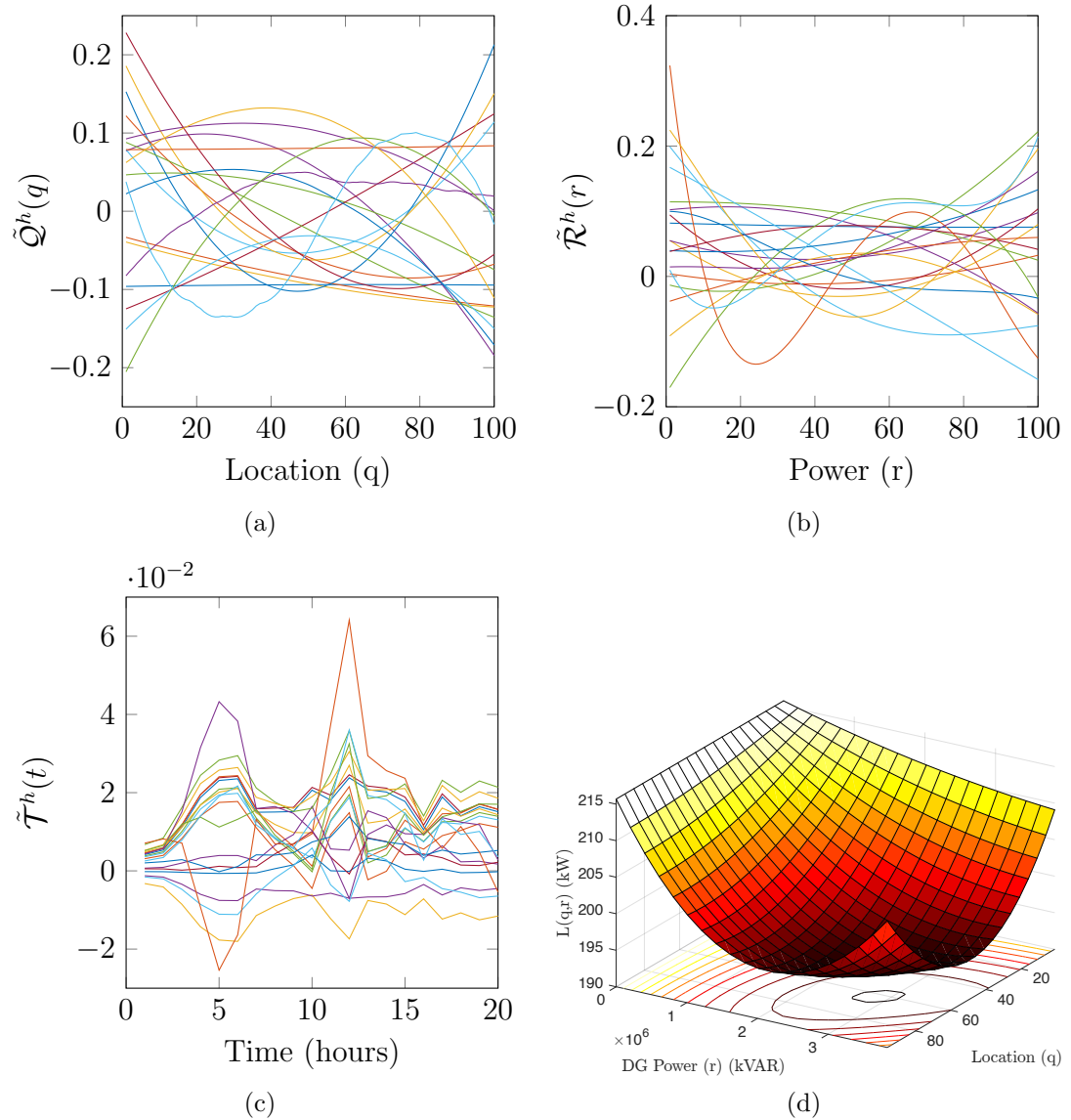
Figure 3.3: Separated form of the three-dimensional power losses. (a)Normalized functions of the DG position q. (b)Normalized function of the DG output reactive power r. (c)Normalized functions of the time t. (d)Reconstructed losses function.

Authors in Martinez and Guerra (2012) reported a run time of 2.5 hours for the execution of Monte Carlo optimization using OpenDSS in this example. With

PGD the execution time to compute the parametric solution is of the order of a few minutes using MATLAB, while optimization can be performed practically in real time.

As in the original paper of Martinez and Guerra and the theoretical analysis presented in Willis (2000), the optimal position is predicted at approximately 2/3 of the total length of the grid, in this case in the node 65 out of 100.

Further considerations and more examples are analyzed in references Borzacchiello et al. (2016) and García-Blanco et al. (2016b).

Chapter 4

Error assessment for the power flow problem

Power flow equations have been studied in detail, although the errors during the simulations have not received the corresponding attention. Particularly, the error has been addressed from diverse points of view as identifying errors associated with power controller parameters in Zhu and Abur (2006) or taking into account state estimation method for measurement error and model accuracy in references Chen and Liao (2012); Amini et al. (2015); Rouhani et al. (2016).

When it comes to errors in the application of Reduce Order methods, Rathinam and Petzold (2000) provides an error analysis of the computed solution obtained from POD illustrating the method using a power grid example modeled by nonlinear swing equations and Galbally et al. (2010) provides an analysis of the errors involved in solving a nonlinear initial value problem using a POD method. An error bound on DEIM approximation is provided by Chaturantabut and Sorensen (2009b, 2010) while Barrault et al. (2004) gives an error analyzes for the empirical interpolation procedure and Wirtz, Sorensen, and Haasdonk (Wirtz et al.) presents a posteriori error estimation for POD-DEIM reduced nonlinear systems. The error estimation in Proper Generalized Decomposition (PGD) is still an open question. However, some strategies have been proposed in Ammar et al. (2011, 2010).

This chapter aims at introducing the concept of error assessment in the context of the Parametric Power Flow problem. Although the procedure applied to both versions of the power flow problem is identical, it is necessary to distinguish the algebraic version from the parametric version of the problem. The process is focused on the development of the error equations based on a Quantity of Interest (QoI), particularly the system losses. The classic strategy that has been applied in this thesis, has also been applied to different problems in the field of error estimation for Reduced Order Models, see Ammar et al. (2010); Florentin and Díez (2012); Mozolevski and Prudhomme (2015). As a result, besides the standard stopping criteria for the PGD solver described in chapter 3, novel criteria are devised using goal-oriented error assessment.

4.1   Algebraic formulation of the error assessment

4.1.1   Error equation

The error is readily defined as

$$E = V - V_a, \tag{4.1}$$

where vector V is the actual solution of the problem and V_a is an approximation, both in $\mathbb{C}^n$. Moreover, the residual of equation (1.3) associated with V_a (also in $\mathbb{C}^n$) reads

$$R(V_a) = S^* - V_a^* \odot (\mathbf{Y} V_a - I_0). \tag{4.2}$$

The error equation is derived from the identity $R(V) = 0$, that is $R(V_a + E) = 0$. The idea is to linearize $R(\cdot)$ noting that $R(V_a)$ is computable once V_a is obtained. Expanding the expression of $R(\cdot)$, it is found that

$$R(V) = R(V_a + E) = S^* - (V_a^* + E^*) \odot (\mathbf{Y}(V_a + E) - I_0) =$$
$$= S^* - V_a^* \odot (\mathbf{Y} V_a - I_0) - V_a^* \odot \mathbf{Y} E - E^* \odot (\mathbf{Y} V_a - I_0) - E^* \odot \mathbf{Y} E. \tag{4.3}$$

In order to obtain a linear equation for the error, the quadratic term $E^* \odot \mathbf{Y} E$ is neglected, that is

$$R(V) = R(V_a) - V_a^* \odot \mathbf{Y} E - E^* \odot (\mathbf{Y} V_a - I_0) = R(V_a) - \mathbf{A} E - \mathbf{B} E^*, \quad (4.4)$$

where $\mathbf{A} = \mathrm{Diag}(V_a^*)\mathbf{Y}$ and $\mathbf{B} = \mathrm{Diag}(\mathbf{Y} V_a - I_0)$ are matrices in $\mathbb{C}^{n \times n}$. The operator $\mathrm{Diag}(\cdot)$ is introduced to compact the notation such that it produces a square matrix with the elements of a vector on the diagonal, that is for $V \in \mathbb{C}^n$, $\mathbf{W} = \mathrm{Diag}(V) \in \mathbb{C}^{n \times n}$ and $W_{lm} = V_l \delta_{lm}$.

Equation (4.4) results from neglecting the quadratic terms in (4.3) but it is still nonlinear because it involves the conjugate operator. This operator is nonlinear and also non-holomorphic (the Cauchy-Riemann equations are obviously not fulfilled in this case). The non-holomorphic character of the resulting expression precludes using the linearization via the Laurent series truncation strategy (similar to truncating the Taylor expansion for the real-valued functions).

The separation in real and imaginary part is an effective alternative to linearize the resulting equations. Thus, in equation (4.4), vectors and matrices are separated in their real and imaginary parts, using the so-called Cartesian representation. Hence, equation (4.4) is rewritten as a linear system of $2n$ real equations and unknowns, namely

$$\mathbf{C} \hat{E} = \hat{R}(V_a) \quad (4.5)$$

where the matrix $\mathbf{C} \in \mathbb{R}^{2n \times 2n}$, and vectors $\hat{R}(V_a)$ and $\hat{E}$ in $\mathbb{R}^{2n}$ are the real valued representations of the complex matrices and vectors in (4.4), and

$$\mathbf{C} = \begin{pmatrix} \mathbf{A}^{\mathrm{Re}} + \mathbf{B}^{\mathrm{Re}} & -\mathbf{A}^{\mathrm{Im}} + \mathbf{B}^{\mathrm{Im}} \\ \mathbf{A}^{\mathrm{Im}} + \mathbf{B}^{\mathrm{Im}} & \mathbf{A}^{\mathrm{Re}} - \mathbf{B}^{\mathrm{Re}} \end{pmatrix}.$$

4.1.2 Error representation via adjoint problem and error estimates

The objective of the optimization problems in this thesis is to minimize the power losses, thus, they are assumed as the Quantity of Interest (QoI) in the simulation. This is a standard choice for grid optimization, where energy losses are the objective quantity to be minimized. In general, given a generic vector of voltages W,

the positive number representing the losses associated with this vector is:

$$l(W) = (W^{*\mathsf{T}}\mathbf{Y}_{\mathcal{L}}W)^{\mathrm{Re}} \tag{4.6}$$

where the matrix $\mathbf{Y}_{\mathcal{L}}$ coincides with the admittance matrix $\mathbf{Y}$ almost everywhere. The difference between $\mathbf{Y}_{\mathcal{L}}$ and $\mathbf{Y}$ corresponds to the admittance values of the generators which in $\mathbf{Y}_{\mathcal{L}}$ are taken to be 0. In other words, $\mathbf{Y}_{\mathcal{L}}$ is the admittance matrix corresponding to the grid, accounting for all the lines and buses but not including the terms associated with the generators. Note that the form $l(\cdot)$ is non-linear and has to be linearized in order to define a goal-oriented error assessment strategy.

The expression of the losses in terms of the approximated solution and the error reads

$$
\begin{aligned}
l(V) &= (V^{*\mathsf{T}}\mathbf{Y}_{\mathcal{L}}V)^{\mathrm{Re}} = ((V_a^* + E^*)^{\mathsf{T}}\mathbf{Y}_{\mathcal{L}}(V_a + E))^{\mathrm{Re}} \\
&= (V_a^{*\mathsf{T}}\mathbf{Y}_{\mathcal{L}}V_a)^{\mathrm{Re}} + (V_a^{*\mathsf{T}}\mathbf{Y}_{\mathcal{L}}E)^{\mathrm{Re}} + (E^{*\mathsf{T}}\mathbf{Y}_{\mathcal{L}}V_a)^{\mathrm{Re}} + (E^{*\mathsf{T}}\mathbf{Y}_{\mathcal{L}}E)^{\mathrm{Re}}.
\end{aligned}
\tag{4.7}
$$

Following the same procedure as above, the quadratic term is neglected:

$$
\begin{aligned}
l(V) &= l(V_a) + (V_a^{*\mathsf{T}}\mathbf{Y}_{\mathcal{L}}E)^{\mathrm{Re}} + (E^{*\mathsf{T}}\mathbf{Y}_{\mathcal{L}}V_a)^{\mathrm{Re}} \\
&= l(V_a) + (f^{\mathsf{T}}E)^{\mathrm{Re}} + (g^{\mathsf{T}}E^*)^{\mathrm{Re}},
\end{aligned}
\tag{4.8}
$$

where $f = \mathbf{Y}_{\mathcal{L}}^{\mathsf{T}}V_a^*$ and $g = \mathbf{Y}_{\mathcal{L}}V_a$ are vectors in $\mathbb{C}^n$.

Now, using the Cartesian representation:

$$l(V) = l(V_a) + (f^{\mathsf{T}}E)^{\mathrm{Re}} + (g^{\mathsf{T}}E^*)^{\mathrm{Re}} = l(V_a) + \hat{\lambda}^{\mathsf{T}}\hat{E} \tag{4.9}$$

where

$$\hat{\lambda} = \begin{pmatrix} f^{\mathrm{Re}} + g^{\mathrm{Re}} \\ -f^{\mathrm{Im}} + g^{\mathrm{Im}} \end{pmatrix} \in \mathbb{R}^{2n}.$$

That is, the linear approximation for the error in the Quantity of Interest reads

$$E_{QoI} = l(V) - l(V_a) = \hat{\lambda}^{\mathsf{T}}\hat{E} \tag{4.10}$$

The following auxiliary problem (referred to as dual or adjoint problem) is introduced in order to obtain a representation of the error in the quantity of interest:

$$\mathbf{C}^{\mathsf{T}}\hat{\rho} = \hat{\lambda}. \tag{4.11}$$

The solution of this problem, $\hat{\rho}$, is a real vector of dimension $2n$. Assuming that the linearization of equation (4.7) holds, using $\hat{\rho}$ and (4.5), the error in the QoI is readily represented as:

$$E_{QoI} = \hat{\lambda}^{\mathsf{T}} \hat{E} = \hat{\rho}^{\mathsf{T}} \mathbf{C} \hat{E} = \hat{\rho}^{\mathsf{T}} \hat{R}(V_a) \qquad (4.12)$$

The matrix $\mathbf{C}$ and the vectors $\hat{R}(V_a)$, $\hat{\lambda}$ and $\hat{\rho}$ are computable but all of them depend on the approximation V_a at every iteration. This means that the computational cost for computing the adjoint problem at one iteration is almost the same than the cost of a PGD solver iteration. Nevertheless, this can be simplified because $\mathbf{C}$ and the vector $\hat{\lambda}$ become stable after a few iterations: in practice, they are constant along the iterative process, and therefore the corresponding dual solution does not change along the iterative process. That is, $\hat{\rho}$ does not change significantly with the γ iterations and it is not necessary to solve the dual problem at every iteration. This is related to the fact that, once the approximation enters the asymptotic range, the expectation is that V_a suffers slight perturbations along the γ iterations. Note also that $\mathbf{C}$ and $\hat{\lambda}$ depend linearly on V_a and therefore the perturbations in the left and right side of (4.11) do cancel each other producing almost the same solution $\hat{\rho}$. This property is also observed in the numerical experiments, see figure 4.2(a) in section 4.3.2. Once vector $\hat{\rho}$ is obtained, computing the error in the quantity of interest with (4.12) requires only computing the residual $\hat{R}(V_a)$ which is affordable in terms of computational time.

4.2 Parametric formulation of the error assessment

When the grid is optimized diverse parameters can be considered, however for the sake of simplicity and without losing generality, the equations are presented for the parameter r. Note that the dependence on q and t is omitted here (it is equivalent to take $n_q, n_t = 1$). However, this is not a loss of generality because the behaviour of the q and t parametric dimensions is analogous to the r dimension.

4.2.1 Error equation and dual problem

Taking the tensorial representation of the solution, $\mathbf{V}_a \in \mathbb{C}^{n \times n_r}$ is such that

$$\mathbf{V}_a = \sum_{m=1}^{M} \alpha_V^m V^m \otimes \mathcal{R}^m \,, \tag{4.13}$$

the error and the residual are also complex matrices in $\mathbb{C}^{n \times n_r}$,

$$\mathbf{E} = \mathbf{V} - \mathbf{V}_a, \tag{4.14}$$

$$\mathbf{R}(\mathbf{V}) = \mathbf{S}^* - \mathbf{V}^* \odot (\boldsymbol{Y}\mathbf{V} - \mathbf{I}_0). \tag{4.15}$$

In the parametric setup, the QoI is taken as the integration with respect to the parametric dimensions (here, only r) of some nonparametric QoI $l(\cdot)$, namely

$$L(V_a(r)) = \int_r l(V_a(r)) \, dr. \tag{4.16}$$

Recalling the identity between the functional and tensorial representations in (3.2) and (3.3), the integral along r is also determined by the mass matrix $\mathbf{M}_r$ (associated with the 1D mesh discretizing I_r) multiplied by vector $\mathbb{1}_{n_r} = [1, 1, \dots, 1]^{\mathsf{T}} \in \mathbb{C}^{n_r}$:

$$L(\mathbf{V}_a) = \mathbb{1}_{n_r}^{\mathsf{T}} \mathbf{M}_r l(\mathbf{V}_a), \tag{4.17}$$

where $l(\cdot)$ is now the generalization to the tensor representation of the operator introduced in equation (4.6), producing a vector of n_r components, namely

$$l(\mathbf{V}_a) = \mathrm{diag}((\mathbf{V}_a^{*\mathsf{T}} \mathbf{Y}_{\mathcal{L}} \mathbf{V}_a)^{\mathrm{Re}}), \tag{4.18}$$

where the operator $\mathrm{diag}(\cdot)$ maps the elements of the diagonal of the input matrix of size $n_r \times n_r$ into a column vector of size n_r. Similarly as in (4.8),

$$\begin{aligned} l(\mathbf{V}) &= l(\mathbf{V}_a) + (\mathbf{V}_a^{*\mathsf{T}} \mathbf{Y}_{\mathcal{L}} \mathbf{E})^{\mathrm{Re}} + \mathrm{diag}((\mathbf{E}^{*\mathsf{T}} \mathbf{Y}_{\mathcal{L}} V_a)^{\mathrm{Re}}) + \mathrm{diag}((\mathbf{E}^{*\mathsf{T}} \mathbf{Y}_{\mathcal{L}} \mathbf{E})^{\mathrm{Re}}) \\ &= l(\mathbf{V}_a) + \mathrm{diag}((\mathbf{F}\mathbf{E})^{\mathrm{Re}}) + \mathrm{diag}((\mathbf{G}\mathbf{E}^*)^{\mathrm{Re}}) \end{aligned} \tag{4.19}$$

where $\mathbf{F} = \mathbf{V}_a^{*\mathsf{T}} \mathbf{Y}_{\mathcal{L}}$ and $\mathbf{G} = (\mathbf{Y}_{\mathcal{L}} \mathbf{V}_a)^{\mathsf{T}}$ are matrices in $\mathbb{C}^{n_r \times n}$. Assuming that the approximation holds and using the Cartesian representation, this equation is rewritten as:

$$l(\mathbf{V}) = l(\mathbf{V}_a) + \mathrm{diag}(\hat{\boldsymbol{\lambda}}_p^{\mathsf{T}} \hat{\mathbf{E}}) \tag{4.20}$$

where

$$\hat{\boldsymbol{\lambda}}_p = \begin{pmatrix} \mathbf{F}^{\mathrm{Re}} + \mathbf{G}^{\mathrm{Re}} \\ -\mathbf{F}^{\mathrm{Im}} + \mathbf{G}^{\mathrm{Im}} \end{pmatrix}, \hat{\mathbf{E}} = \begin{pmatrix} \mathbf{E}^{\mathrm{Re}} \\ \mathbf{E}^{\mathrm{Im}} \end{pmatrix} \in \mathbb{R}^{2n \times n_r}.$$

Using the tensor contraction notation, equation (4.20) becomes:

$$L(\mathbf{V}) = L(\mathbf{V}_a) + \hat{\boldsymbol{\lambda}}^{\mathsf{T}} : \hat{\mathbf{E}} \tag{4.21}$$

where $\hat{\boldsymbol{\lambda}} = (\mathbb{1}_{2n}\mathbb{1}_{n_r}^{\mathsf{T}}\mathbf{M}_r) \odot \hat{\boldsymbol{\lambda}}_p \in \mathbb{R}^{2n \times n_r}$.

The error equation is derived following the same ideas as in the previous section:

$$\begin{aligned} \mathbf{R}(\mathbf{V}) = \mathbf{R}(\mathbf{V}_a + \mathbf{E}) &= \mathbf{S}^* - (\mathbf{V}_a^* + \mathbf{E}^*) \odot (\mathbf{Y}(\mathbf{V}_a + \mathbf{E}) - \mathbf{I}_0) \\ &= \mathbf{S}^* - \mathbf{V}_a^* \odot (\mathbf{Y}\mathbf{V}_a - \mathbf{I}_0) - \mathbf{V}_a^* \odot \mathbf{Y}\mathbf{E} - \mathbf{E}^* \odot (\mathbf{Y}\mathbf{V}_a - \mathbf{I}_0) - \mathbf{E}^* \odot \mathbf{Y}\mathbf{E}. \end{aligned} \tag{4.22}$$

Neglecting the quadratic term, and enforcing $\mathbf{R}(\mathbf{V}) = 0$, the following equation for the error follows

$$\mathbf{V}_a^* \odot \mathbf{Y}\mathbf{E} + \mathbf{E}^* \odot (\mathbf{Y}\mathbf{V}_a - \mathbf{I}_0) = \mathbf{R}(\mathbf{V}_a). \tag{4.23}$$

Taking every column of the matrix $\mathbf{V}_a$, it is possible to build two tensors $\underline{\mathbf{A}}(\cdot,\cdot,\ell) = \mathrm{Diag}(\mathbf{V}_a^*(\cdot,\ell))\mathbf{Y}$ and $\underline{\mathbf{B}}(\cdot,\cdot,\ell) = \mathrm{Diag}((\mathbf{Y}\mathbf{V}_a(\cdot,\ell) - \mathbf{I}_0(\cdot,\ell)))\mathbf{Y}$ for $\ell = 1,\ldots,n_r$ in $\mathbb{C}^{n \times n \times n_r}$. Thus, (4.23) is rewritten as:

$$\underline{\mathbf{A}} \overset{\cdot}{\odot} \mathbf{E} + \underline{\mathbf{B}} \overset{\cdot}{\odot} \mathbf{E}^* = \mathbf{R}(\mathbf{V}_a) \tag{4.24}$$

where the operation $\overset{\cdot}{\odot}$ denotes a contraction of one index and a Hadamard product in another index. For instance, in the particular case of $\underline{\mathbf{A}} \in \mathbb{C}^{n \times n \times n_r}$ and $\mathbf{E} \in \mathbb{C}^{n \times n_r}$, it reads

$$\left[\underline{\mathbf{A}} \overset{\cdot}{\odot} \mathbf{E}\right]_{i\ell} = \sum_{j=1}^{n} \underline{\mathbf{A}}_{ij\ell}\mathbf{E}_{j\ell} \text{ , with no sum on } \ell. \tag{4.25}$$

Note that the definition is general for the field ($\mathbb{C}$ can be replaced by $\mathbb{R}$) and for the dimensions of the tensors, the only restriction being that the two last indices of tensor $\underline{\mathbf{A}}$ have the same range as the the two indices of tensor $\mathbf{E}$.

Using the Cartesian representation, the equation becomes linear:

$$\underline{\mathbf{C}} \overset{\cdot}{\odot} \hat{\mathbf{E}} = \hat{\mathbf{R}}(\mathbf{V}_a) \tag{4.26}$$

53

where tensor $\underline{\mathbf{C}} \in \mathbb{R}^{2n \times 2n \times n_r}$ is:

$$\underline{\mathbf{C}}(\cdot, \cdot, \ell) = \begin{pmatrix} \underline{\mathbf{A}}(\cdot, \cdot, \ell)^{\mathrm{Re}} + \underline{\mathbf{B}}(\cdot, \cdot, \ell)^{\mathrm{Re}} & -\underline{\mathbf{A}}(\cdot, \cdot, \ell)^{\mathrm{Im}} + \underline{\mathbf{B}}(\cdot, \cdot, \ell)^{\mathrm{Im}} \\ \underline{\mathbf{A}}(\cdot, \cdot, \ell)^{\mathrm{Im}} + \underline{\mathbf{B}}(\cdot, \cdot, \ell)^{\mathrm{Im}} & \underline{\mathbf{A}}(\cdot, \cdot, \ell)^{\mathrm{Re}} - \underline{\mathbf{B}}(\cdot, \cdot, \ell)^{\mathrm{Re}} \end{pmatrix},$$

$\forall \ell = 1, \ldots, n_r$ and

$$\hat{\mathbf{R}} = \begin{pmatrix} \mathbf{R}^{\mathrm{Re}} \\ \mathbf{R}^{\mathrm{Im}} \end{pmatrix} \in \mathbb{R}^{2n \times n_r}.$$

The dual problem is readily introduced as:

$$\underline{\mathbf{C}}^{\mathsf{T}} \overset{\cdot}{\odot} \hat{\boldsymbol{\rho}} = \hat{\boldsymbol{\lambda}}, \tag{4.27}$$

where $\underline{\mathbf{C}}^{\mathsf{T}}(\cdot, \cdot, \ell) = \underline{\mathbf{C}}(\cdot, \cdot, \ell)^{\mathsf{T}}$, $\forall \ell$ (transposing only the two first dimensions of the tensor). Hence the error in the quantity of interest using equation (4.26) is:

$$\begin{aligned} E_{QoI} = L(\mathbf{V}) - L(\mathbf{V}_a) = \hat{\boldsymbol{\lambda}}^{\mathsf{T}} : \hat{\mathbf{E}} = \hat{\boldsymbol{\lambda}}^{\mathsf{T}} : (\underline{\mathbf{C}}^{\dagger} \overset{\cdot}{\odot} \hat{\mathbf{R}}(\mathbf{V}_a)) = \\ = \hat{\boldsymbol{\rho}}^{\mathsf{T}} : \hat{\mathbf{R}}(\mathbf{V}_a) \end{aligned} \tag{4.28}$$

where $\underline{\mathbf{C}}^{\dagger}(\cdot, \cdot, \ell) = \underline{\mathbf{C}}^{-1}(\cdot, \cdot, \ell)$, $\forall \ell$ (sectionally inverting the two first dimensions of the tensor). The previous identity is straightforwardly derived by analyzing the component-wise expression:

$$E_{QoI} = \sum_{i,\ell} \hat{\boldsymbol{\lambda}}_{\ell i} \hat{\mathbf{E}}_{i\ell} = \sum_{i,j,\ell} \hat{\boldsymbol{\lambda}}_{\ell i} \underline{\mathbf{C}}_{ij\ell}^{\dagger} \hat{\mathbf{R}}(\mathbf{V}_a)_{j\ell} = \sum_{j,\ell} \hat{\boldsymbol{\rho}}_{j\ell} \hat{\mathbf{R}}(\mathbf{V}_a)_{j\ell}$$

using the definition of the dual problem in equation (4.27).

The error representation provided in (4.28) describes the scalar E_{QoI} as the double contraction of $\hat{\boldsymbol{\rho}}^{\mathsf{T}}$ and $\hat{\mathbf{R}}(\mathbf{V}_a)$, both $n \times n_r$ tensors. This is because the residual error equation (4.26) is in fact a set of n_r algebraic residual equations similar to (4.5), one for each possible value of parameter r. The same occurs with the adjoint problem (4.27), which can be seen as a collection of n_r algebraic adjoint problems like (4.11).

The error assessment technique using the solution $\hat{\boldsymbol{\rho}}^{\mathsf{T}}$ of (4.27) and the error representation (4.28) is in practice computationally unaffordable. This is due to the multidimensional character of both $\hat{\boldsymbol{\rho}}^{\mathsf{T}}$ and $\hat{\mathbf{R}}(\mathbf{V}_a)$, which are tensors of order $n \times n_q \times n_r \times n_t$. Moreover, once $\hat{\boldsymbol{\rho}}^{\mathsf{T}}$ and $\hat{\mathbf{R}}(\mathbf{V}_a)$ are obtained, all the tensorial dimensions must be contracted (this requires four nested loops) to compute the

scalar quantity E_{QoI}. In the following, a numerical strategy that condensates all the parametric dimensions in order to devise an amenable error assessment methodology is introduced.

4.2.2 Error estimates

The QoI introduced in (4.16) (or its matrix form (4.17)) is integrating the effect of the parametric dimensions and one expects the resulting problem to depend only on the physical dimension (represented here by the vector of voltages of size n). Accordingly, it is expected to provide an error representation having the form

$$E_{QoI} = (\hat{\rho}^A)^\mathsf{T} \hat{R}^A(\mathbf{V}_a), \tag{4.29}$$

where $\hat{\rho}^A$ and $\hat{R}^A(\mathbf{V}_a)$ are vectors in $\mathbb{R}^{2n}$ that have to be obtained condensing the parametric dimensions (here, integrating with respect to parameter r).

The condensation of $\hat{\mathbf{R}}(\mathbf{V}_a) \in \mathbb{R}^{2n \times n_r}$ and $\underline{\mathbf{C}} \in \mathbb{R}^{2n \times 2n \times n_r}$ into $\hat{R}^A(\mathbf{V}_a) \in \mathbb{R}^{2n}$ and $\mathbf{C}^A \in \mathbb{R}^{2n \times 2n}$ (superscript A is used to denote that the quantities are condensed into an *accumulated* value) is readily obtained by just integrating the parametric dimension, namely

$$\hat{R}^A(\mathbf{V}_a) = \int_r \hat{R}(\cdot, r)\, dr = \hat{\mathbf{R}}(\mathbf{V}_a) \mathbf{M}_r \mathbb{1}_{n_r}, \tag{4.30}$$

and

$$\mathbf{C}^A = \int_r \underline{\mathbf{C}}(\cdot, \cdot, r)\, dr = \underline{\mathbf{C}}\, \mathbf{M}_r \mathbb{1}_{n_r}. $$

It is assumed that there exists some vector $\hat{E}^A \in \mathbb{R}^{2n}$, representing an *average* value of $\hat{\mathbf{E}}(\cdot, r)$, such that

$$\int_r \underline{\mathbf{C}}(\cdot, \cdot, r) \odot \hat{\mathbf{E}}(\cdot, r)\, dr = \mathbf{C}^A \hat{E}^A. \tag{4.31}$$

Consequently, the equation for the mean error $\hat{E}^A$ is precisely the following linear system of dimension $2n$

$$\mathbf{C}^A \hat{E}^A = \hat{R}^A(\mathbf{V}_a). \tag{4.32}$$

Note that the existence of vector $\hat{E}^A$ is guaranteed by the integral Mean Value Theorem applied to the left-hand-side of (4.26), under the hypothesis of having a

continuous dependence of $\hat{\mathbf{E}}(\cdot, r)$ on r. In this case, there exists some value of r such that $\hat{E}^A = \hat{\mathbf{E}}(\cdot, r)$. Note that continuity of $\hat{\mathbf{E}}(\cdot, r)$ is ensured by the continuity of the parametric description of the solution $\mathbf{V}_a(r)$. If the modes are not continuous, the existence of $\hat{E}^A$ is also guaranteed provided that $\mathbf{C}^A$ is a regular matrix. In this case, $\hat{E}^A$ does not necessarily coincide with any value of $\hat{\mathbf{E}}(\cdot, r)$.

In the parametric case, the error in the QoI reads

$$E_{QoI} = L(\mathbf{V}) - L(\mathbf{V}_a) = \int_r \operatorname{diag}(\hat{\boldsymbol{\lambda}}_p(\cdot, r)^{\mathsf{T}} \hat{\mathbf{E}}(\cdot, r)) \, dr = \operatorname{diag}(\hat{\boldsymbol{\lambda}}_p^{\mathsf{T}} \hat{\mathbf{E}}) \mathbf{M}_r \mathbb{1}_{n_r}, \quad (4.33)$$

where the last term in the right uses the multidimensional tensor structure to express the integrals along the r range by a scalar product.

An accumulated value of $\hat{\boldsymbol{\lambda}}_p$, $\hat{\lambda}^A \in \mathbb{R}^{2n}$, is readily introduced

$$\hat{\lambda}^A = \int_r \hat{\boldsymbol{\lambda}}_p(\cdot, r) \, dr = \hat{\boldsymbol{\lambda}}_p \mathbf{M}_r \mathbb{1}_{n_r}.$$

In order to obtain a suitable error representation, it must be take for granted that the following assumption is true.

Assumption 1. The quantity of interest E_{QoI} is expressed using the accumulated value of $\hat{\boldsymbol{\lambda}}_p$ and the vector $\hat{E}^A$, that is to say,

$$E_{QoI} = (\hat{\lambda}^A)^{\mathsf{T}} \hat{E}^A.$$

This can be interpreted as a new application of the mean value theorem in (4.33), with the additional assumption that the *average* value of $\hat{E}$ is again $\hat{E}^A$. Actually in this case there is no a unique average value: there exist an affine space of dimension $2n - 1$ where all the possible vectors $\hat{E}^A$ fulfilling the equation above lie. Thus, the assumption claiming that $\hat{E}^A$ from equation (4.31) fulfils also (4.33) (at least approximately) is very likely to hold. This assumption is further supported by noting that the dependence on r of $\underline{\mathbf{C}}$ and $\hat{\boldsymbol{\lambda}}_p$ is directly given by the dependence on r of $\mathbf{V}_a$ (the matrices $\mathbf{F}$, $\mathbf{G}$, $\mathbf{A}$ and $\mathbf{B}$ and the tensors $\underline{\mathbf{A}}$ and $\underline{\mathbf{B}}$ depend on the solution $\mathbf{V}_a$ linearly). Thus, the dominant r mode in $\mathbf{V}_a$ is going to be the dominant r mode also in $\underline{\mathbf{C}}$ and $\hat{\boldsymbol{\lambda}}_p$ and hence $\hat{E}^A$ from equation (4.31) is expected to fulfil also (4.33). An error indicator is introduced in section 4.3.1 in order to numerically check the validity of assumption 1.

Hence, the dual problem in the condensed form reads

$$\mathbf{C}^{A\mathsf{T}}\hat{\rho}^A = \hat{\lambda}^A \,, \tag{4.34}$$

and the corresponding error representation is

$$E_{QoI} = (\hat{\rho}^A)^\mathsf{T}\hat{R}^A(\mathbf{V}_a) \,. \tag{4.35}$$

Thus, also in the parametric form of the problem, the error in the quantity of interest can be affordably assessed by solving the condensed dual problem (4.34) and computing the error estimate using (4.35).

4.3 Simulation results

4.3.1 Tolerances and stopping criteria

The aim at introducing the goal-oriented error estimates in the algorithm 1 presented in chapter 3 is to control the accuracy of the approximation solution through the incorporation of stopping criteria into the procedure. Hence, a new value for the error indicators $\xi_\star^\square$ is introduced when $\square = QoI$ for the error in the quantity of interest as described above. The definitions of the additional error indicators are:

1. Loop in γ

$$\xi_\gamma^{QoI} = \frac{|(\hat{\rho}^A)^\mathsf{T}\hat{R}^A(\mathbf{V}_a^{[\gamma+1]})|}{|L(\mathbf{V}_a^{[\gamma+1]})|} \tag{4.36}$$

2. Loop in M

$$\xi_M^{QoI} = \frac{|\hat{\lambda}^\mathsf{T}(\mathbf{V}_a^{[\gamma],M} - \mathbf{V}_a^{[\gamma],M-1})|}{|L(\mathbf{V}_a^{[\gamma]})|} \,, \tag{4.37}$$

Moreover, in order to check the stabilization of $\hat{\lambda}^A$ and $\hat{\rho}^A$, the following indicator is introduced:

$$d_\rho = \frac{\|\rho^{A[\gamma+1]} - \rho^{A[\gamma]}\|_2}{\|\rho^{A[\gamma+1]}\|_2} \,. \tag{4.38}$$

If the value of d_ρ is small enough, the assumption on the stability of $\hat{\rho}^A$ is going to be confirmed. Besides, for checking that the assumption 1 holds, another indicator is introduced:

$$e_{\hat{E}} = \frac{|E_{QoI} - (\hat{\lambda}^A)^\mathsf{T} \hat{E}^A|}{|E_{QoI}|}. \tag{4.39}$$

Note that $\hat{E}^A$ is computed using equation (4.32) straightforwardly.

Similarly, the verification of the obtained solution and the corresponding losses is performed with the following error measures (with respect to a reference solution $\mathbf{V}$):

$$e_V = \frac{\|\mathbf{V} - \mathbf{V}_a\|_2}{\|\mathbf{V}\|_2} \tag{4.40}$$

$$e_L = \frac{\|l(\mathbf{V}) - l(\mathbf{V}_a)\|_2}{\|l(\mathbf{V})\|_2}. \tag{4.41}$$

4.3.2 Illustrative Examples

In all the following examples, the algorithm 1 is applied to both the algebraic and parametric version of the power flow problem taking into account the proposed goal-oriented error estimates.

The diagram of the test system is shown in figure 4.1. The model, taken from Martinez and Guerra (2013); Guerra and Martinez-Velasco (2016), is a three-phase system with different topologies and load characteristics including a simplified representation of the high-voltage system. The three-phase grid has 256 nodes (located in 3 different branches), and therefore the number of degrees of freedom is $n = 3 \times 256 = 768$. However, the number of geometrical nodes in figure 4.1 is only 155, numbered from $a701$ to $a777$ (first branch), from $b701$ to $b746$ (second branch), from $c701$ to $c729$ (third branch), and three more: $a700$ connecting the three branches, the transformer and the slack node. The additional 101 nodes correspond to the duplication of the 101 nodes of the mesh where the distributed generator (DG) can be located. These new 101 nodes are identified by adding an l, for instance $lc701$ is the duplication of $c701$. This duplication is necessary because each DG is connected to the system through a step-up interconnection transformer allowing the switch from high-voltage to low-voltage.

Some of the main characteristics of the substation transformer are given below:

- High-voltage rating: 230 kV

- Low-voltage rating: 4.16 kV
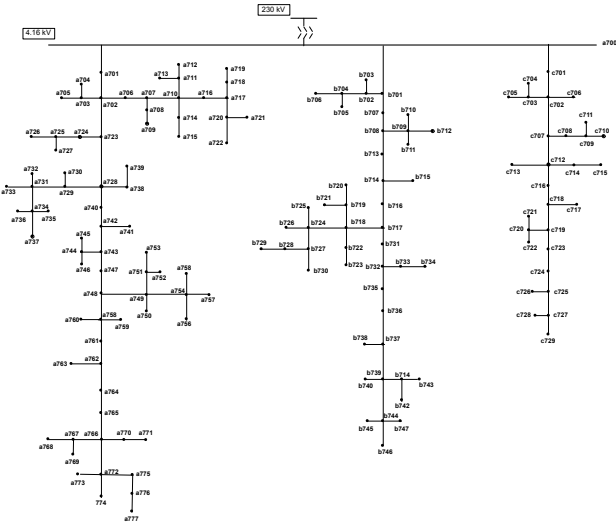
Figure 4.1: Diagram of the test system network

The main objective in the below examples is to solve an optimization problem: find the optimal position and power of a distributed generator that minimizes the system losses, quantity of interest in this work. Considering the error assessment in the implementation of the solver allows one to compute the solution taking them into consideration. As a first step, the computation of the solution is carried out while the evaluation for calculating the losses is seen as a post-process or second step where the value that optimizes the problem statement is sought.

4.3.2.1 Example 1: Algebraic approach

The efficiency of the procedure for linearizing the residual and the losses equation explained in section 4.1 is shown in this first example. In this case, fixing the position $q = lc707$, the power $r = 850$ kW of the DG and the hour of the year $t = 759$, the power flow problem associated with these values is solved. Consequently, $n_q, n_r, n_t = 1$ and the number of degrees of freedom is $n = 768$.

For computing the relative errors, for instance e_L, it is considered as real so-lution the one calculated using Newton-Raphson algorithm while tolerances tol_γ^R, tol_γ^S and $\mathrm{tol}_\gamma^{QoI}$ are 10^{-8}. As mentioned above, it is not necessary to calculate the solution of the dual problem at every γ iteration. In figure 4.2(a), it is observed this fact, plotting ξ_γ^{QoI} and $\xi_{\hat{\gamma}}^{QoI}$. Note that the notation $\xi_{\hat{\gamma}}^{QoI}$ for indicating that the vector $\hat{\rho}$ is just calculated until the tolerance for the indicator d_ρ is reached is introduced, in this particular case that tolerance is 10^{-3}. The standard nota-tion ξ_γ^{QoI} implies that the dual problem is solved at every single iteration. It is noticed that $\hat{\rho}$ barely changes, thus the E_{QoI} does not either. In this example the stability is evident, as figure 4.2(b) shows after only 4 iterations the indicator d_ρ verifies that $d_\rho < 10^{-4}$, and the same fact was noticed in other simulations. That is the reason why from now on in the examples below, once the tolerance for the indicator d_ρ is reached, the vector $\hat{\rho}$ is reused in the following iterations. Hence at some point, the cost of calculating the error in the quantity of interest has the same computational cost as the residual calculation because there is no need to update $\mathbf{C}$, $\hat{\lambda}$ or $\hat{\rho}$.

Figure 4.3(a) shows the growth of ξ_γ^{QoI} when $\mathrm{tol}_\gamma^{QoI}$ increases. The numbers in the graph represent the number of iterations required until the tolerance is reached. It is logically observed that this number decreases when $\mathrm{tol}_\gamma^{QoI}$ increases. Moreover, in order to show the efficiency of the error indicator ξ_γ^{QoI} used as stopping criteria in the algorithm, the effectivity index is shown in figure 4.3(b) comparing the relative error with respect to the reference solution e_L versus ξ_γ^{QoI}.

4.3.2.2   Example 2: Parametric approach

The goal in this second example is to seek the optimal nominal and position of the DG over a year when the parameter time t is introduced. Three DGs are introduced in the network, each of them is set in a different branch. The parameters associated to this problem are the position of the DGs q_1, q_2 and q_3, the active power of the DGs r_1, r_2 and r_3 and the time t. The representation of the solution is given by

$$\mathbf{V}_a = \sum_{m=1}^M \alpha_V^m V^m \otimes \mathcal{Q}^m \otimes \mathcal{R}^m \otimes \mathcal{T}^m \,, \tag{4.42}$$
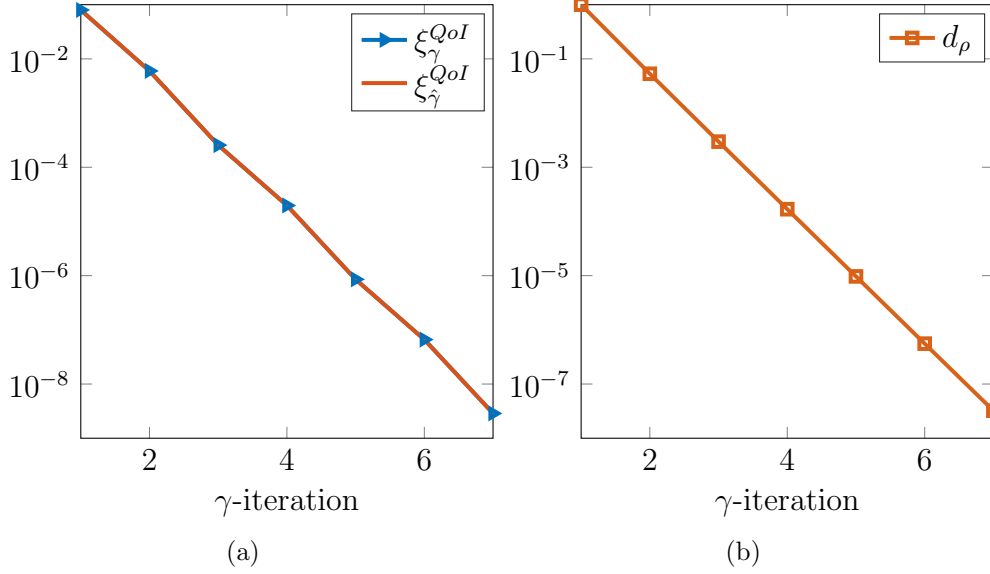
Figure 4.2: Convergence diagrams at iteration γ. (a)Relative error in the losses and error in quantity of interest with the iteration index γ. (b)Stagnation criteria for the solution of the dual problem ρ.

while the representation of the load term $\mathbf{S}$ requires more terms:

$$
\mathbf{S} = \sum_{h=1}^{24} \alpha_S^h \breve{S}^h \otimes \breve{Q}^h \otimes \breve{\mathcal{R}}^h \otimes \breve{\mathcal{T}}^h + \alpha^1 S^1 \otimes \mathcal{Q}^1 \otimes \mathcal{R}^1 \otimes \mathcal{T}^1 + \alpha^2 S^2 \otimes \mathcal{Q}^2 \otimes \mathcal{R}^2 \otimes \mathcal{T}^2 +
$$
$$
+ \alpha^3 S^3 \otimes \mathcal{Q}^3 \otimes \mathcal{R}^3 \otimes \mathcal{T}^3 ,
$$
(4.43)

where $\forall l = 1, 2, 3$ S^l are n vectors representing the nodal positions of the network, $\mathcal{Q}^l$ are zero vectors of n_q components except for the position of the DGs and $\mathcal{R}^l$ corresponds to the variation of the power. The functions $\mathcal{T}^l$ expresses the load curves that represent the DGs for every hour of the year. Apart from these three terms, the load demand and the generation profiles during a year are represented by the load curves $\breve{\mathcal{T}}^h(t), \forall h = 1, \ldots, 24$. For this particular system, 24 load curves were generated using the software HOMER described in Lambert et al. (2006). These load curves are mainly based on solar and wind data but also depend on the customer type (commercial, industrial or residential).

(a)   (b)
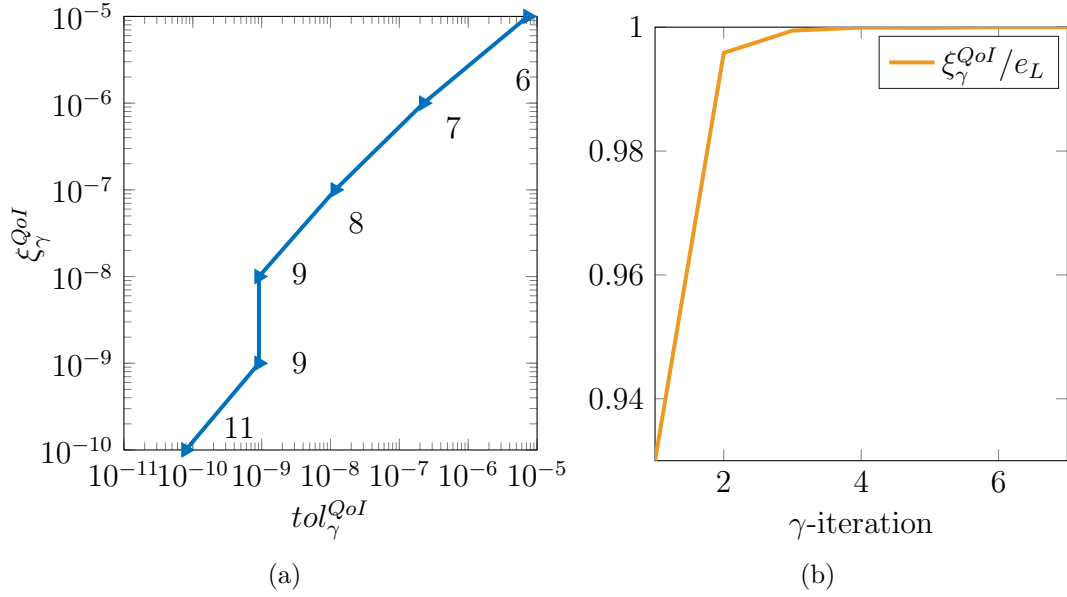
Figure 4.3: Diagrams of E_{QoI} and effectivity index. (a)Error in the quantity of interest for different simulations varying the tolerances. The numbers reported on the curve represent number of iterations. (b)Effectivity index in the losses.

The parametric modes in the representation of $\mathbf{V}_a$ and $\mathbf{S}$ are discretized in the parametric space. Specifically, the parameters q_1, q_2 and $q_3 \in I_q = [1, q_{max}]$ where $q_{max} = 19$ is the number of possible location for the DG in the three branches at the same time, thus $n_q = 19$. Due to the characteristics of the first two branches, the variation of r_1 and r_2 is the same, that is, the partition of the interval $I_{r_1} = [0, r_{max_1}]$ where the increment is $r_{max_1}/(n_r - 1)$ with $r_{max_1} = 400$ kW and n_r is equal to 100. The generator situated in the third branch can provide a maximum power of 2200 kW, thus the parameter r_3 varies in the interval $I_{r_2} = [0, r_{max_2}]$ with $r_{max_2} = 2000$ kW. The time parameter t is varied from 1 to 8760 with a time step of 1h, thus $n_t = 8760$.

The goal is to set different tolerances and compare the obtained solutions in order to validate the goal-oriented error estimates in terms of controlling the quality of the approximations. In figure 4.4, the stopping criteria for γ and M respectively for the first set of tolerances in the algorithm, $\text{tol}_\gamma^\square = 10^{-4}$, $\text{tol}_M^\square = 10^{-5}$ and

$\text{tol}_k^\square = 10^{-6}$ for $\square = S, R, QoI$ are shown in figures 4.4(a) and 4.4(b). The numbers in 4.4(a) represent the amount of modes that the solution contains at every iteration γ. In this case, the final solution consists of 41 modes after 9 iterations. It is remarkable that in all M iterations, at some point the criterion ξ_M^R stabilizes after some iterations. This is possible because at every iteration M, a new term is added hence more information is considered. However,it is possible that the added information is not enough for changing significantly the quality of the solution, thus the residual in the first step of the algorithm does not decrease.

The same quantities are shown in figures 4.5(a) and 4.5(b) but the fixed tolerances are $\text{tol}_\gamma^\square = 10^{-5}$, $\text{tol}_M^\square = 10^{-6}$ and $\text{tol}_k^\square = 10^{-7}$ for $\square = S, R, QoI$ in this case. As can be seen, the amount of terms of the solution changes, more terms are needed, 52 in this simulation and also the number of iterations 9 against 15.

The introduction of error estimators in the algorithm 1 allows to control the whole procedure and specifically the construction of the solution $\mathbf{V}_a$. By adding more modes to the final solution, its accuracy can increase when it is compared to the solution obtained using the algebraic version of the algorithm (it is used as reference solution). In figures 4.4(c) and 4.5(c) where the relatives error are plotted this fact is observed, the accuracy of the solution and the losses improve when the tolerances are lower because the solution has more modes, i.e. 52 versus 41, thus it is more precise.

Besides, in figure 4.6, the proof that the assumption 1 holds in the numerical examples is shown using the indicator $e_{\hat{E}}$. At every γ iteration, the difference between the two average vectors $\hat{E}^A$ is insignificant.

The reconstruction of the losses is shown in figure 4.7 where the positions of the DGs $la724, lb726$ and $lc726$ that provided the annual optimal losses 341 kW can be seen. In terms of the parameters, the values that provide this minimal loss are $r_1 = 121$ kW, $r_2 = 365$ kW and $r_3 = 311$ kW. More examples are detailed in García-Blanco et al. (2016a).

(a)

(b)

(c)
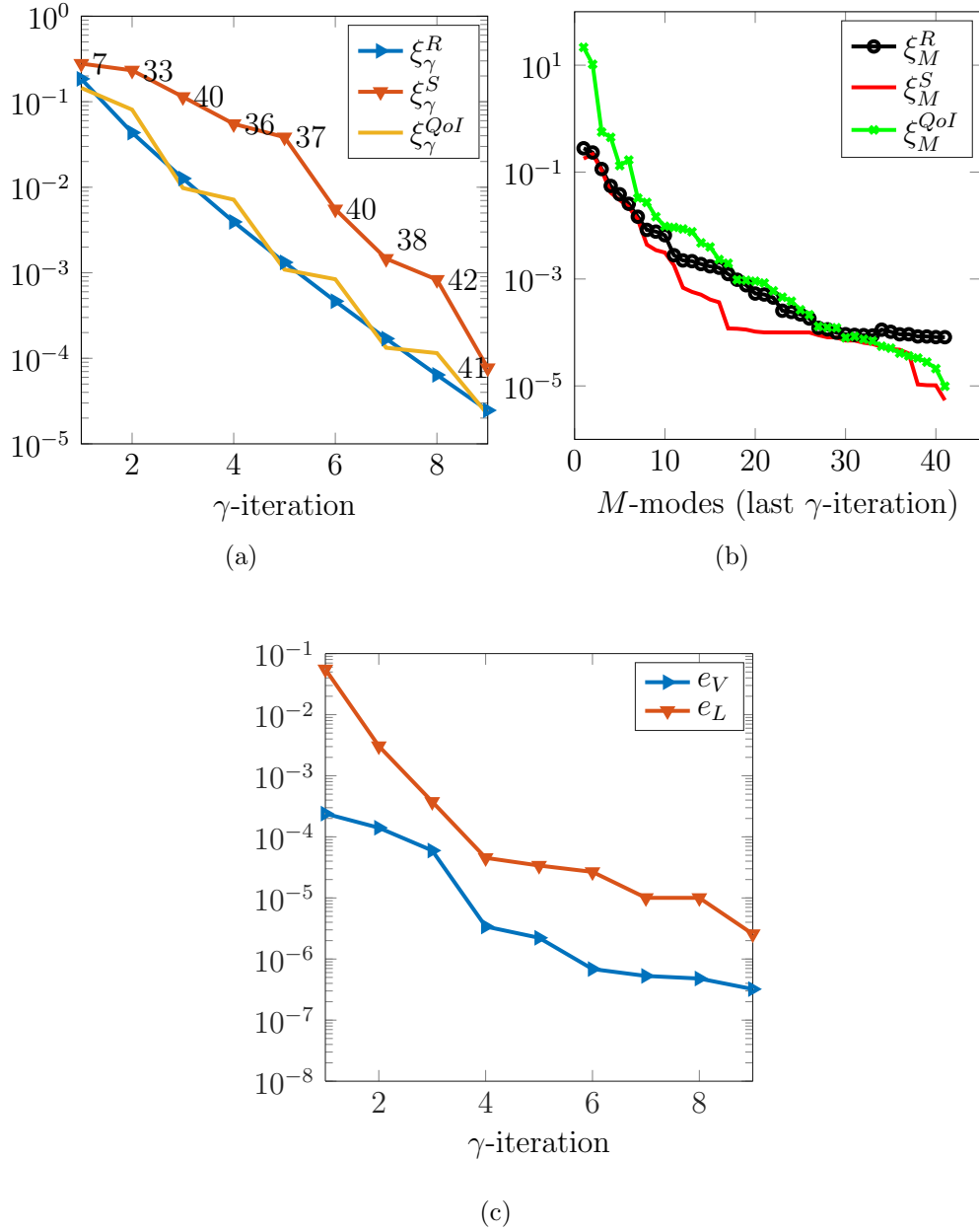
Figure 4.4: Diagrams of convergence when the tolerances are $\text{tol}_\gamma^\square = 10^{-4}$, $\text{tol}_M^\square = 10^{-5}$ and $\text{tol}_k^\square = 10^{-6}$. (a)Convergence diagram of the stopping criteria for the outer loop with the iteration index γ. The numbers along the curves refer to the number of modes that the solution contains. (b)Convergence diagram of the enrichment algorithm in the last M iteration (last γ-iteration). (c)Relative errors comparing the real and the approximated solution.

(a)

(b)

(c)
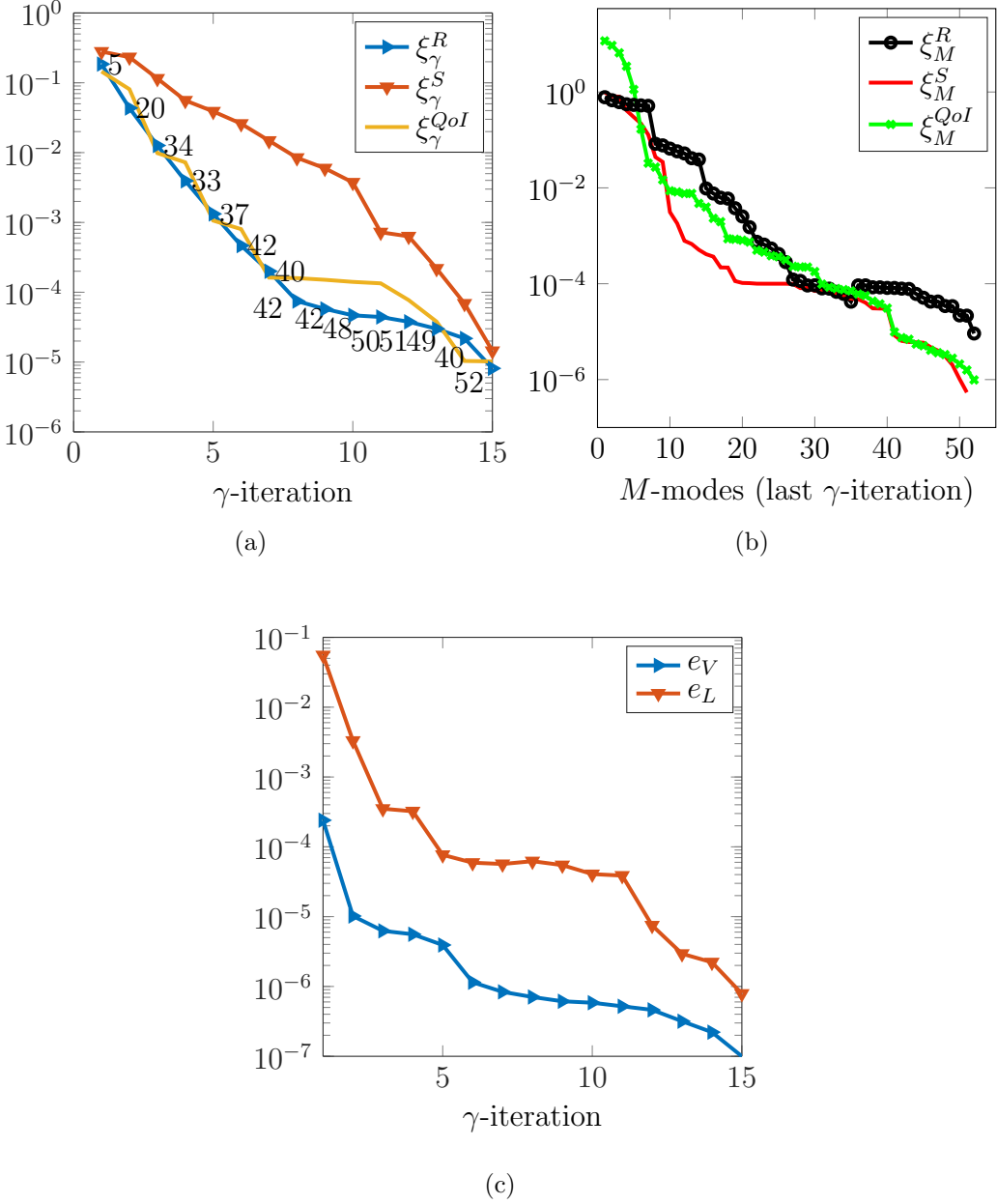
Figure 4.5: Diagrams of convergence when the tolerances are $\text{tol}_\gamma^\square = 10^{-5}$, $\text{tol}_M^\square = 10^{-6}$ and $\text{tol}_k^\square = 10^{-7}$. (a)Convergence diagram of the stopping criteria for the outer loop with the iteration index γ. The numbers along the curves refer to the number of modes that the solution contains. (b)Convergence diagram of the enrichment algorithm in the last M iteration (last γ-iteration). (c)Relative errors comparing the real and the approximated solution.
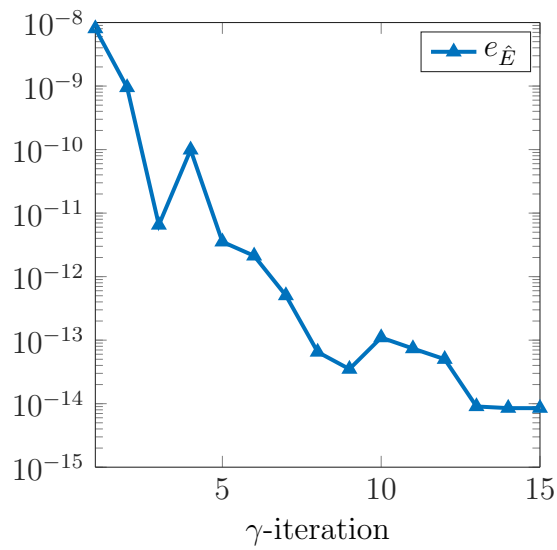
Figure 4.6: Convergence diagram of the error indicator $e_{\hat{E}}$ with the iteration index γ.
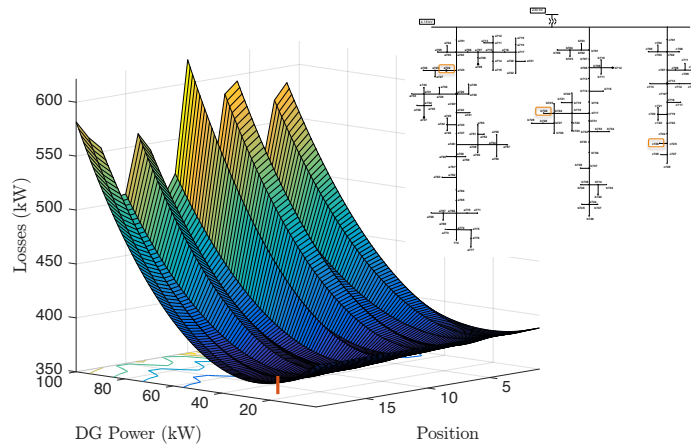

Figure 4.7: Reconstructed System Losses

Chapter 5

Conclusions

In the following chapter, the main contributions of this thesis are summarized and research lines for future development are presented.

5.1 Contributions

- **A family of iterative solvers for the power flow problem**

  The power flow equations are quadratic equations, but just one of the mathematical solutions corresponds to the physical, high voltage or operative solution. One classical adversity for the power flow solvers is that the convergence to the physical solution is not always guaranteed. Besides this, when the number of nodes in the network is considerably large, assemble the Jacobian matrix may be computationally unfordable. Taking advantage of the algebraic structure of the governing equation (1.3), the application of the Alternating Search Directions method (ASDM) to the power flow problem was successful. As a result, a family of solvers depending on search directions emerged.

  The possibility of tuning the search directions allows achieving a good performance in term of computational time. The reason behind this is that the choice of constant search directions yield stationary methods, that is to say,

there is no need to assemble Jacobian matrices. Moreover, by construction, regardless of the choice of the search directions, the convergence to operative solution is enforced throughout the whole iterative process. Accordingly, the obtained solutions are demonstrated to be accurate because the methods are not designed based on the practical properties of the system but on the algebraic structure of the power flow problem.

Another interesting remark is the fact that, unlike Newton-Raphson and Fast Decoupled Load Flow methods, the convergence does not depend on the choice of the initial guess. There also exists the possibility of recovering classical methods choosing search directions, for instance, Gauss-Seidel, Newton-Raphson and Z-matrix bus method.

This family of methods is presented in chapter 2 and discussed in detail in paper A.

- **Successful strategy for implementing nonlinear PGD**

The optimal allocation of generators in networks requires to compute power flow calculations in different scenarios. Hence, the introduction of parameters in the power flow equations is necessary. Moreover, the aim is to make decisions in real-time for operation and control of networks in case of voltage drop or other possible failures. Both ideas are represented when the solution of the problem is assumed to have a separated representation depending of numerous parameters. In order to computed the parametrized solutions, the Proper Generalized Decomposition technique is applied. Nevertheless, it is well-known that the application of the PGD methodology to nonlinear problems is not straightforward. Actually, the procedure for tackling the problem depends on the characteristics of the equations to be solved. In this thesis, PGD strategy was implemented for the power flow problem successfully. Besides, this adopted technique presents a double advantage. The separated representation of the solution scales linearly the dimension of the problem and it is easily computed as a succession of one dimensional problems. Consequently, the memory storage requirements is insignificant.

The PGD technique allows to store the information associated to the resolu-

tion of a highly dimensional problem in a compressed separated variables format. Once the PGD solution is computed in the "offline" phase and stored, the optimization can be performed effortlessly in the "online" step, because the objective function (in this case the power losses) is explicitly available, that is to say, it might be possible to optimize networks in real-time.

More details about the algorithm proposed for solving these parametrized problems and some applications are given in chapter 3 and in paper B and C.

- **Control of the accuracy of the solutions based on the Quantity of Interest**

Proper Generalized Decomposition (PGD) has been developed in diverse areas, although the associated error associated is still an open problem. An error assessment approach was applied defining stopping criteria added in the nonlinear PGD solver. These criteria guarantee that the error in the losses is lower than a prescribed tolerance.

Since the power flow problem is a system of complex equations, the development of the error assessment following standard procedures was challenging. In order to linearize the equations is necessary to use Cartesian representations of the vector and matrices. Furthermore, in the parametric version of the problem, the error in the QoI is also a number implying that the dependence on the parameters is condensed integrating the equations. In order to integrate, the Mean Value Theorem is applied and it is essential to assume that accumulated value of the errors after integrating both equations coincides. Another singular characteristic of the this procedure is that the solution of the dual problem it is observed to be stationary along the iterative process saving computational resources.

The resulting error equations and indicators are described in detail in chapter 4 and in paper D.

5.2 Open research lines

- **Improved efficiency of the family of iterative solvers by exploring optimal search directions**

  Diverse choices of the search directions in the proposed family of methods have been analyzed in this thesis. Indeed, one of them seems optimal based on the numerical results. An idea to be explored is the possibility of using a variable search direction at each iteration, which would yield non-stationary iterative methods and offer a possible margin for improvement. Besides this, the PGD technique was implemented just in the case of a particular choice of the search directions. This fact opens the possibility of choosing another combination that may improve the accuracy of the solution and even the computational time.

- **Parametrizing variation of topology as an application of the Parametric Power Flow problem**

  In this thesis, Parametric Power Flow problem was presented in the framework of optimal allocation of generators based on losses minimization. However, the availability of parametric solutions in explicit form is a commodity for many power engineering applications like power system design or real-time simulation control. Further investigation is to add parameters describing physical characteristics of the wires, all these parameters are in the admittance matrix. That way, it would be possible establish the state of a network in real-time even when the topology of the networks changes due to voltage drop or other failure.

- **Uncertainty quantification (UQ) in power systems as a post-process of the explicit parametric solution**

  Another interesting open line is to extent the parametric solutions when the input power data are random variables. For instance, the introduced generator depends on a wind farm, hence it is related to high uncertainty. Thus, the Parametric Power Flow problem would take into account random parameters. As a result after applying the PGD strategy proposed in this

thesis, the probability density function of the voltage can be represented together with other amounts of interest.

- **Advanced modeling of electrical networks**

  All examples included in this thesis and in the indexed papers are based on theoretical networks. Thus, another future goal is to incorporate realistic data to the model improving the input of the problem. As an illustration, the input power is characterized using time variations and the correlation between generators in the case of solar panels or wind turbines is also taking into account when generators are set in the grid.

Bibliography

Abido, M. (2002). Optimal power flow using particle swarm optimization. *International Journal of Electrical Power & Energy Systems 24*(7), 563–571.

Abookazemi, K., M. Y. Hassan, and M. S. Majid (2010). A review on optimal placement methods of distribution generation sources. In *Power and Energy (PECon), 2010 IEEE International Conference on*, pp. 712–716.

Acharya, N., P. Mahat, and N. Mithulananthan (2006, December). An analytical approach for DG allocation in primary distribution network. *International Journal of Electrical Power & Energy Systems 28*(10), 669–678.

Aghighi, M., A. Ammar, C. Metivier, M. Normandin, and F. Chinesta (2013). Non-incremental transient solution of the RayleighBnard convection model by using the PGD. *Journal of Non-Newtonian Fluid Mechanics 200*(0), 65 – 78. Special Issue: Advances in Numerical Methods for Non-Newtonian Flows.

Allan, R. N. and M. R. G. Al-Shakarchi (1977). Probabilistic techniques in a.c. load-flow analysis. *Electrical Engineers, Proceedings of the Institution of 124*(2), 154–160.

Amini, M. H., M. D. Ili, and O. Karabasoglu (2015). DC power flow estimation utilizing bayesian-based lmmse estimator. In *2015 IEEE Power Energy Society General Meeting*, pp. 1–5.

Ammar, A., F. Chinesta, and E. Cueto (2011). Coupling finite elements and proper generalized decompositions. *International Journal for Multiscale Computational Engineering 9*(1), 17–33.

Ammar, A., F. Chinesta, P. Diez, and A. Huerta (2010). An error estimator for separated representations of highly multidimensional models. *Computer Methods in Applied Mechanics and Engineering 199*(2528), 1872 – 1880.

Arritt, R. and R. Dugan (2010, April). The IEEE 8500-node test feeder. In *Transmission and Distribution Conference and Exposition, 2010 IEEE*, pp. 1–6.

Atwa, Y. and E. El-Saadany (2011). Probabilistic approach for optimal allocation of wind-based distributed generation in distribution systems. *Renewable Power Generation, IET 5*(1), 79–88.

Barrault, M., Y. Maday, N. C. Nguyen, and A. T. Patera (2004, November). An empirical interpolation method: application to efficient reduced-basis discretization of partial differential equations. *Comptes Rendus Mathematique 339*(9), 667–672.

Bijwe, P. R., B. Abhijith, and G. K. V. Raju (2009). Robust three phase fast decoupled power flow. In *Power Systems Conference and Exposition, 2009. PSCE '09. IEEE/PES*, pp. 1–5.

Borkowska, B. (1974, May). Probabilistic load flow. *IEEE Trans. on Power App. and Syst. PAS-93*(3), 752–759.

Borzacchiello, D., F. Chinesta, R. García-Blanco, and P. Diez (2016). Introduction to the proper generalized decomposition for the solution of the parametrized power equations. *Submitted*.

Borzacchiello, D., M. Malik, F. Chinesta, R. García-Blanco, and P. Diez (2016). Unified formulation of a family of iterative solvers for power systems analysis. *Electric Power Systems Research 140*, 201 – 208.

Brameller, A. and J. Denmead (1962). Some improved methods for digital network analysis. *Proceedings of the IEEE-Part A: Power Engineering 109*(43), 109–116.

Brown, H., G. Carter, H. Happ, and C. Person (1963). Power flow solution by impedance matrix iterative method. *Power Apparatus and Systems, IEEE Transactions on 82*(65), 1–10.

Brown, H. E., G. K. Carter, H. H. Happ, and C. E. Person (1968). Z-matrix algorithms in load-flow programs. *IEEE Transactions on Power Apparatus and Systems PAS-87*(3), 807–814.

Brown, H. E., C. E. Person, L. K. Kirchmayer, and G. W. Stagg (1960). Digital calculation of 3-phase short circuits by matrix method. *Transactions of the American Institute of Electrical Engineers. Part III: Power Apparatus and Systems 79*(3), 1277–1281.

Brown, R. J. and W. F. Tinney (1957). Digital solutions for large power networks. *Transactions of the American Institute of Electrical Engineers. Part III: Power Apparatus and Systems 76*(3), 347–351.

Chaturantabut, S. and D. Sorensen (2009a). Application of POD and DEIM on dimension reduction of non-linear miscible viscous fingering in porous media. *Mathematical and Computer Modelling of Dynamical Systems*.

Chaturantabut, S. and D. Sorensen (2009b, Dec). Discrete empirical interpolation for nonlinear model reduction. In *Decision and Control, 2009 held jointly with the 2009 28th Chinese Control Conference. CDC/CCC 2009. Proceedings of the 48th IEEE Conference on*, pp. 4316–4321.

Chaturantabut, S. and D. Sorensen (2010). Nonlinear model reduction via discrete empirical interpolation. *SIAM Journal on Scientific Computing 32*(5), 2737–2764.

Chen, J. and Y. Liao (2012). State estimation and power flow analysis of power systems. *JOURNAL OF COMPUTERS 7*(3), 685.

Chen, P., Z. Chen, and B. Bak-Jensen (2008, April). Probabilistic load flow: A review. In *Electric Utility Deregulation and Restructuring and Power Technologies, 2008. DRPT 2008. Third International Conference on*, pp. 1586–1591.

Chen, Y. and C. Shen (2006). A Jacobian-free Newton-GMRES (m) method with adaptive preconditioner and its application for power flow calculations. *Power Systems, IEEE Transactions on 21*(3), 1096–1103.

Cheng, C. . F. Z. (1997). A modified Newton method for radial distribution system power flow analysis. *IEEE Transactions on Power Systems 12*(1), 389–397.

Chiang, H. D., T. Q. Zhao, J. J. Deng, and K. Koyanagi (2014). Convergence/divergence analysis of implicit Z-bus power flow for general distribution networks. In *2014 IEEE International Symposium on Circuits and Systems (IS-CAS)*, pp. 1808–1811.

Chinesta, F., A. Ammar, and E. Cueto (2010). Recent advances and new challenges in the use of the proper generalized decomposition for solving multidimensional models. *Archives of Computational methods in Engineering 17*(4), 327–350.

Chinesta, F., P. Ladeveze, and E. Cueto (2011, October). A Short Review on Model Order Reduction Based on Proper Generalized Decomposition. *Archives of Computational Methods in Engineering 18*(4), 395–404.

Chinesta, F., A. Leygue, F. Bordeu, J. Aguado, E. Cueto, D. Gonzalez, I. Alfaro, A. Ammar, and A. Huerta (2013a). PGD-based computational vademecum for efficient design, optimization and control. *Archives of Computational Methods in Engineering 20*(1).

Chinesta, F., A. Leygue, F. Bordeu, J. V. Aguado, E. Cueto, D. Gonzalez, I. Alfaro, A. Ammar, and A. Huerta (2013b, January). Pgd-based computational vademecum for efficient design, optimization and control. *Archives of Computational Methods in Engineering 20*(1), 31–59.

De Leon, F. and A. Semlyen (2002). Iterative solvers in the Newton power flow problem: preconditioners, inexact solutions, and partial jacobian updates. *IEEE Proceedings-Generation, Transmission and Distribution 149*(4), 479–484.

De Souza, A., C. Junior, I. Lima Lopes, R. Leme, and O. Carpinteiro (2007, May). Non-iterative load-flow method as a tool for voltage stability studies. *IET Gener. Transm. Distrib. 1*(3), 499–505.

Derakhshandeh, S. Y. and R. Pourbagher (2016). Application of high-order Newton-like methods to solve power flow equations. *IET Generation, Transmission Distribution 10*(8), 1853–1859.

Dimitrovski, A. and K. Tomsovic (2004, Sept). Slack bus treatment in load flow solutions with uncertain nodal powers. In *Probabilistic Methods Applied to Power Systems, 2004 International Conference on*, pp. 532–537.

Dommel, H. and W. Tinney (1968, Oct). Optimal power flow solutions. *IEEE Trans. on Power App. and Syst. PAS-87*(10), 1866–1876.

Dopazo, J. F., O. A. Klitin, and A. M. Sasson (1975). Stochastic load flows. *IEEE Transactions on Power Apparatus and Systems 94*(2), 299–309.

Dugan, R. and T. McDermott (2013, june). *Reference Guide. The Open Distribution System Simulator*.

El-Khattam, W., Y. G. Hegazy, and M. M. A. Salama (2003). Stochastic power flow analysis of electrical distributed generation systems. In *Power Engineering Society General Meeting, 2003, IEEE*, Volume 2, pp. 1144 Vol. 2.

Elgerd, O. I. (1972). *Electric Energy Systems Theory*. New York: McGraw-Hill.

Fang, S., H. Cheng, G. Xu, L. Yao, and P. Zeng (2014). A stochastic power flow method based on polynomial normal transformation and quasi monte carlo simulation. In *Power System Technology (POWERCON), 2014 International Conference on*, pp. 75–82.

Favuzza, S., G. Graditi, M. Ippolito, and E. Sanseverino (2007, May). Optimal electrical distribution systems reinforcement planning using gas micro turbines by dynamic ant colony search algorithm. *Power Systems, IEEE Transactions on 22*(2), 580–587.

Florentin, E. and P. Díez (2012). Adaptive reduced basis strategy based on goal oriented error assessment for stochastic problems. *Computer Methods in Applied Mechanics and Engineering 225228*, 116 – 127.

Frank, S., I. Steponavice, and S. Rebennack (2012). Optimal power flow: a bibliographic survey I. *Energ. Syst. 3*(3), 221–258.

Galbally, D., K. Fidkowski, K. Willcox, and O. Ghattas (2010). Non-linear model reduction for uncertainty quantification in large-scale inverse problems. *International Journal for Numerical Methods in Engineering 81*(12), 1581–1608.

Gandomkar, M., M. Vakilian, and M. Ehsan (2005). A combination of genetic algorithm and simulated annealing for optimal dg allocation in distribution networks. In *Canadian Conference on Electrical and Computer Engineering, 2005.*, pp. 645–648.

Garcia, P., J. Pereira, J. Carneiro, S., V. Da Costa, and N. Martins (2000). Three-phase power flow calculations using the current injection method. *IEEE Trans. Power Syst. 15*(2), 508–514.

García-Blanco, R., D. Borzacchiello, F. Chinesta, and P. Diez (2016a). Monitoring a PGD solver for parametric power flow problems with goal-oriented error assessment. To appear in. *Int. J. Numer. Meth. Engng.*.

García-Blanco, R., D. Borzacchiello, F. Chinesta, and P. Diez (2016b, April). A reduced order modeling approach for optimal allocation of distributed generation in power distribution systems. In *Energy Conference (ENERGYCON), 2016 IEEE International*.

Georgilakis, P. and N. Hatziargyriou (2013). Optimal distributed generation placement in power distribution networks: Models, methods, and future research. *Power Systems, IEEE Transactions on 28*(3), 3420–3428.

Glimn, A. and G. Stagg (1957). Automatic calculation of load flows. *Power apparatus and systems, Part III. transactions of the american institute of electrical engineers 76*(3), 817–825.

Gómez-Expósito, A., A. J. Conejo, and C. Cañizares (2008). *Electric energy systems: analysis and operation*. CRC Press.

Grainer, J. J. and W. Stevenson (2008). *Power System Analysis*.

Griffin, T., K. Tomsovic, and A. Law. Placement of dispersed generation systems for reduced losses. In *Proceedings of the 33rd Hawaii International Conference on System Sciences- 2000*, Number c, pp. 1–9.

Guerra, G. and J. A. Martinez-Velasco (2016). Optimum allocation of distributed generation in multi-feeder systems using long term evaluation and assuming voltage-dependent loads. *Sustainable Energy, Grids and Networks 5*, 13 – 26.

Gupta, N. (2016). A review on the inclusion of wind generation in power system studies. *Renewable and Sustainable Energy Reviews 59*, 530 – 543.

Gupta, P. and M. Humphrey Davies (1961). Digital computers in power system analysis. *Proceedings of the IEEE-Part A: Power Engineering 108*(41), 383–398.

G.W.Stagg and A.H.El-Abiad (1968). *Computer Methods in Power System-Analysis*. New York: McGraw-Hill.

Hale, H. and R. Goodrich (1959). Digital computation or power flow - some new aspects. *Power Apparatus and Systems, Part III. Transactions of the American Institute of Electrical Engineers 78*(3), 919–923.

He, J., B. x. Zhou, Q. Zhang, Y. c. Zhao, and J. h. Liu (2012). An improved power flow algorithm for distribution networks based on Z-bus algorithm and forward/backward sweep method. In *Control Engineering and Communication Technology (ICCECT), 2012 International Conference on*, pp. 1–4.

Hinze, M. and M. Kunkel (2012). Discrete empirical interpolation in POD model order reduction of drift-diffusion equations in electrical networks. In B. Michielsen and J.-R. Poirier (Eds.), *Scientific Computing in Electrical Engineering SCEE 2010*, Mathematics in Industry, pp. 423–431. Springer Berlin Heidelberg.

Hochman, A., B. N. Bond, and J. K. White (2011). A stabilized discrete empirical interpolation method for model reduction of electrical, thermal, and microelectromechanical systems. In *Proceedings of the 48th Design Automation Conference on - DAC '11*, New York, New York, USA, pp. 540. ACM Press.

Huneault, M. and F. Galiana (1991, May). A survey of the optimal power flow literature. *IEEE Trans. Power Syst. 6*(2), 762–770.

Idema, R., D. Lahaye, K. Vuik, and L. van der Sluis (2010). Fast newton load flow. In *IEEE PES T D 2010*, pp. 1–7.

Idema, R., D. J. Lahaye, C. Vuik, and L. Van der Sluis (2012). Scalable Newton-Krylov solver for very large power flow problems. *Power Systems, IEEE Transactions on 27*(1), 390–396.

Idema, R., G. Papaefthymiou, D. Lahaye, C. Vuik, and L. van der Sluis (2013). Towards faster solution of large power flow problems. *IEEE Transactions on Power Systems 28*(4), 4918–4925.

Iwamoto, S. and Y. Tamura (1981). A load flow calculation method for ill-conditioned power systems. *Power Apparatus and Systems, IEEE Transactions on* (4), 1736–1743.

Kim, J. O., S. K. Park, K. W. Park, and C. Singh. Dispersed Generation Planning Using Improved Hereford Ranch Algorithm. In *1998 IEEE International Conference on Evolutionary Computation Proceedings. IEEE World Congress on Computational Intelligence*, pp. 0–5.

Kim, K.-H., Y.-J. Lee, S.-B. Rhee, S.-K. Lee, and S.-K. You (2002). Dispersed generator placement using fuzzy-ga in distribution systems. In *Power Engineering Society Summer Meeting, 2002 IEEE*, Volume 3, pp. 1148–1153 vol.3.

Knoll, D. and D. Keyes (2004). Jacobian-free NewtonKrylov methods: a survey of approaches and applications. *Journal of Computational Physics 193*(2), 357 – 397.

Ladevèze, P. and J. Simmonds (1999). *Nonlinear Computational Structural Mechanics: New Approaches and Non-Incremental Methods of Calculation*. Mechanical Engineering Series. Springer New York.

Lambert, T., P. Gilman, and P. Lilienthal (2006). *Micropower System Modeling with HOMER*. John Wiley.

Laughton, M. A. and M. W. H. Davies (1964). Numerical techniques in solution of power-system load-flow problems. *Electrical Engineers, Proceedings of the Institution of 111*(9), 1575–1588.

Li, G. and X. P. Zhang (2009). Comparison between two probabilistic load flow methods for reliability assessment. In *2009 IEEE Power Energy Society General Meeting*, pp. 1–7.

Li, Y., Y. Luo, B. Zhang, and C. Mao (2011). A modified Newton-Raphson power flow method considering wind power. In *Power and Energy Engineering Conference (APPEEC), 2011 Asia-Pacific*, pp. 1–5.

Lin, G., M. Elizondo, S. Lu, and X. Wan (2014). Uncertainty quantification in dynamic simulations of large-scale power system models using the high-order probabilistic collocation method on sparse grids. *Int. J. Uncert. Quant. 4*(3), 185–204.

Lin, W.-M. and J.-H. Teng (2000, June). Three-phase distribution network fast-decoupled power flow solutions. *International Journal of Electrical Power & Energy Systems 22*(5), 375–380.

Maffei, A., L. Iannelli, and L. Glielmo (2015). A colored Gauss-Seidel approach for the distributed network flow problem. In *2015 54th IEEE Conference on Decision and Control (CDC)*, pp. 4934–4939.

Martinez, J. A. and G. Guerra (2012). Optimum placement of distributed generation in three-phase distribution systems with time varying load using a Monte Carlo approach. In *Power and Energy Society General Meeting, 2012 IEEE*, pp. 1–7. IEEE.

Martinez, J. A. and G. Guerra (2013). A monte carlo approach for distribution reliability assessment considering time varying load and system reconfiguration.

Martinez, J. A. and G. Guerra (2014, Nov). A parallel monte carlo method for optimum allocation of distributed generation. *IEEE Transactions on Power Systems 29*(6), 2926–2933.

Mithulananthan, N., T. Oo, and L. V. Phu (2004). Distributed Generator in Power Distribution Placement System Using Genetic Algorithm to Reduce Losses. *Thammasat International Journal of Science and Technology 9*(3).

Monticelli, A., A. Garcia, and O. Saavedra (1990). Fast decoupled load flow: hypothesis, derivations, and testing. *Power Systems, IEEE Transactions on 5*(4), 1425–1431.

Mozolevski, I. and S. Prudhomme (2015). Goal-oriented error estimation based on equilibrated-flux reconstruction for finite element approximations of elliptic problems. *Computer Methods in Applied Mechanics and Engineering 288*, 127 – 145. Error Estimation and Adaptivity for Nonlinear and Time-Dependent Problems.

Nara, K., Y. Hayashi, K. Ikeda, and T. Ashizawa (2001). Application of Tabu search to optimal placement of distributed generators. Number C, pp. 918–923. IEEE.

Ness, J. V. (1959, Aug.). Iteration methods for digital load flow studies. *Power Apparatus and Systems. Transactions of the American Institute of Electrical Engineers 78*, 583–588.

Niroomandi, S., I. Alfaro, D. Gonzlez, E. Cueto, and F. Chinesta (2013). Model order reduction in hyperelasticity: a proper generalized decomposition approach. *International Journal for Numerical Methods in Engineering 96*(3), 129–149.

Ou, T. C. and W. M. Lin (2009). A novel Z-matrix algorithm for distribution power flow solution. In *PowerTech, 2009 IEEE Bucharest*, pp. 1–8.

Parrilo, P., S. Lall, F. Paganini, G. C. Verghese, B. Lesieutre, and J. Marsden (1999). Model reduction for analysis of cascading failures in power systems. In *American Control Conference, 1999. Proceedings of the 1999*, Volume 6, pp. 4208–4212 vol.6.

Pinnau, R. (2008). Model reduction via proper orthogonal decomposition. In *Model Order Reduction: Theory, Research Aspects and Applications*, Volume 13, pp. 95–109. Springer Berlin Heidelberg.

Rao, S., Y. Feng, D. J. Tylavsky, and M. K. Subramanian (2015). The holomorphic embedding method applied to the power-flow problem. *IEEE Transactions on Power Systems PP*(99), 1–13.

Rathinam, M. and L. R. Petzold (2000). An iterative method for simulation of large scale. In *Proceedings of the 39th IEEE Conference on Decision and Control, Sydney 2000*, pp. 4630–4635.

Rau, N. and C. Necsulescu (1990). Solution of probabilistic load flow equations using combinatorics. *International Journal of Electrical Power & Energy Systems 12*(3), 156 – 164.

Rau, N. S. and Y.-H. Wan (1994). Optimum location of resources in distributed planning. *IEEE Transactions on Power Systems 9*(4), 2014–2020.

Rios, R., J. Espinosa, and C. Mejía (2010). In *ANDESCON, 2010 IEEE*.

Rouhani, M., M. Mohammadi, and A. Kargarian (2016). Parzen window density estimator-based probabilistic power flow with correlated uncertainties. *IEEE Transactions on Sustainable Energy 7*(3), 1170–1181.

Rozza, G.and Huynh, D. B. P. P. A. T. (2008). Reduced basis approximation and a posteriori error estimation for affinely parametrized elliptic coercive partial differential equations. *Archives of Computational Methods in Engineering 15*(3), 229.

S. M. L. Kabir, A. H. Chowdhury, M. R. and J. Alam (2014). Inclusion of slack bus in Newton Raphson load flow study. *Electrical and Computer Engineering (ICECE), 2014 International Conference on, Dhaka*, 282–284.

Sachdev, M. S. and T. K. P. Medicherla (1977). A second order load flow technique. *IEEE Transactions on Power Apparatus and Systems 96*(1), 189–197.

Sameni, A., A. B. Nassif, C. Opathella, and B. Venkatesh (2012). A modified Newton-Raphson method for unbalanced distribution systems. In *Smart Grid Engineering (SGE), 2012 IEEE International Conference on*, pp. 1–7.

Sauer, P. (1981, Aug). Explicit load flow series and functions. *IEEE Trans. on Power App. and Syst. PAS-100*(8), 3754–3763.

Schaffer, M. D. and D. J. Tylavsky (1988). A nondiverging polar-form Newton-based power flow. *IEEE Transactions on Industry Applications 24*(5), 870–877.

Shareef, S. D. M. and T. V. Kumar (2014). A review on models and methods for optimal placement of distributed generation in power distribution system. *International Journal of Education and Applied Research 4*, 161–169.

Shrivastava, V. K., O. Rahi, V. K. Gupta, and J. S. Kuntal (2012). Optimal Placement Methods of Distributed Generation:A Review. *IEEE Transactions on Power Systems*, 978–981.

Sirovich, L. (1987). Turbulence and the dynamics of coherent structures. *IIII. Quart. Appl. Math. 45*, 561–590.

Stott, B. (1971). Effective starting process for Newton-Raphson load flows. *Electrical Engineers, Proceedings of the Institution of 118*(8), 983–987.

Stott, B. (1974, July). Review of load-flow calculation methods. *Proceedings of the IEEE 62*(7), 916–929.

Stott, B. and O. Alsac (1974, May). Fast Decoupled Load Flow. *Power Apparatus and Systems, IEEE Transactions on PAS-93*(3), 859–869.

Su, C.-L. (2005). Probabilistic load-flow computation using point estimate method. *IEEE Transactions on Power Systems 20*(4), 1843–1851.

Subramanian, M. K., Y. Feng, and D. Tylavsky (2013). PV bus modeling in a holomorphically embedded power-flow formulation. In *North American Power Symposium (NAPS), 2013*, pp. 1–6.

Sun, D. I., B. Ashley, B. Brewer, A. Hughes, and W. F. Tinney (1984). Optimal power flow by newton approach. *IEEE Transactions on Power Apparatus and Systems PAS-103*(10), 2864–2880.

Tang, J., F. Ni, F. Ponci, and A. Monti (2015). Dimension-adaptive sparse grid interpolation for uncertainty quantification in modern power systems: Probabilistic power flow. *Power Systems, IEEE Transactions on PP*(99), 1–13.

Taylor, D. and J. Treece (1967). Load flow analysis by the Gauss-Seidel method. *Symp. on Power SystemsLoad Flow Analysis, University of Manchester Institute of Saence and Technology, Manchester, U. K.*.

Teng, J.-H. (2002). A modified Gauss-Seidel algorithm of three-phase power flow analysis in distribution networks. *International Journal of Electrical Power & Energy Systems 24*(2), 97–102.

Thorp, J. S. and S. A. Naqavi (1997). Load-flow fractals draw clues to erratic behaviour. *IEEE Computer Applications in Power 10*(1), 59–62.

Thorp, J. S., S. A. Naqavi, and H. D. Chiang (1990). More load flow fractals. In *Decision and Control, 1990., Proceedings of the 29th IEEE Conference on*, pp. 3028–3030 vol.6.

Tinney, W. F. and C. E. Hart (1967). Power Flow Solution by Newton's Method. *IEEE Transactions on Power Apparatus and Systems*, (11).

Trias, A. (2012, July). The holomorphic embedding load flow method. In *Power and Energy Society General Meeting, 2012 IEEE*, pp. 1–8.

Trias, A. (2015, Sep). Fundamentals of the holomorphic embedding load-flow method. *ArXiv e-prints* (1509), 02421.

Trias, A. and J. L. Marn (2016). The holomorphic embedding loadflow method for dc power systems and nonlinear dc circuits. *IEEE Transactions on Circuits and Systems I: Regular Papers 63*(2), 322–333.

Tripathy, S. C., G. D. Prasad, O. P. Malik, and G. S. Hope (1982). Load-flow solutions for ill-conditioned power systems by a newton-like method. *IEEE Power Engineering Review PER-2*(10), 25–26.

Ward, J. B. (1949). Equivalent circuits for power-flow studies. *AIEE Trans. Power. App.Syst 68*(9), 373–382.

Ward, J. B. and H. W. Hale (1956, January). Digital computer solution of power-flow problems [includes discussion]. *Transactions of the American Institute of Electrical Engineers. Part III: Power Apparatus and Systems 75*(3).

Wasley, R. and M. Shlash (1974). Newton-Raphson algorithm for 3-phase load flow. In *Proceedings of the Institution of Electrical Engineers*, Number 7.

Willis, H. L. (2000). Analytical methods and rules of thumb for modeling dg-distribution interaction. In *Power Engineering Society Summer Meeting, 2000. IEEE*, Volume 3, pp. 1643–1644. IEEE.

Wirtz, D., D. Sorensen, and B. Haasdonk. A-posteriori error estimation for DEIM reduced nonlinear dynamical systems. *SIAM Journal on Scientific Computing*, 1–31.

Wu, F. (1977). Theoretical study of the convergence of the fast decoupled load flow. *Power Apparatus and Systems, IEEE Transactions on 96*(1), 268–275.

Xu, W., Y. Liu, J. Salmon, T. Le, and G. Chang (1998, May). Series load flow: a novel noniterative load flow method. *IEE Proc.-Gener. Transm. Distrib. 145*(3), 251–256.

Yang, N. C. (2016). Three-phase power flow calculations using direct Z-bus method for large-scale unbalanced distribution networks. *IET Generation, Transmission Distribution 10*(4), 1048–1055.

Yi-Shan, Z. and C. Hsiao-Dong (2010, May). Fast Newton-FGMRES solver for large-scale power flow study. *Power Systems, IEEE Transactions on 25*(2), 769–776.

Yong, T. and R. H. Lasseter (2000). Stochastic optimal power flow: formulation and solution. In *Power Engineering Society Summer Meeting, 2000. IEEE*, Volume 1, pp. 237–242 vol. 1.

Yu, H., C. Y. Chung, K. P. Wong, H. W. Lee, and J. H. Zhang (2009). Probabilistic load flow evaluation with hybrid latin hypercube sampling and cholesky decomposition. *IEEE Transactions on Power Systems 24*(2), 661–667.

Zhang, H. and P. Li (2013). Application of sparse-grid technique to chance constrained optimal power flow. *Generation, Transmission Distribution, IET 7*(5), 491–499.

Zhang, P. and S. T. Lee (2004). Probabilistic load flow computation using the method of combined cumulants and gram-charlier expansion. *IEEE Transactions on Power Systems 19*(1), 676–682.

Zhang, Z., H. D. Nguyen, K. Turitsyn, and L. Daniel (2015). Probabilistic power flow computation via low-rank and sparse tensor recovery. *IEEE Trans. Power Systems*.

Zhao, T. Q., H. D. Chiang, and K. Koyanagi (2016). Convergence analysis of implicit Z-bus power flow method for general distribution networks with distributed generators. *IET Generation, Transmission Distribution 10*(2), 412–420.

Zhu, J. and A. Abur (2006). Identification of errors in power flow controller parameters. In *Probabilistic Methods Applied to Power Systems, 2006. PMAPS 2006. International Conference on*, pp. 1–6.

Zimmerman, R. D. and H.-D. Chiang (1995). Fast decoupled power flow for unbalanced radial distribution systems. *IEEE Transactions on Power Systems 10*(4), 2045–2052.

Paper A

Unified formulation of a family of iterative solvers for power systems analysis

D. Borzacchiella, F. Chinesta, M.H. Malik, R. García-Blanco, P. Díez

ATTENTION ¡

Pages 87 to 95 of the thesis, containing the txet mentioned above,
should be consulted on the editor's web
https://www.sciencedirect.com/science/article/pii/S0378779616302292

Paper B

Introduction to the proper generalized decomposition for the solution of the parametrized power equations

D. Borzacchiello, R. García-Blanco, P. Díez,
F. Chinesta

Introduction to the Proper Generalized Decomposition for the solution of the parametrized power flow equations

D. Borzacchiello[a,*], R. García-Blanco[b], P. Díez[b], F. Chinesta[a]

[a]*Institut de Calcul Intensif (ICI), École Centrale de Nantes, 1 rue de la Noë, 44321 Nantes cedex 3, France*
[b]*Laboratori de Càlcul Numèric (LaCàN), Universidad Politécnica de Cataluña, C2 Campus Nord UPC, 08034 Barcelona, Spain*

Abstract

This paper concerns parametric modeling in power flow analysis and introduces a novel technique capable of producing fully explicit parametric solutions of the power flow equations accounting for the variability of power loads and generation. The key element of the method is the appropriate parametrization of load and generation profiles through the use of separated variable representations to express the functional dependence from the parameters. Reduced order solutions are computed numerically using the Proper Generalized Decomposition (PGD) technique. The paper introduces the fundamentals of the PGD method applied to the power flow equations and shows how to extend the traditional implicit Z bus method to compute parametric solutions in explicit form using a monolithic solution strategy. To discuss the potential advantages related to parametric modeling in power flow analysis an example application to the optimal placement of distributed generation is considered.

Keywords: Power System Simulation, Power Flow Analysis, Proper Generalized Decomposition, Reduced Order Modeling, Parametric Power Flow, Optimal Distributed Generation Allocation.

*Corresponding author
Email addresses:* `domenico.borzacchiello@ec-nantes.fr` (D. Borzacchiello),
`raquel.garcia.blanco@upc.edu` (R. García-Blanco), `pedro.diez@upc.edu` (P. Díez),
`francisco.chinesta@ec-nantes.fr` (F. Chinesta)

1. Introduction

1.1. Motivation and background

Power flow analysis is an important field of power system engineering that deals with the study of transmission and distribution of electrical power. It is the core of many applications based on computer simulation for power grids, such as real-time monitoring, optimal control, contingency analysis, operation and expansion planning. In power system design and analysis, a power flow solver routine is invoked as many times as particular system configurations need to be evaluated in order to take a decision. For some particular cases, like optimization and uncertainty quantification, specific formulations of the power flow equations have been defined. These are known as the Optimal Power Flow[10, 19, 13] and the Probabilistic Load Flow [3, 7].

When the dependance from many parameters need to be assessed, the extensive exploration of the state space through a parametric sweep study becomes computationally intensive. Considering that each sample of the space requires a computer simulation to solve the associated power flow, the computational cost diverges rapidly and sometimes it becomes unpractical for real systems. This complexity is typical of high dimensional problems and is known as the *curse of dimensionality.*

For this reason, the study of monolithic solvers for the *Parametric Power Flow* (PPF) becomes of practical interest. In this sense, instead of sweeping the parametric space and solving for each particular choice of the parameters, we propose to solve the set of parametric equations over the whole state space at once, treating the parameters of the problem as additional coordinates. The great drawback that comes with this approach is that the solution of the PPF lives in a higher dimensional space than the one of the original power flow problem. It implies that even if the solution algorithm for a single solve is optimally designed and has a linear complexity, the amount of computational work needed to explore a parametric space increases exponentially with its dimension.

Reduced Order Modeling (ROM) techniques can be thought of as a dimensionality reduction strategy to tame the exponential scaling associated with the parametric modeling. Among these, Proper Generalized Decomposition (PGD) has proven to be an efficient method for the numerical solution of high dimensional and parametric equations [9, 8]. The PGD exploits the concept of low rank approximations based on the separation of variables in order to compute reduced order solutions of parametric problems.

2

1.2. Related work

The concept of ROM has been known for long time in the field of power system engineering. Indeed, grid equivalencing techniques like Ward reduction [33] are commonly used to reduce the computational cost of power flow analysis of large systems. In this work, ROM techniques are not intended to reduce the physical degrees of freedom (i.e. the nodes) of a system but the computational complexity associated to the resolution of high-dimensional parametric equations.

Recent works dealing with either OPF or PLF using order reduction techniques rely on Sparse Grid approaches [21, 35, 31] or Sparse Tensor Recovery [36]. Both techniques can be classified as collocation approaches, since the solution is reconstructed in the high dimensional space from the values it assumes in a set of particular and well-chosen points called the collocation points.

In contrast with this concept, projection methods recover the solution using a Galerkin projection technique to guarantee global optimality. Proper Orthogonal Decomposition (POD) belongs to this category [2, 29] and has been used for transient simulation of electrical systems [24, 28, 27]. To the authors knowledge PGD still has not found an application in the field of power system simulation. Contrarily to POD, which produces a surrogate model from the results of previously computed results, PGD discovers the true dimensionality of the model as a part of the solution of the parametrized equations and does not need train simulations as in the Reduced Basis method [25]. As shown in this paper, careful treatment of the nonlinearity is required when using PGD. Diversified strategies exist, depending on the problem at hand, and can be found in the specialized literature [9].

1.3. Contributions

In this work we focus on the solution of the Parametric Power Flow using PGD, and we show how it is possible to extend a traditional iterative algorithm, the implicit Z bus method, to the case of parametric solutions. The proposed approach is introduced with an academic example of optimal allocation of Distributed Generation (DG), although this technique is not limited to this application but can be in principle extended to all the cases in which a parametric power flow problem arises.

The layout of the paper is organized as follows: in section 2 an overview of power flow equations and the nonlinear iterative method to solve them is given. The Proper Generalized Decomposition is illustrated in detail in

3

section 3 with a single parameter. The formalism of separated variables representations is also introduced in this section. In section 4, numerical examples are presented for problem in three and four parametric dimensions, while conclusions and perspectives are discussed in section 6.

2. Numerical Solution of Power Flow equations

In this section we review the governing equations for the power flow problem to make the paper self contained. We also motivate the choice of the iterative numerical method adopted for the solution.

2.1. The Power Flow equations

The Power Flow problem seeks the value of the voltages and currents (injected or withdrawn) at specified nodal locations in a grid representative of a power transmission or distribution system. The unknowns are assembled in vectors of n components V and $I \in \mathbb{C}^n$, where n is the number of nodes. The input data are the complex power source vector $S \in \mathbb{C}^n$, the network admittance matrix $\mathbf{Y} \in \mathbb{C}^{n \times n}$ including the characteristics of all power transmission devices like lines and transformers and the vector $I_0 \in \mathbb{C}^n$ accounting for constant current sources. In this formulation, the contribution of the slack node and other voltage sources is transformed into equivalent currents distributed in the neighboring nodes and is also included in I_0.

Writing Kirchhoff's current law at any node, the following algebraic linear system is obtained:

$$\mathbf{Y}V = I_0 + I \,, \tag{1}$$

where $\mathbf{Y}V$ denotes the matrix-vector product. Currents, voltages and powers are nonlinearly related through power balance equations, which can be written in vector form as:

$$S = V \odot I^* \,, \tag{2}$$

where I^* denotes the complex conjugate of the current vector I, and the symbol $\odot$ denotes the Hadamard product of vectors (component wise product). By incorporating equation (2) into (1), the following nonlinear system is obtained:

$$\mathbf{Y}V = I_0 + S^* \oslash V^* \,, \tag{3}$$

where the symbol $\oslash$ denotes the component-wise quotient between vectors. Equation (3) is referred to as the injected current form. Multiplying both right and left hand side by V^* one obtains the power form:

$$V^* \odot [\mathbf{Y}V - I_0] = S^* \,. \tag{4}$$

4

2.2. The implicit Z bus method

The resolution of the above problem has been addressed through diverse iterative methods. The linearization technique adopted in this work is the implicit Z bus method [6, 5, 18].

When the power flow equations are expressed in the current form this fixed point algorithm can be formulated as follows:

$$\mathbf{Y}V^{[l+1]} = I_0 + S^* \oslash V^{[l]^*}, \tag{5}$$

where l is the nonlinear iteration index.

Although this algorithm has a lower convergence rate compared to standard Newton-Raphson (NR) method [32, 16, 17], it can still be a preferred choice when solving parametric power flow problems with PGD. Indeed, in the implicit Z bus method only the admittance matrix needs to be inverted at each iteration and, unlike the Jacobian matrix in NR method, this does not depend on the solution. As it will be shown later in this work, this feature is a key point that greatly simplifies the structure of the parametric power flow solver. Note that a similar linearization strategy is adopted in other works [30, 1, 4] and in the open source code OpenDSS [11, 12], although not in the framework of parametric solutions.

In order to extend the Z bus method to compute fully parametric solution with PGD, it is useful to reformulate the fixed point (5) as a two-step procedure. Given the injected current $I^{[l]}$ at iteration l, the first step involves the update of the voltages from the solution of the linear system:

$$V^{[l+1]} = \mathbf{Y}^{-1}[I^{[l]} + I_0]. \tag{6}$$

while the second step is to update the injected currents from:

$$V^{*[l+1]} \odot I^{[l+1]} = S^*, \tag{7}$$

Note that the sub steps (7) and (6) are formally equivalent to (5), however the currents I are reintroduced as an auxiliary variables. The iterations are initiated assuming that initially the injected currents are zero. Therefore after one step the voltage are set to $V^{[1]} \equiv V_0 = \mathbf{Y}^{-1}I_0$, that is the solution of the problem in absence of loads and generations. Convergence is assessed by checking the variation of the voltage levels between successive iterations. The convergence in the norm $\left\| (V^{[l+1]} - V^{[l]}) \right\|$ criterion ensures that also the injection current mismatches tend to zero. Indeed, subtracting $\mathbf{Y}V^{[l]}$ from both members of (5) and taking the euclidean norm yields:

$$\left\| I_0 + S^* \oslash V^{[l]^*} - \mathbf{Y}V^{[l]} \right\| = \left\| \mathbf{Y}(V^{[l+1]} - V^{[l]}) \right\| \le \rho_{\mathbf{Y}} \left\| (V^{[l+1]} - V^{[l]}) \right\|, \tag{8}$$

5
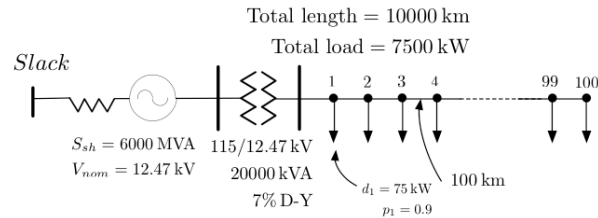
Figure 1   Schematics of the distribution grid used in the numerical examples of this paper. Data extracted from reference [22].

in which $\rho_{\mathbf{Y}}$ is the supremum among the magnitudes of the eigenvalues of $\mathbf{Y}$. The last inequality in equation (8) provides an upper bound of the residual norm (i.e. the current mismatches) and also guarantees that the stagnation of the fixed point implies that current, and hence power, mismatches tend to zero if the spectral radius of $\mathbf{Y}$ is bounded.

3. Numerical solution of the parametric power flow with PGD

In order to analyze how the PGD method works in the context of the PPF problem in a easy way, a practical optimization problem is introduced. This is only one particular case where a PPF naturally arises among those discussed in section 1.

3.1. Test problem

The problem considered requires to determine the optimal location and size of a capacitor bank in a distribution network in order to minimize the power losses over a year. The system analyzed is the three-phase radial distribution grid extracted from [22, 23] and is represented in figure 1. This consists of 100 buses and a transformer, therefore the number of nodes, considering the slack bus, is $n = 306$. Although the test system is not a realistic one, the associated power flow problem has the required algebraic structure needed to present and test the procedure that is proposed in this paper.

The variables that need to be optimized are p, q, that is, the position of the capacitor bank and the nominal power (in this case the capacitor bank is modeled as a purely reactive power source).

The search space for optimization is defined by:

$$q, p \in [q_{min}, q_{max}] \times [p_{min}, p_{max}] \tag{9}$$

6

Hourly variable loads are considered, therefore time is considered as additional parameter

$$t \in [0, t_{max}] \tag{10}$$

Traditional optimization algorithms require on-the-fly solutions of the power flow problem to evaluate the cost function (in this case the power losses) and possibly its gradient (if gradient based minimization can be used). Instead of following this approach we chose to pre-compute the parametric solution of the problem as an explicit function of the parameters p, q and t so that the evaluation of the objective function in the optimization algorithm does not require any further simulation.

It is important to emphasize that simulation and optimization are now separate steps and any optimization algorithm can be elected since this is completely unrelated to the solution of the power flow. For brevity, we do not address the choice of the optimization algorithm in this work. In the following examples extensive grid search was used to locate the minimum of the objective function.

Without losing generality, we start by considering the problem as depending from the single parameter q while keeping p and t fixed for the moment. In particular we assume $t = 0$ and $p = 100$.

The input power on the last bus now varies explicitly with the parameter q and therefore this can be taken into account into the vector S as follows:

$$S(q) = S_0 + iS_1 q \quad \forall q \in [q_{min}, q_{max}], \tag{11}$$

where i is the imaginary unit. In equation (11), S_0 is the vector of constant loads, while S_1 contains the reactive power variation in the last bus due to the presence of the capacitor bank. Hence, S_1 is zero for all buses except the last one.

Solving the PPF for this problem implies computing $V(q)$, $q \in [q_{min}, q_{max}]$, representing the voltage at each node of the power grid as an explicit function of the parameter q, representing the reactive power level in the last bus.

3.2. The separated varibles approximation

In the framework of the PGD, reduced order modeling is achieved through the separation of variables in the solution. For instance, for the injected currents a separated variable approximation is expressed in the following form:

$$I(q) \approx \sum_m^M I_m \mathcal{Q}_m(q). \tag{12}$$

7

This choice of representation allows to express a vector-valued function of the variable q

$$I\left(q\right) : [q_{min}, q_{max}] \subset \mathbb{R} \mapsto \mathbb{C}^n$$

as linear combination of scalar functions

$$\mathcal{Q}_m\left(q\right) : [q_{min}, q_{max}] \subset \mathbb{R} \rightarrow \mathbb{C}$$

by vector coefficients $I_m \in \mathbb{C}^n$.

Thus, the functions $\mathcal{Q}_m(q)$, expressing the functional dependency from q, are used to weight the space modes I_m expressing the dependency from the nodal position in the network. Note that the parametrization of the power given by expression (11) is also a separated variable representation made of two terms.

The symbol $\approx$ denotes the fact that we seek a numerical approximation of the solution and not an exact representation. The number of terms M in the summation is also referred to as the *rank* of the approximation and is not known apriori but can be progressively increased in order to improve the accuracy of the solution, as explained in the next section.

In practice, a numerical approximation requires the discretization of the parametric space using a suitable sampling strategy based on N_q discrete points. In this case, a PGD reduced order solution expressed by (12) has $M \cdot (n + N_q)$ degrees of freedom. On the other hand, a traditional parametric sweep approach for this problem would require to compute a full order solution consisting of $n \cdot N_q$ degrees of freedom, since a new solution would be computed for each of the N_q values of the parametric sampling. It is evident that an effective reduction is achieved if the rank of the separated variables approximation M is small.

3.3. Parametrized version of the implicit Z bus method

When the implicit Z bus method is used to solve a parametric problem, we first assume that a separated variables representations for $I\left(q\right)$ is available at iteration l,

$$I(q)^{[l]} \approx \sum_{m}^{M} I_m^{[l]} \mathcal{Q}_m^{[l]}(q). \tag{13}$$

The first step (7) of the iterative solver consists in solving equation:

$$V(q)^{[l+1]} = \mathbf{Y}^{-1}[I_0 + I(q)^{[l]}]. \tag{14}$$

8

Since the matrix $\mathbf{Y}$ does not depend on the parameter q, it is straightforward to show that $V(q)^{[l+1]}$ has the form

$$V(q)^{[l+1]} \approx V_0 + \sum_m^M V_m^{[l+1]} \mathcal{Q}_m^{[l]}(q) \tag{15}$$

with

$$V_m^{[l+1]} = \mathbf{Y}^{-1} I_m^{[l]} \quad \forall m = 1, \ldots, M\,, \tag{16}$$

and

$$V_0 = \mathbf{Y}^{-1} I_0\,.$$

This means that, once the injected currents is known, that the voltage inherits all the parametric functions from the current, while the space modes are easily computed using (16) once the factorization of the matrix $\mathbf{Y}$ is performed once and for all. This result is possible because $\mathbf{Y}$ does not depend on the solution. In Jacobian based iterative methods computing $V(q)^{[l+1]}$ would be more complicated due to the necessity of evaluating the Jacobian from the separated variable representation of $V(q)^{[l]}$ at current iteration.

Once the voltage is known the currents needs to be updated from:

$$V(q)^{*[l+1]} \odot I(q)^{[l+1]} = S(q)^*\,, \tag{17}$$

This step is less straightforward than the first, since it requires to find a low rank approximation for $I(q)$ as the quotient of two separated variable functions $V(q)^{*[l+1]}$ and $S(q)^*$. This is explained in the following section. As usual the procedure can be started by taking zero initial injected currents and is stopped when the difference between two successive iterations is small enough.

3.4. The Proper Generalized Decomposition

The computational bottleneck of the parametric Z bus solver is the determination of the current $I(q)$ in a separated variables form, from equation (17). The Proper Generalized Decomposition is based on *greedy enrichment* strategy that starts by computing a rank one approximation for the current

$$I(q) \approx I_1 Q_1(q) \tag{18}$$

Equations (17) express a set of $n \times N_q$ constraints while $I(q)$ has only $n + N_q$ degrees of freedom. Therefore, using a rank one approximation may not be sufficient to fulfill all the equations exactly. In this case the system is

9

overdetermined and therefore the equations must solved in an approximate sense by minimizing the residual norm, which corresponds to minimizing the nodal power mismatch.

Since the voltage and the power are expressed in a separated variables form, the residual of equations (17) can also be expressed in a separated variables form

$$R(q) = V(q)^* \odot I(q) - S(q)^* = \sum_{m=1}^{M_R} R_m \mathcal{W}_m(q) \,.$$

The norm of the residual can be defined as follows:

$$\|R(q)\|^2 = \sum_{j,k=1}^{M_R} \left\langle R_j^H R_k \right\rangle \int_{q_{min}}^{q_{max}} \mathcal{W}_j(q)^* \mathcal{W}_k(q) dq \,, \qquad (19)$$

where $\langle R_j^H R_k \rangle$ is the classical inner product in $\mathbb{C}^n$, R_j^H being the conjugate transpose of the vector R_j, while $\int_{q_{min}}^{q_{max}} W_j(q)^* W_k(q) dq$ denotes the inner product between continuous functions defined over $[q_{min}, q_{max}]$.

The best approximation for the current can be found from the condition

$$I_1 \mathcal{Q}_1(q) = \underset{I\mathcal{Q}(q)}{\arg\min} \left\{ \|R(q)\|^2 \right\}. \qquad (20)$$

Since this is not necessarily enough to reduce the nodal power mismatches to the desired tolerance, the rank of the approximation is increased by one and the new term $I_2 \mathcal{Q}_2(q)$ is computed using an analogous minimization procedure. New terms are added until the power mismatch is less than a given tolerance parameter ϵ_l.

The minimization problem (20) can be solved at each enrichment step using any algorithm and valid numerical integration technique for computing the integrals appearing in (19). What works well in practice is an *Alternating Minimization* approach. This starts from a random guess for $I_m \mathcal{Q}_m(q)$ and then gradually improves the approximation quality by fixing one factor and minimizing the residual norm over the other factor. The first order optimality condition dictated by the residual minimization over a single factor results in a linear diagonal system that can be easily solved with any direct solver. The procedure is detailed in Appendix A.

3.5. Overview of the algorithm and convergence criteria

The algorithm presented in the previous sections consists of three nested iterative loops. The outer solver is needed to deal with the nonlinearity is

the implicit Z bus method (iteration index l), while the inner solver (PGD) is used to find a separated variable approximation of the solution at current nonlinear iteration. PGD is further broken down in a Greedy Enrichment algorithm that adds new terms until the residual of the equations is sufficiently small (iteration index m), and the Alternating Minimization fixed point needed to compute each new term in the separated form of $I(q)$. The pseudo-code (1) provides a step by step outline of the overall procedure.

Algorithm 1: PGD - Power Flow

    Data: $V^0 = \boldsymbol{Y}^{-1}I_0$

1   **for** $l = 0, 1, \ldots$ *(Nonlinear iteration)* **do**

2      $I^{0,l+1} \leftarrow 0$;

3      $m = 0$;

4   **while** $\|R(q)\| > \epsilon_g$ *(Add new enrichment)* **do**

5          $m \leftarrow m + 1$;

6          $I_m \leftarrow$ random;

7          $\mathcal{Q}_m(q) \leftarrow$ random;

8   **while** $\max\left(\frac{\Delta I_m}{I_m}, \frac{\Delta \mathcal{Q}_m(q)}{\mathcal{Q}_m(q)}\right) > \epsilon_f$ *(Alternating Minimization)* **do**

9   Minimize the residual norm over I_m with $\mathcal{Q}_m(q)$ fixed ;

10   Minimize the residual norm over $\mathcal{Q}_m(q)$ with I_m fixed ;

11          $I^{m,l+1} \leftarrow I^{m-1,l+1} + I_m \mathcal{Q}_m(q)$;

12   Compute V^{l+1} from eq. (14);

13   **if** $\left\| V^{l+1} - V^l \right\| / \left\| V^{l+1} \right\| < \epsilon_l$ **then**

14   break;

Convergence is checked using the guidelines described in [8]. In algorithm 1, we adopt a stagnation criterion to check the convergence of both the nonlinear loop and the inner fixed point loop using ϵ_l and ϵ_f as tolerance parameters. The convergence of the greedy algorithm is controlled by the norm of the residual, which is required to be smaller than ϵ_g. In the numerical examples presented in this paper we adopt $\epsilon_f = 10^{-4}$, $\epsilon_l = 10^{-7}$ and $\epsilon_g = 10^{-7}$. When the problem dimensionality is higher than two, the described algorithm is directly applicable with the only variant being that Alternating Minimization is now applied iteratively over each individual dimension.

11
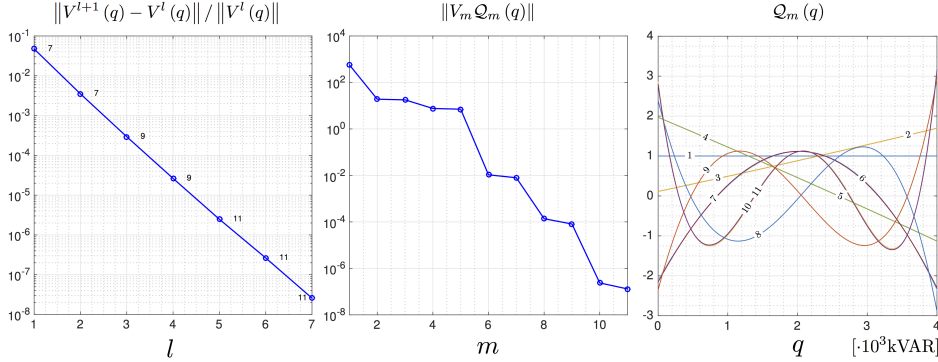
Figure 2   Parametric Power Flow solution with PGD. Convergence diagram of nonlinear-PGD with the iteration index l (left). The numbers reported on the curve represent number of terms M in the solution at each nonlinear iteration l. Norm of each individual term in the separated representation of the converged solution for $m = 1, 2, \ldots, 11$ (middle). Normalized functions $\mathcal{Q}_m(q)$ expressing the functional dependency form the reactive power variation q of the node 100 (right). Note that, in order to visualize $\mathcal{Q}_m(q)$ for this case, we constrained the PGD algorithm to work with real output for the parametric dimension. In general, using complex functions results in a more compact representation (i.e. with fewer terms).

3.6. Numerical results

We report hereafter the convergence results for the problem described in section 3.2. The values for the reactive power in this example were taken as $q_{min} = 0$ and $q_{max} = 4 \cdot 10^3$ kVAR. The parametric space is discretized using $N_q = 1000$ points and trapezoidal rule is used for numerical integration. The convergence of the outer loop for the implicit Z bus method is shown in figure 2, where the number of enrichment computed at each iteration is also reported. The separated representation of the converged solution is composed of 11 terms. The Euclidean norm of each term is also represented in figure 2, this values are a measure of the relative importance of individual term in the low rank approximation. The rate at which these coefficient decay gives some insight on the reducibility of the model. In this case the fact that the decay is quite fast indicates that the model is fairly well reducible. Finally the normalized functions $\mathcal{Q}_m(q)$ are also shown. By recombining the vectors V_m with these, the solution of the power flow for any value of q in the considered interval can be retrieved, without any further simulation needed.

12

4. Application to the optimal allocation of DG

In this section results related to the application of the nonlinear PGD solver for a high dimension version of the PPF are shown.

4.1. Optimal positioning and sizing of a capacitor bank

In this example, we reintroduce the location p of the capacitor as parametric coordinates of the PPF and seek to minimize the power losses over p and q. The resulting PPF problem is three-dimensional (one physical coordinate and two parameters) and is solved using the PGD. The same problem is solved by Martinez and Guerra using Monte Carlo Simulation [22]. Here we follow an "offline-online" approach, in the sense that first we solve the PPF to compute the loss function $\mathcal{L}(q, p)$ explicitly for every point of the parametric space (offline) and then proceed to its minimization (online). The offline stage consists in determining a separated variables representation of the voltage solution:

$$V(q,p) \approx \sum_{m=1}^{M} V_m \mathcal{Q}_m(q) \mathcal{P}_m(p) \,, \text{where} \tag{21}$$

$$\mathcal{Q}_m(q) : [q_{min}, q_{max}] \subset \mathbb{R} \mapsto \mathbb{C} \tag{22}$$

are functions of the injected reactive power q and

$$\mathcal{P}_m(p) : [p_{min}, p_{max}] \subset \mathbb{N} \mapsto \mathbb{C} \tag{23}$$

are functions of the capacitor bank position p.

Once the solution is obtained, a separated variables representation for the losses can be computed as a part of the post-processing of the solution:

$$\mathcal{L}(q,p) \approx \sum_{m=1}^{\tilde{M}} \tilde{\mathcal{Q}}_m(q) \tilde{\mathcal{P}}_m(p) \,. \tag{24}$$

In the above expression the losses are also approximated using separated variables representation.

The online phase consists in determining the optimal positioning and sizing of the capacitor bank as the minimizers of the loss function

$$\tilde{q}, \tilde{p} = \arg\min_{q,p} \left\{ \mathcal{L}(q,p) \right\}. \tag{25}$$

The injected reactive power q is varied between $q_{min} = 0$ and $q_{max} = 4 \cdot 10^3$ kVAR, while candidate positions for the capacitor bank are considered

13

from bus 1 to bus 100. Therefore the number of available positions N_p is 100. Again, the interval $[q_{min}, q_{max}]$ is discretized in $N_q = 1000$ points and the trapezoidal integration rule is adopted.

The desired accuracy is obtained after 7 nonlinear iterations of the implicit Z bus method and the final solution approximation for the voltage contains only $M = 13$ enrichments. The first 5 functions $\tilde{\mathcal{Q}}_m(q)$ and $\tilde{\mathcal{P}}_m(p)$, from the separated variable representation of the losses are shown respectively in figure 3 together with the reconstruction of the two dimensional loss function.

In practice, for this problem a $2D - 1D$ separation is adopted, since the fully separated representation of the power S needs exactly as many terms as possible positions p. For this reason two dimensions are kept together: the bus coordinate and the DG position. In this way, only two terms are needed for the separated representation of the power, as in the previous example.

To understand the advantage of slow rank approximation, note that the computational work needed to obtain an equivalent solution with a traditional parametric sweep in the optimization space corresponds to 100×1000 different calls of the power flow solver. This amounts to compute $306 \times 100 \times 1000$ unknowns, whereas using PGD a separated variable approximation of the parametric solution only requires computing $13 \times (306 * 100 + 1000)$ unknowns to have the desired accuracy. Therefore the reduced order solution is about 75 times smaller than the full order solution.

The final step involves performing a global minimization procedure. This can be done using any optimization technique by reconstructing the objective function "on-the-fly" only in the points where evaluations are needed by the minimization algorithm. Function evaluations are now no longer associated with power flow solutions but with the reconstruction of the separated variables representation which only involves simple arithmetic operations and can be done practically in real time on a standard laptop computer.

As in the original paper of Martinez and Guerra and the theoretical analysis present in [34], the optimal position is predicted at approximately 2/3 of the total length of the grid.

4.2. Long term losses evaluation with hourly variable loads

In this last example we turn our attention to the case where loads are varying in time. The voltage solution can be written as:

$$V(q,p,t) \approx \sum_{m=1}^{M} V_m \mathcal{Q}_m(q)\mathcal{P}_m(p)\mathcal{T}_m(t)\,, \tag{26}$$

14
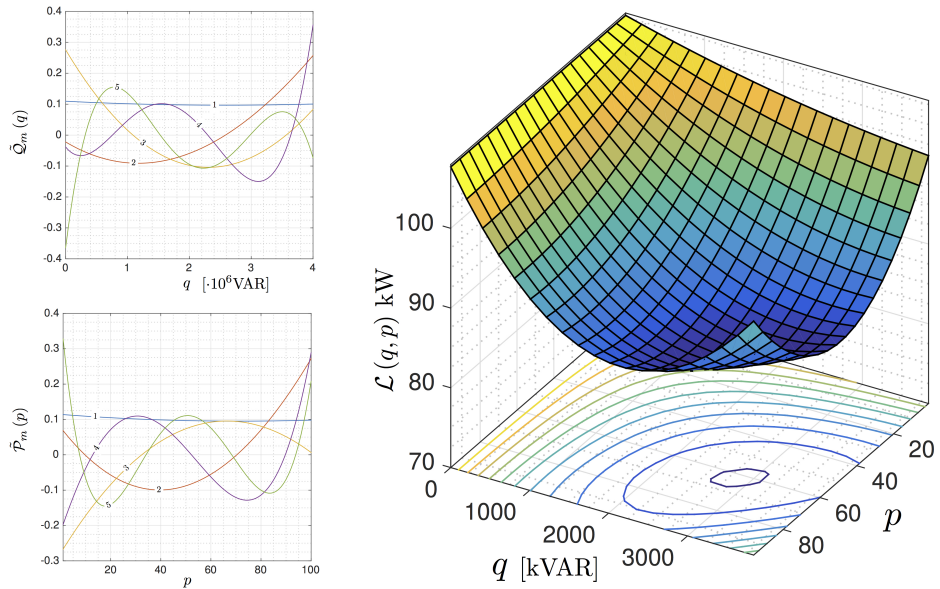
Figure 3 Separated form of the power losses as a function of the nodal position p and the generated reactive power q of the capacitor bank. Functions of the DG output reactive power (top-left). Functions of the DG position (bottom-left). Reconstructed losses function (right).
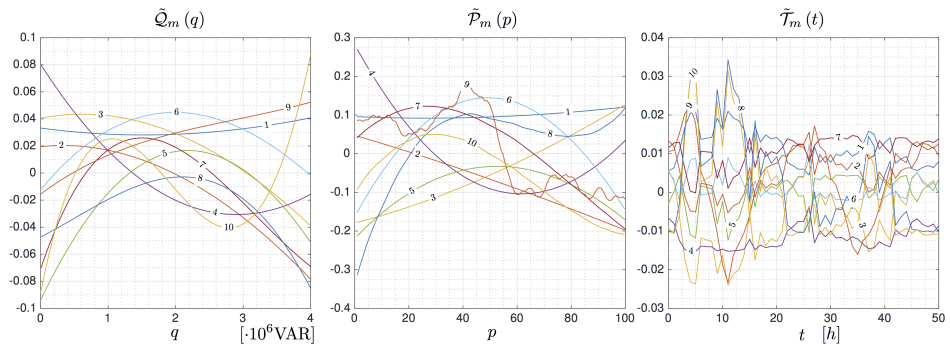

Figure 4 Separated form of the three-dimensional power losses, computed for the case of time varying loads. Normalized function of the DG output reactive power q (left). Normalized functions of the DG position p (middle). Normalized functions of the time t (right).

15

with

$$\mathcal{T}_m(t) : [0, t_f] \subset \mathbb{R} \mapsto \mathbb{C} \qquad (27)$$

being the parametric functions of the time t. In the present example $t_f = 8760h$ and the load variations are recorded hourly, therefore time is discretized in $N_t = 8760$ points. Load profiles can be either obtained by direct measurements over time or, as in this case, generated with an appropriate model. Load and generation shapes data were obtained from reference [22] based on the models implemented in [20]. For this case, the power can be written as a sum of five terms, one for the base loads and four describing the loads variations in time:

$$S(q, p, t) = \sum_{m=1}^{5} \bar{\mathcal{S}}_m(p) \bar{\mathcal{Q}}_m(q) \bar{\mathcal{T}}_m(t) \,. \qquad (28)$$

Following the same reasoning of section 4.1, we represent the now four-dimensional voltage solution using a $2D - 1D - 1D$ separation. As in the previous exemple the nonlinear iterative method converges in 7 iterations, but the rank of final solution is now 65. The power loss function

$$\mathcal{L}(q, p, t) \approx \sum_{m=1}^{\tilde{M}} \tilde{\mathcal{Q}}_m(q) \tilde{\mathcal{P}}_m(p) \tilde{\mathcal{T}}_m(t) \qquad (29)$$

can be computed directly by post-processing the separated form of the voltage solution and incorporated in the objective function to minimize. The first ten individual terms of the separated variables representation of the power loss are represented in figure 4. In this case the reduced order solution obtained with 65 modes is approximately 5 orders of magnitude smaller than the full order solution.

This evidences how the separated variables approximation becomes more and more efficient as the dimensionality of the problem increases. Authors in [22] reported a run time of 2.5 hours for the execution of Monte Carlo optimization using OpenDSS in time mode for this example. With PGD the execution time to compute the parametric solution is of the order of a few minutes using MATLAB, while optimization can be performed practically in real time.

16

5. Further considerations

When the system depends on more parameters $\xi = \{\xi_1, \xi_2, \ldots, \xi_D\}$, a separated variable approximation can be written in a general form as:

$$V(\xi_1, \xi_2, \ldots, \xi_D) \approx \sum_m^M V_m X_m^1(\xi_1) X_m^2(\xi_2) \ldots X_m^D(\xi_D),$$

where V_m are vector coefficients, $X_m^d(\xi_d)$, $d = 1, 2, \ldots, D$ are functions expressing the solution dependency from the individual parameters ξ_d. From the numerical viewpoint a parametric sweep based on a sampling strategy with N points per dimension requires N^D simulations. However, the exponential scaling is avoided using separated variables representations. In this case the complexity of the solution is $M \times N \times D$, hence it scales linearly with the dimension of the parametric space. The PGD attempts to compute a low rank approximation by breaking down the original problem into a succession of smaller problems each depending on a single parameter.

The reducibility of the problem and the existence of low rank approximations of parametric solutions depend on the nature of the problem at hand. This subject is rather broad and will not be addressed in this work. The interested read may refer to [26] chapter 5. Our experience so far with different power systems, indicates that the power flow problem solutions are good candidates for dimensionality reduction, meaning that low rank representations with reasonable accuracy can be computed using PGD. Further examples of the application of this technique can be found in [14].

6. Conclusions and perspectives

The computational strategy adopted in this paper is intended as a first step in the introduction of the PGD for low rank approximations of the parametric solutions of the power flow problem. The efficiency of the proposed method relies on a robust nonlinear iterative solver that can accommodate the Proper Generalized Decomposition in order to reduce the exponential algorithmic complexity naturally arising in high-dimensional parametric problems.

The results presented in this work show a double advantage. In the first place, the representation of the solution through the separated variables formalism, and by consequence the memory storage requirements, scale linearly with the dimensionality of the problem. Second, the alternating minimization algorithm breaks down the original multiparametric problem into a succession of subproblems each depending on a single parameter.

17

This new computational strategy was presented in the framework of optimal allocation of DG based on losses minimization and will hopefully be extended to other application areas, in which parametric modeling is applicable. Indeed, the availability of parametric solutions in explicit form is a commodity for many power engineering applications like power system design and optimization, real time simulation-based control and uncertainty quantification due to non-deterministic power generations and loads.

For the method proposed in this paper, we have developed a robust error estimation strategy for the quantity of interest (the losses for instance) allowing to monitor the convergence of the PGD algorithm, which is the subject of a parallel publication [15].

Appendix A. Alternating Minimization Method

Given a representation of rank M_s for the nodal powers

$$S(q) = \sum_{m=1}^{M_s} S_m \bar{\mathcal{Q}}_m(q) \tag{A.1}$$

and a representation of rank M_v for the voltage

$$V(q) = \sum_{m=1}^{M_v} V_m \mathcal{Q}'_m(q) , \tag{A.2}$$

a low rank approximation of the current $I(q)$ is sought from the linear relation:

$$V(q)^* \odot I(q) - S(q)^* = 0 , \tag{A.3}$$

In the following a generic method is explained supposing that $M - 1$ terms have already been computed. Given the approximation of rank $M - 1$:

$$I^{M-1}(q) = \sum_{m=1}^{M-1} I_m \mathcal{Q}_m(q) \tag{A.4}$$

the corresponding nodal power mismatch is given by

$$R^{M-1}(q) = \sum_{j=1}^{M-1} \sum_{k=1}^{M_v} I_j \odot V_k^* \mathcal{Q}_j(q) \mathcal{Q}'_k(q)^* - \sum_{m=1}^{M_s} S_m^* \bar{\mathcal{Q}}_m(q)^* \tag{A.5}$$

18

If the norm $\left\|R^{M-1}(q)\right\|$ is higher than the admissible tolerance, an improved rank M approximation for the current can be obtained by adding a rank one correction to $I^{M-1}(q)$:

$$I^M(q) = \sum_{m=1}^{M-1} I_m \mathcal{Q}_m(q) + I_M \mathcal{Q}_M(q) \qquad (A.6)$$

The new term $I_M \mathcal{Q}_M(q)$ is found from the requirement that the norm of power mismatch $R^M(q)$ is minimized. Using equation (A.5), this can be written as:

$$R^M(q) = R^{M-1}(q) + [I_M \mathcal{Q}_M(q)] \odot V(q)^* . \qquad (A.7)$$

By consequence, the following relation holds for the norm of $R^M(q)$:

$$\left\|R^M(q)\right\|^2 = \|[I_M \mathcal{Q}_M(q)] \odot V(q)^*\|^2 + \left\|R^M(q)\right\|^2 +$$
$$\left\langle R^M(q)^*, [I_M \mathcal{Q}_M(q)] \odot V(q)^* \right\rangle +$$
$$\left\langle [I_M \mathcal{Q}_M(q)]^* \odot V(q), R^M(q) \right\rangle \quad (A.8)$$

The algorithm for minimizing $\left\|R^M(q)\right\|$ is started by assuming random values for I_M and $\mathcal{Q}_M(q)$.

First, the factor $\mathcal{Q}_M(q)$ is fixed. Minimizing the power mismatch norm over the other factor results in the following first order optimality condition, derived from equation (A.8):

$$\left[\sum_{j,k=1}^{Mv} \alpha_{jk} V_j \odot V_k^* \right] \odot I_M = \sum_{j=1}^{Ms} \sum_{k=1}^{Mv} \gamma_{jk} S_j^* \odot V_k - \sum_{h=1}^{M-1} \sum_{j,k=1}^{Mv} \beta_{hjk} I_h \odot V_j \odot V_k^* \qquad (A.9)$$

from which I_M is updated. The coefficients appearing in (A.9) are defined by the integrals:

$$\alpha_{jk} = \int_{q_{min}}^{q_{max}} \mathcal{Q}_M(q)^* \mathcal{Q}_M(q) \mathcal{Q}_j'(q) \mathcal{Q}_k'(q)^* \, dq$$

$$\beta_{hjk} = \int_{q_{min}}^{q_{max}} \mathcal{Q}_M(q)^* \mathcal{Q}_h(q) \mathcal{Q}_j'(q) \mathcal{Q}_k'(q)^* \, dq$$

$$\gamma_{jk} = \int_{q_{min}}^{q_{max}} \bar{\mathcal{Q}}_j(q)^* \mathcal{Q}_k'(q) \, dq$$

19

These can be approximated using standard quadrature rules. Note that (A.9) is a linear system that is straightforwardly solved for I_M since the operator is diagonal. Then, I_M is considered fixed and the minimization is performed over the factor $\mathcal{Q}_M(q)$, which results into the following first order optimality condition:

$$
\left[\sum_{j,k=1}^{Mv} \tilde{\alpha}_{jk} \mathcal{Q}'(q)_j \mathcal{Q}'_j(q)^* \right] \mathcal{Q}_M(q) =
$$
$$
\sum_{j=1}^{Ms} \sum_{k=1}^{Mv} \tilde{\gamma}_{jk} \bar{\mathcal{Q}}_j(q)^* \mathcal{Q}'_k(q) - \sum_{h=1}^{M-1} \sum_{j,k=1}^{Mv} \tilde{\beta}_{hjk} \mathcal{Q}_h(q) \mathcal{Q}'_j \mathcal{Q}'_k{}^* \quad \text{(A.10)}
$$

with coefficients defined by

$$
\begin{aligned}
\tilde{\alpha}_{jk} &= \left\langle (V_j^* \odot I_M)^H, V_k^* \odot I_M \right\rangle \\
\tilde{\beta}_{hjk} &= \left\langle (V_j^* \odot I_h)^H, V_k^* \odot I_M \right\rangle \\
\tilde{\gamma}_{jk} &= \left\langle S_j^H, V_k \right\rangle
\end{aligned}
$$

In practice the function $\mathcal{Q}_M(q)$, is solved for a set of N_q discrete points in $[q_{min}, q_{max}]$ using the linear relation (A.10).

This procedure is iterated until convergence, when both factors reach stagnation. At this point, if the power mismatch norm is still too high a new rank one enrichment is added and the algorithm is started again.

Similarly, for higher dimensional problems, the minimization is alternated over each parametric dimension until convergence.

References

[1] R. Benato, A. Paolucci, and R. Turri, "Power flow solution by a complex admittance matrix method," *Eur. T. Electr. Power*, vol. 11, no. 3, pp. 181–188, 2001.

[2] G. Berkooz, P. Holmes, and J. L. Lumley, "The proper orthogonal decomposition in the analysis of turbulent flows," *Annu. Rev. Fluid Mech.*, vol. 25, no. 1, pp. 539–575, 1993.

[3] B. Borkowska, "Probabilistic load flow," *IEEE Trans. on Power App. and Syst.*, vol. PAS-93, no. 3, pp. 752–759, May 1974.

[4] D. Borzacchiello, M. Malik, F. Chinesta, R. García-Blanco, and P. Diez, "Unified formulation of a family of iterative solvers for power systems analysis," *Electr. Pow. Syst. Res.*, 2016.

[5] A. Brameller and J. Denmead, "Some improved methods for digital network analysis," *Proc. Inst. Elec. Eng*, vol. 109A, no. 43, pp. 109–116, February 1962.

[6] H. Brown, G. Carter, H. Happ, and C. Person, "Power flow solution by impedance matrix iterative method," *IEEE Trans. on Power App. and Syst.*, vol. 82, no. 65, pp. 1–10, April 1963.

[7] P. Chen, Z. Chen, and B. Bak-Jensen, "Probabilistic load flow: A review," in *Proc. 3rd Int. Conf. Electr. Utility Deregulation Restructuring Power Technol.* IEEE, 2008, pp. 1586–1591.

[8] F. Chinesta, R. Keunings, and A. Leygue, *The Proper Generalized Decomposition for Advanced Numerical Simulations: A Primer*, ser. SpringerBriefs in Applied Sciences and Technology.

[9] F. Chinesta, A. Leygue, F. Bordeu, J. Aguado, E. Cueto, D. Gonzalez, I. Alfaro, A. Ammar, and A. Huerta, "PGD-based computational vademecum for efficient design, optimization and control," *Arch. Comput. Methods Eng.*, vol. 20, no. 1, pp. 31–59, 2013.

[10] H. Dommel and W. Tinney, "Optimal power flow solutions," *IEEE Trans. on Power App. and Syst.*, vol. PAS-87, no. 10, pp. 1866–1876, Oct 1968.

[11] R. Dugan and T. McDermott, "An open source platform for collaborating on smart grid research," in *IEEE PES Gen. Meeting*, July 2011, pp. 1–7.

[12] R. Dugan, *Reference Guide. The Open Distribution System Simulator.*, june 2013.

[13] S. Frank, I. Steponavice, and S. Rebennack, "Optimal power flow: a bibliographic survey I," *Energ. Syst.*, vol. 3, no. 3, pp. 221–258, 2012.

[14] R. García-Blanco, D. Borzacchiello, F. Chinesta, and P. Diez, "A reduced order modeling approach for optimal allocation of distributed generation in power distribution systems," in *Energy Conference (ENERGYCON), 2016 IEEE International*, April 2016.

21

[15] R. García-Blanco, D. Borzacchiello, F. Chinesta, and P. Diez, "Monitoring a PGD solver for parametric power flow problems with goal-oriented error assessment (article in review)," in *Int. J. Numer. Meth. Engng.*, 2016.

[16] P. Garcia, J. Pereira, J. Carneiro, S., V. da Costa, and N. Martins, "Three-phase power flow calculations using the current injection method," *IEEE Trans. Power Syst.*, vol. 15, no. 2, pp. 508–514, May 2000.

[17] A. Gómez-Expósito, A. J. Conejo, and C. Cañizares, *Electric energy systems: analysis and operation.* CRC Press, 2008.

[18] P. Gupta and M. Humphrey Davies, "Digital computers in power system analysis," *Proc. Inst. Elec. Eng.*, vol. 108A, no. 41, pp. 383–398, October 1961.

[19] M. Huneault and F. Galiana, "A survey of the optimal power flow literature," *IEEE Trans. Power Syst.*, vol. 6, no. 2, pp. 762–770, May 1991.

[20] T. Lambert, P. Gilman, and P. Lilienthal, *Micropower System Modeling with HOMER.* John Wiley, 2006.

[21] G. Lin, M. Elizondo, S. Lu, and X. Wan, "Uncertainty quantification in dynamic simulations of large-scale power system models using the high-order probabilistic collocation method on sparse grids," *Int. J. Uncert. Quant.*, vol. 4, no. 3, pp. 185–204, 2014.

[22] J. A. Martinez and G. Guerra, "Optimum placement of distributed generation in three-phase distribution systems with time varying load using a Monte Carlo approach," in *Proc. IEEE PES General Meeting.* IEEE, 2012, pp. 1–7.

[23] J. Martinez and G. Guerra, "A parallel monte carlo method for optimum allocation of distributed generation," *IEEE Trans. Power Syst.*, vol. 29, no. 6, pp. 2926–2933, Nov 2014.

[24] P. Parrilo, S. Lall, F. Paganini, G. C. Verghese, B. Lesieutre, and J. Marsden, "Model reduction for analysis of cascading failures in power systems," in *Proc. Amer. Control Conf.*, vol. 6, 1999, pp. 4208–4212 vol.6.

22

[25] C. Prud'homme, D. V. Rovas, K. Veroy, L. Machiels, Y. Maday, A. T. Patera, and G. Turinici, "Reliable real-time solution of parametrized partial differential equations: Reduced-basis output bound methods," *J. Fluid. Eng.*, vol. 124, no. 1, pp. 70–80, 2001.

[26] A. Quarteroni, A. Manzoni, and F. Negri, *Reduced Basis Methods for Partial Differential Equations: An Introduction*, Springer International Publishing, 2016.

[27] M. Rathinam, "An iterative method for simulation of large scale modular systems using reduced order models," in *Decision and Control, 2000. Proceedings of the 39th IEEE Conference on*, vol. 5. IEEE, 2000, pp. 4630–4635.

[28] M. Rathinam and L. R. Petzold, "Dynamic iteration using reduced order models: a method for simulation of large scale modular systems," *SIAM J. Numer. Anal.*, vol. 40, no. 4, pp. 1446–1474, 2002.

[29] M. Rathinam and L. R. Petzold, "A new look at proper orthogonal decomposition," *SIAM J. Numer. Anal.*, vol. 41, no. 5, pp. 1893–1925, 2003.

[30] K. Sunderland, M. Coppo, M. Conlon, and R. Turri, "A correction current injection method for power flow analysis of unbalanced multiple-grounded 4-wire distribution networks," *Electr. Pow. Syst. Res.*, vol. 132, pp. 30 – 38, 2016.

[31] J. Tang, F. Ni, F. Ponci, and A. Monti, "Dimension-adaptive sparse grid interpolation for uncertainty quantification in modern power systems: Probabilistic power flow," *IEEE Trans. Power Syst.*, vol. PP, no. 99, pp. 1–13, 2015.

[32] W. Tinney and C. Hart, "Power flow solution by Newton's method," *IEEE Trans. on Power App. and Syst.*, vol. PAS-86, no. 11, pp. 1449–1460, November 1967.

[33] J. B. Ward, "Equivalent circuits for power-flow studies," *AIEE Trans. Power. App.Syst*, vol. 68, no. 9, pp. 373–382, 1949.

[34] H. L. Willis, "Analytical methods and rules of thumb for modeling dg-distribution interaction," in *Proc. IEEE Power Eng. Soc. Summer Meet.*, vol. 3. IEEE, 2000, pp. 1643–1644.

23

[35] H. Zhang and P. Li, "Application of sparse-grid technique to chance constrained optimal power flow," *Gener. Transm. Distrib. IET*, vol. 7, no. 5, pp. 491–499, May 2013.

[36] Z. Zhang, H. D. Nguyen, K. Turitsyn, and L. Daniel, "Probabilistic power flow computation via low-rank and sparse tensor recovery," *arXiv preprint arXiv:1508.02489*, 2015.

24

Paper C

A reduced order modeling approach for optimal allocation of distributed generation in power distribution systems

R. García-Blanco, D. Borzacchiello, F. Chinesta, P. Díez,

ATTENTION ¡

Paper D

Monitoring a PGD solver for parametric power flow problems with goal-oriented error assessment

R. García-Blanco, D. Borzacchiello, F. Chinesta, P. Díez